

UNIVERSITY OF CAPE COAST

NONLINEAR POLARIZATION EFFECTS IN A BIREFRINGENT SINGLE MODE OPTICAL FIBER

2006002

BY

GEORGE CHUKWUJI ISHIEKWENE

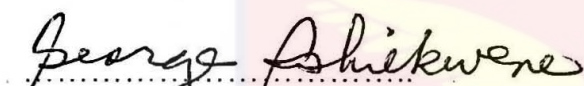
THESIS SUBMITTED TO THE DEPARTMENT OF PHYSICS OF
THE FACULTY OF SCIENCE, UNIVERSITY OF CAPE COAST IN
PARTIAL FULFILMENT OF THE REQUIREMENTS FOR THE
AWARD OF DOCTOR OF PHILOSOPHY DEGREE IN PHYSICS

LIBRARY
UNIVERSITY OF CAPE COAST

MAY 2000

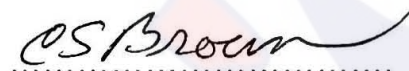
DECLARATION

"I hereby declare that this thesis is the result of my own original research and that no part of it has been presented for another degree in this University or elsewhere.

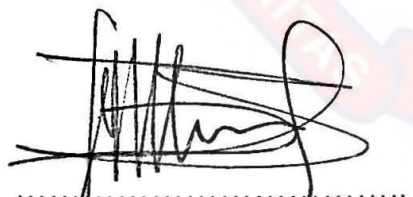

George Chukwui Ishiekwene

Date: *May 11, 2000*

"We hereby declare that the preparation and presentation of the thesis were supervised in accordance with the guidelines on supervision of thesis laid down by the University of Cape Coast."


Professor Charles S. Brown
Principal Supervisor

Date: *11th May 2000*

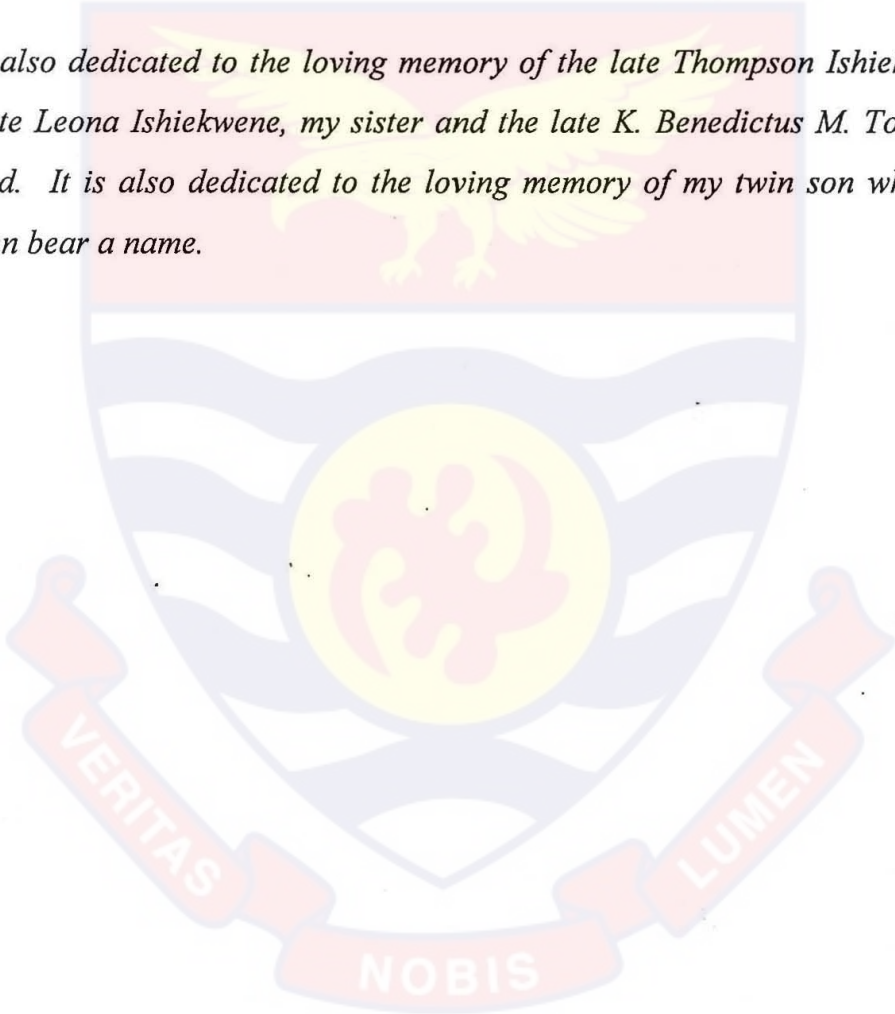

Professor S. Yeboah Mensah
Supervisor

Date: *11th May 2000*

DEDICATION

This work is dedicated to my mother, my wife Martha and my son Pius. It is also dedicated to George Junior, my twin son, who was born few days before the completion of this thesis.

This work is also dedicated to the loving memory of the late Thompson Ishiekwene, my father; the late Leona Ishiekwene, my sister and the late K. Benedictus M. Torborg, my favorite friend. It is also dedicated to the loving memory of my twin son who did not survive to even bear a name.



ACKNOWLEDGEMENTS

Fristly, I would like to thank God for the blessing in completing this work. I wish to express sincere gratitude to my wife, Martha Boema Ishiekwene; my mother, Janet Ada Ishiekwene; my son Pius Chukwuemeke Khine-Llango Ishiekwene; my sister, Victoria Bendu Sirleaf and the rest of my family including Claudius Chukwuka Ishiekwene and Georgette Ada Ishiekwene for their love, understanding, sacrifice, encouragement and support.

Indeed, I am very grateful to Professors Charles S. Brown and S.Yeboah Mensah for their guidance, advice and numerous discussions during this research effort. I wish to thank Professors G. Denardo, F.K.A. Allotey and H. Winful for their concern, helpful discussions, and recommendations regarding this research. Special thanks to Dr. A.M. Dikande for his assistance.

I would also like to thank Drs Frederick Gbegbe, Al-Hassan Conteh, and Dean Hunder for their support. I am thankful to Messrs P.K. Mensah and Alex Asante for their friendship and encouragement. Special gratitude go to my colleagues Joshua Oladipo and Jojo Eghan.

I would also like to express my utmost gratitude to the International Atomic Energy Agency (IAEA) for the magnanimous gesture made during the entire period of my programme. Special thanks to the Abdus Salam International Centre for Theoretical Physics (ICTP) through its Office of External Activities for the outstanding contribution to my research. I am deeply indebted to the University of Cape Coast through the Laser and Fibre Optics Centre (LAFOC) and the University of Liberia for their support.

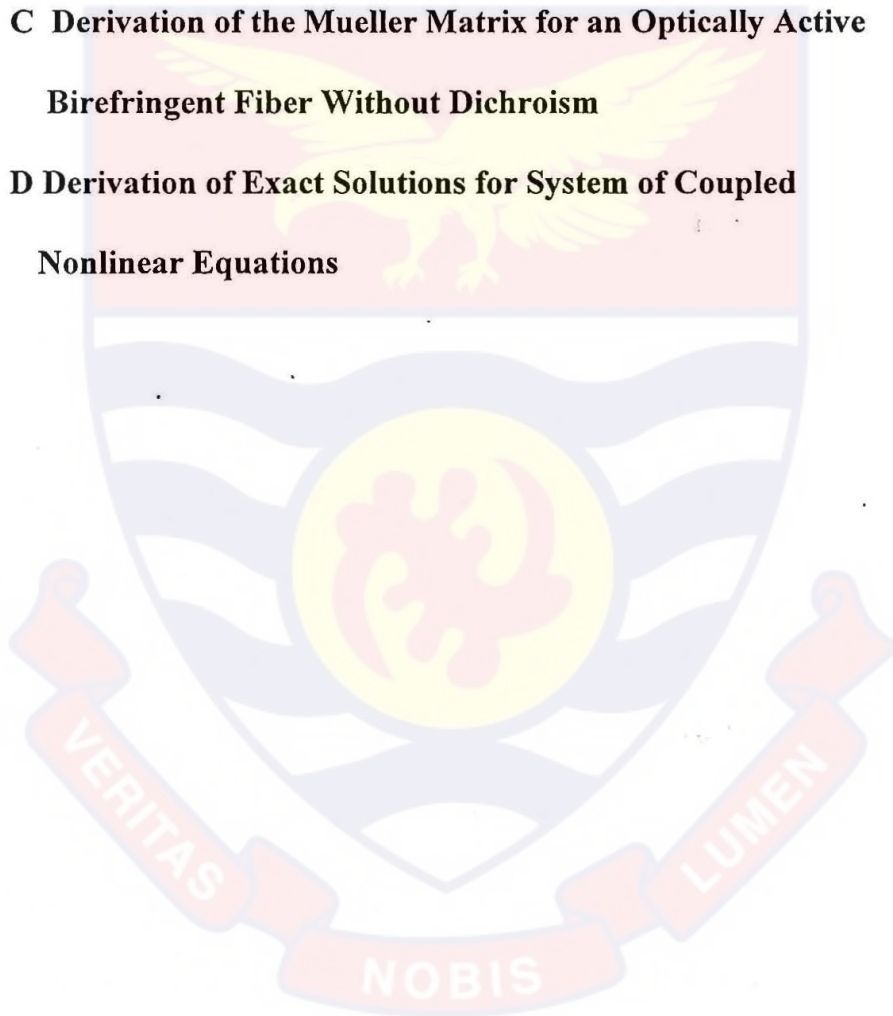
Finally, I am also very grateful for the invaluable support I received from the Zinnahs, Kamaras, Mensahs, Massaquois, Seminarians and many others too numerous to list for lack of space. Many thanks to all.

TABLE OF CONTENTS

List of Figures	viii
List of Symbols	xiii
Abstract	xvi
1 INTRODUCTION	1
2 BACKGROUND AND THEORY OF PROPAGATION IN SINGLE MODE FIBERS	6
2.1 Historical Review of Polarization Phenomena in single Mode Fibers . .	7
2.2 Concepts and Definitions	10
2.2.1 Constitutive Equations: The Linear Case.	13
2.2.2 Constitutive Equation: The Nonlinear Case	16
2.2.3 Symmetry Conditions for Susceptibility Tensors	18
2.2.4 Constitutive Equations for Optical Effects in a Single Mode Fiber	24
2.3 Characteristics of Single Mode Fibers	26
2.3.1 Refractive Index Profile	26
2.3.2 Fiber Modes	30
2.3.3 Fiber Losses	33
2.3.4 Dispersion in Single Mode Fibers	36
2.4 Propagation in Single Mode Fibers - Coupled Mode Theory	38

3	POLARIZATION PHENOMENA IN SINGLE MODE OPTICAL FIBERS	40
3.1	Definition and Evolution of Polarization	40
3.1.1	Stokes Parameters	45
3.1.2	Poincare Sphere	48
3.1.3	Mueller Matrix	48
3.2	Stokes Parameters Equation of Motion	50
3.3	Polarization Ellipse	56
3.3.1	Polarization Ellipse Plane Rotation	57
3.4	Polarization Mode Dispersion	59
4	POLARIZATION FORMALISM AND MODEL: THE LINEAR CASE	61
4.1	The Unified Formalism	61
4.2	Polarization Formalism for an Optically Active Birefringent Fiber without Dichroism	70
4.3	Polarization Formalism for an Optically Active Birefringent Fiber with Dichroism	84
5	POLARIZATION FORMALISM AND MODEL: THE NONLINEAR CASE	97
5.1	Evolution Equations for Stokes Parameters in Nonlinear Fiber	97
5.2	Nonlinear Polarization Effects	104
5.2.1	Nonlinear Anisotropic Effects	105
5.2.2	Nonlinear Polarization Self-Ellipse Rotation	107
5.2.3	Polarization Instability	108
5.2.4	Nonlinear Optical Activity	121

6	DISCUSSION OF RESULTS	123
7	CONCLUSIONS	132
	REFERENCES	134
	APPENDIX A Derivation of Coupled-Mode Equation	141
	APPENDIX B Derivation of the Stokes Parameters Equation of Motion	147
	APPENDIX C Derivation of the Mueller Matrix for an Optically Active Birefringent Fiber Without Dichroism	151
	APPENDIX D Derivation of Exact Solutions for System of Coupled Nonlinear Equations	156



LIST OF FIGURES

2 - 1	Measured loss profile of a single mode fiber	34
3 - 1	Evolution of the state of polarization along a birefringent fiber when the input beam is linearly polarized at 45° with respect to the slow axis .	44
3 - 2	Illustration of the polarization state of a light wave on the Poincare sphere	47
3 - 3	Poincare's sphere representation of optical activity in a lossless birefringent fiber	58
4 - 1	Variation in output stokes parameters as a function of fiber length for linearly horizontally polarized input light. Circular birefringence present but linear birefringence off-axis not allowed	75
4 - 2	Variation in output stokes parameters as a function of fiber length for linear $+45^\circ$ polarized input light. Circular birefringence assumed present but linear birefringence off-axis not allowed	76
4 - 3	Output Stokes parameters as a function of fiber length for right circularly polarized input light. Circular birefringence present but linear birefringence off-axis not allowed	76
4 - 4	Variation in output stokes parameters as a function of fiber length for elliptically polarized input light (45° azimuth and 22.5° ellipticity). Circular birefringence is present but linear birefringence off-axis not allowed	77

4 - 5	Output Stokes parameters as a function of fiber length for linearly horizontally polarized input light. Both circular and linear off-axis birefringence are absent.	78
4 - 6	Output Stokes parameters as a function of fiber length for linear +45° polarized input light. Circular and linear birefringence off-axis are both absent	78
4 - 7	Output Stokes parameters as a function of fiber length for right circularly polarized input light. Circular birefringence and linear birefringence off-axis are both absent	79
4 - 8	Variation in output stokes parameters as a function of fiber length for elliptically polarized input light (45° azimuth and 22.5° ellipticity). Circular and linear birefringence off-axis are both absent	79
4 - 9	Output stokes parameters as a function of fiber length for linearly horizontally polarized input light. Circular birefringence assumed absent and liner off-axis birefringence allowed	82
4 - 10	Output stokes parameters as a function of fiber length for linear +45° polarized input light. Circular birefringence assumed absent and linear birefringence off-axis allowed	82
4 - 11	Output stokes parameters as a function of fiber length for right circularly polarized input light. Circular birefringence is assumed absent and linear birefringence off-axis allowed.	83

4 - 12	Output Stokes parameters as a function of fiber length for elliptically polarized input light (45° azimuth and 22.5° ellipticity). Circular birefringence is assumed absent and linear birefringence off-axis allowed.	83
4 - 13	Variation in output stokes parameters as a function of fiber length for linearly horizontally polarized input light. Circular birefringence assumed present and linear birefringence off-axis allowed.	84
4 - 14	Variation in output stokes parameters as a function of fiber length for linear $+45^\circ$ polarized input light. Circular birefringence present and linear birefringence off-axis allowed.	85
4 - 15	Variation in output stokes parameters as a function of fiber length for right circularly polarized input light. Circular birefringence present and linear birefringence off-axis allowed.	85
4 - 16	Variation in output stokes parameters as a function of fiber length for elliptically polarized (45° azimuth and 22.5° ellipticity) input light. Circular birefringence assumed present and linear birefringence off-axis allowed.	86
4 - 17	Output stokes parameters for linearly horizontally polarized input light as a function of fiber length. Circular birefringence and dichroism only are assumed present.	88
4 - 18	Output stokes parameters for linearly $+45^\circ$ polarized input light as a function of the fiber length. Circular birefringence and dichroism only are assumed present.	89

4 - 19	Variation in output stokes parameters for right circularly polarized input light as a function of the fiber length. Circular birefringence and dichroism only are assumed present.	89
4 - 20	Output stokes parameters for elliptically polarized (45° azimuth and 22.5° ellipticity) input light as a function of the fiber length. Circular birefringence and dichroism only are assumed present.	90
4 - 21	Output stokes parameters for linearly horizontally polarized input light as a function of the fiber length. Circular birefringence and dichroism are assumed absent.	93
4 - 22	Output stokes parameters for linear +45° polarized input light as a function of the fiber length. Circular birefringence and dichroism are assumed absent.	94
4 - 23	Variation in output stokes parameters for right circularly polarized input light as a function of the fiber length. Circular birefringence and dichroism are assumed absent.	94
4 - 24	Output stokes parameters for elliptically polarized (45° azimuth and 22.5° ellipticity) input light as a function of the fiber length. Circular birefringence and dichroism are assumed absent.	95
5 - 1	Jacobian parameter m as a function of the ratio r for initial polarization states S_{10} , S_{20} , and S_{30} of (1) 1, 0, 0; (2) 0, 0.3, 1; (3) 0, 0.71, 0.71; (4) 1, 0, 0.8; (5) -1, 0, 0.8.	118
5 - 2	Variation of stokes parameters as a function of fiber length for the initial polarization state $S_{10} = 0$, $S_{20} = 0.71$ and $S_{30} = 0.71$. In this figure, $r = 2.3$ and $m = 0.58$	119

5 - 3	Variation of stokes parameters as a function of fiber length for the initial polarization state $S_{10} = 0, S_{20} = 0.71$ and $S_{30} = 0.71$. In this figure, $r = 4$ and $m = 1$	120
5 - 4	Variation of stokes parameters as a function of fiber length for the initial polarization state $S_{10} = 0, S_{20} = 0.3$ and $S_{30} = 1$. In this figure, $r = 2.3$ and $m = 1.2$	120
5 - 5	Variation of stokes parameters as a function of fiber length for the initial polarization state $S_{10} = 0, S_{20} = 0.3$ and $S_{30} = 1$. In this figure, $r = 4$ and $m = 2.7$	121
6 - 1	Variation in output stokes parameters as a function of orientation angle for elliptically polarized (45° azimuth and 22.5° ellipticity) input light. Circular birefringence is assumed absent.	127
6 - 2	Variation in output stokes parameters as a function of orientation angle for elliptically polarized (45° azimuth and 22.5° ellipticity) input light. Circular birefringence is assumed present.	127
6 - 3	Jacobian parameter m as a function of the ratio r for initial polarization states S_{10}, S_{20} , and S_{30} of (1) 0, 0, 1; (2) 0, 0.5, 1; (3) 0.4, 0.4, 1; (4) 0, 1, 0; (5) -0.5, 0, 0.3.	130

LIST OF SYMBOLS

$A, A_j, a_\gamma(z)$	electromagnetic wave amplitude
a	fiber core radius
\hat{B}	birefringent operator
cn, sn, dn	Jacobian elliptic functions
\hat{D}	dichroic operator
D	degeneracy factor
\mathbf{D}	electric displacement vector
$\vec{d} \equiv (d_1, d_2, d_3)$	dichroism in Stokes 3-vector representation
E, \mathbf{E}, E_z	electric field
H, \mathbf{H}, H_z	magnetic field
HE_{11}, LP_{01}	fundamental fiber mode, linearly polarized mode
HE_{lm}, EH_{lm}	fiber modes
\hat{I}	4×4 unit matrix
$\mathcal{I}(z)$	coherency matrix, density matrix
J_l, K_l	Bessel functions
k	Jacobian modulus

k_z, \mathbf{k}, k	wave vector, wave number
k_i	birefringence
L	fiber length
$\widehat{\mathbf{M}}$	Mueller matrix
$n \in Z$	n is an integer
n_1, n_2	core index, cladding index
NA	numerical aperture
\mathbf{P}	electric field polarization response
P	degree of polarization
P_T, P_0	transmitted power, initial power
$P_i^{(n)}$	nth order induced polarization tensor
$\hat{\mathbf{P}}, u_{ij}$	perturbative coupling terms
\mathbf{r}	spatial coordinate vector
S_i, S_μ	Stokes parameters
$\overline{\mathbf{S}}$	three-dimensional Stokes coordinate space
$\overline{\overline{\mathbf{S}}}$	four-dimensional Stokes coordinate space
TM, TE	transverse magnetic mode, transverse electric mode
V	cutoff parameter, V number
v	phase velocity
$w_{\alpha\beta}$	expansion coefficient
α	attenuation constant, fiber loss
β	phase constant
$\overline{\beta} \equiv (\beta_1, \beta_2, \beta_3)$	birefringence in Stokes 3-vector representation
β_{lm}	eigenvalue solution to characteristic Bessel equation
γ	damping parameter of the oscillator
Δ	relative index of refraction difference
δ	arbitrary phase
δ_{ij}	kronecker delta symbol

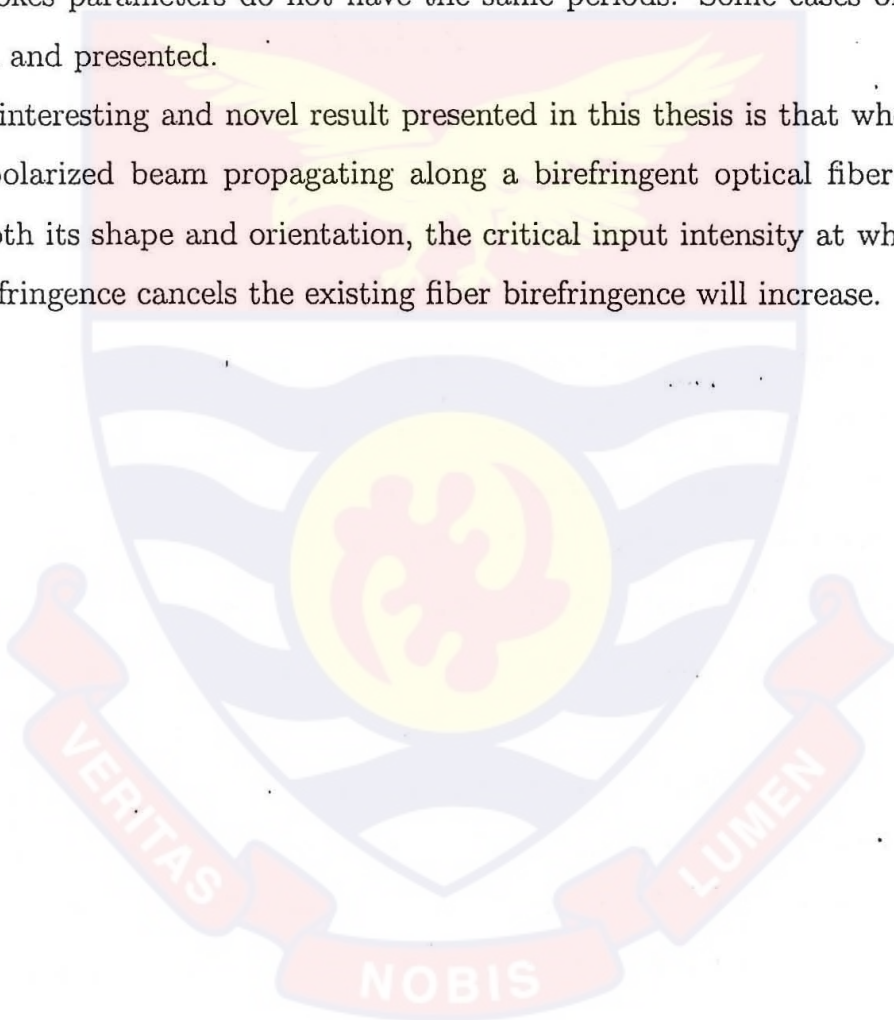
δn_p	phase index of refraction difference
ϵ_0	permittivity of free space
ϵ_{ij}	dielectric tensor
$\epsilon_{ijk}, \epsilon_{\alpha\beta\gamma}$	Levi-Civita symbol
η	angle of ellipticity
Θ	azimuthal angle
λ	wavelength
μ	magnetic permeability
ρ	relative coordinate
$\sigma^{(i)}$	Pauli matrices
τ	time delay between two events
$\chi_{ij}^{(1)}$	first order local susceptibility
$\chi_{ijk}^{(2)}$	second order local susceptibility
$\chi_{ijkl}^{(3)}$	third order local susceptibility
$\Psi^{(n)}$	fiber response function
ψ	dielectric function of perturbed function
$\Omega_\alpha, \Omega^{NL}$	self-action vector in nonlinear case
$\Omega_\alpha^L, \Omega^L$	self-action vector in linear case
ω	angular frequency of electromagnetic oscillation
$\Gamma_{ij}^{(1)}$	first order nonlocal susceptibility tensor
$\Gamma_{ijk}^{(2)}$	second order nonlocal susceptibility tensor
$\Gamma_{ijkl}^{(3)}$	third order nonlocal susceptibility tensor
\dagger	complex conjugate transpose, self adjoint operator

ABSTRACT

In this thesis, an investigation is conducted on the nonlinear polarization effects in a birefringent single mode optical fiber. The thesis begins with an introduction that gives current interests as well as a general review of polarization behavior in a birefringent single mode fiber. The theory on propagation of light in single mode optical fibers is also introduced to serve as a basis for understanding the concepts of nonlinear polarization effects. Then Stokes parameters and the Stokes formalism are introduced and related to the traditional measures of light polarization such as ellipticity and azimuth. The use of Stokes parameters to analyze polarization effects as the beam propagates in a birefringent optical fiber forms the central theme of this thesis. The evolution equations for Stokes parameters when the optical fiber is considered linear are derived using the methods of Brown's Unified Formalism for Polarization Optics. Several Mueller matrices which characterize the polarization effects of birefringence and dichroism are obtained analytically. This provides a means to model the evolution of the Stokes parameters as function of fiber length and orientation angle. Graphical illustrations showing the output polarization change are presented in this thesis. Furthermore, general solutions to the Stokes parameters evolution equations when the optical fiber is considered nonlinear have been obtained analytically in terms of the Jacobian elliptic functions. Graphical illustration showing the nonlinear behavior of the output polarization are also presented.

A fundamental and noteworthy aspect of the results presented in this thesis is that when the fiber is considered linear the output Stokes parameters are either periodic or constant with length or orientation angle depending on whether the fiber is assumed to have losses or not. When the solutions are periodic, the three Stokes parameters are observed to have the same periods. However, when the fiber response to propagation is considered nonlinear, the output Stokes parameters are generally doubly periodic and the three Stokes parameters do not have the same periods. Some cases of aperiodicity are observed and presented.

Another interesting and novel result presented in this thesis is that when an intense elliptically polarized beam propagating along a birefringent optical fiber undergoes a change in both its shape and orientation, the critical input intensity at which the light-induced birefringence cancels the existing fiber birefringence will increase.



Chapter 1

INTRODUCTION

In recent years, single mode optical fibers have become the transmission medium of choice for long-distance telecommunications networks [1]. These networks take advantage of the high-data-rate characteristics of a single mode fiber. In addition, these fibers are not only utilized in applications such as local area networks, cable TV networks, sensors and integrated optical device components but also as tools to facilitate measurement objectives in a variety of scientific and technological areas. In these applications, a thorough understanding of polarization and its effects are fundamental to the design and characterization of all these devices.

This research investigates the nonlinear polarization effects in a birefringent single mode fiber. It also involves the simulation of a model that determines the nonlinear polarization behavior of the fiber as a function of the input field intensity and polarization. Such a research is significant because the nonlinear effects resulting from polarization behavior lead to various applications including pulse shaping, optical switching, intensity discriminators and all-optical logic gates [2]. Some of the nonlinear polarization dependent effects are also of keen interest in optical fiber telecommunications. This research, therefore, addresses problems related to the nonlinear polarization dynamics in single mode optical fibers.

In an ideal optical fiber, it is generally supposed that the fiber has perfect circular symmetry and that the polarization vectors are degenerate. However, in real optical fibers, the degeneracy is split by birefringence that may be introduced either intentionally or randomly. Birefringence may be defined as the difference between the two effective mode indices of refraction and can be either due to intrinsic geometrical asymmetries and imperfections in the fiber or due to extrinsic externally applied perturbations such as bending, squeezing, or twisting of the fiber [3]. In general, the pair of orthogonal modes are coupled by perturbations which vary along the length of the fiber. Therefore, the propagating optical field in a birefringent fiber can be expressed as a superposition of two orthogonal linearly polarized modes. The birefringence induces a phase shift between the modes.

It was usually assumed that the birefringence is locally linear in a single mode fiber [4]. However, in recent years, the availability of fibers with low dichroism has led not only to a revolution in the field of optical fiber communications [5] but has also given birth to the field of nonlinear fiber optics [6]. Dichroism relates to the polarization dependent loss effects of a fiber. It represents the attenuation of the light power transmitted by the fiber and arises from intrinsic material properties such as absorption or scattering and from waveguide properties due to manufacturing influence. It has been reported that polarization dependent losses influence systems containing several elements connected by optical fibers [78]. Several nonlinear phenomena including optically induced birefringence [7], polarization instability [8 – 11], and solitons [4, 11] have led to important advances from the fundamental as well as technological point of view. Self-induced birefringence is a nonlinear coupling between the two orthogonally polarized components of an optical wave resulting in changes in the fiber refractive index by different amounts for the two components. The nonlinearity in fibers is responsible for a nonlinear exchange in energy between the orthogonal modes [12]. In addition, interest in nonlinear fiber optics is expected to develop further in view of the current emphasis on photonics-based technologies for information management. Photonics summarizes and symbolizes the current effort to

replace and/or supplement electronics with optics in signal processing, computing, and related technologies. In fact, a polarization diversity detection system for distributed sensing of polarization mode coupling in high birefringence fibers has been implemented using a pump-probe architecture based on the optical Kerr effect [79]. Optical Kerr effect is a nonlinear process in which the birefringence in a medium is caused by an intensity-induced change in the refractive index of the medium. Single mode fibers offer unique opportunities for observing nonlinear phenomena in relatively simple experimental conditions. These fibers exhibit nonlinear behavior depending on the power density which travels through them. In spite of the weak nonlinear response of silica, fibers are capable of confining the electromagnetic field over small cross-sections (typically ten squared microns) and for long distances with little loss (down to 0.2db/km) [11]. In contrast with other fields of application such as plasma physics and fluid mechanics, in fiber optics, one needs a minimum level of approximation in order to derive a set of coupled equations from the basic principles for a small number of modal amplitudes. This is true for the linear [73, 74] and nonlinear [75] regime of pulse propagation in fibers. Whereas in the linear case, a weak transverse anisotropy of the linear susceptibility tensor and longitudinal inhomogeneities of the fiber act as perturbing terms and lead to mode coupling, in the nonlinear case the role of the perturbation is played by the presence of a weak nonlinearity. In both linear and nonlinear cases, the separation between transverse and longitudinal variables that is at the basis of the coupled mode theory allows one to deal with only two independent variables, namely the time and the distance traveled along the longitudinal axis of the fiber. Coupled mode theory is a powerful method used to study the change in the propagation characteristics of the light caused by perturbations in an optical medium. A detailed discussion on this theory as it pertains to an optical fiber is presented in subsequent chapters.

This research, therefore, involves the study of the propagation of an optical field through a single mode fiber with small nonlinearity and anisotropy in the framework of the coupled mode theory and in terms of a rather simple formalism. The emphasis will

be on the analytical approach to solving the problem of nonlinear polarization effects in single mode fibers. The use of Stokes parameters to calculate polarization changes as the beam propagates along a birefringent optical fiber will form the central theme throughout this thesis. This will permit an immediate global insight into the physical properties of the solutions for both linear and nonlinear polarization effects in an optical fiber. Where necessary, geometrical considerations will be provided to enhance the visualization of the resulting effects. The approach used in this work is based on the qualitative theory in this field advanced in a recently published textbook [12]. The investigation in this thesis is limited to the study of induced nonlinear birefringence resulting from coupling between the two orthogonally polarized components of an optical wave in a single mode fiber. The coupling between the polarization components of the optical wave is then analyzed after including the effects of both intrinsic linear birefringence and optically induced nonlinear birefringence. Thus, this research investigates the effects and interplay of both linear and nonlinear birefringence in single mode optical fibers and their implications for communications as well as their potential for device applications. Nondegenerate three-wave mixing modes in regimes where dispersion plays a crucial role will not be considered since the full wave dynamics in the fiber would be governed by partial differential equations in 1+1 dimensions [11]. In other words, dispersion is not considered a critical factor in this work. This assumption has several advantages. There is no group velocity dispersion (GVD) which is responsible for pulse broadening. Other effects such as solitons and pulse compression which depend on the presence of GVD will not be considered in this research. However, even though dispersion is neglected, it can be included to first order for analysis on polarization mode dispersion in birefringent fibers [14, 83]. Lastly, the analysis in this research is purely deterministic so that stochastic effects resulting from randomly varying birefringence are not given consideration.

The above discussions signify the importance of polarization phenomena in bulk optics, fiber optics, and photonics. It is the aim of this thesis, therefore, to analyze the polarization behavior of a single mode fiber with special emphasis on nonlinear effects.

The methods of the unified formalism for polarization optics [1] and the Jacobian elliptic functions [61, 77] are used to obtain and interpret the physical behavior of the fiber based on its local and nonlocal properties.

The plan for the rest of this thesis is as follows: chapter 2 provides the historical background and propagation theory on single mode fibers to serve as the basis for understanding the concepts presented in later chapters. Stokes parameters and Mueller matrix theory are introduced in chapter 3 to describe, respectively, the propagating field polarization and characteristics of the fiber. The derivation of Stokes parameter equation of motion is also presented to establish the connection between the field amplitudes and the optical properties of the fiber. Stokes equation of motion form the unifying feature common to both the linear and nonlinear cases under investigation. In chapter 4, an overview of the unified formalism for polarization optics is presented to provide the analytical approach used for modeling the fiber considered in this work. In addition, Mueller matrices describing polarization effects for specific cases of optically active fibers with and without dichroism when nonlinear effects are negligible are deduced and presented. Chapter 5 focuses on polarization effects that occur when the incident power and fiber length are such that nonlinear effects occur. Evolution equations for Stokes parameters in a nonlinear fiber are also derived and presented. Central in this section is the presentation of a Mueller matrix which contains terms that depend on the cubic optical nonlinearity of the fiber. Chapter 6 is on the discussions of the analytical and numerical results obtained for all possible effects observed within the scope of this research. Chapter 7 is on the conclusions of the thesis. Several suggestions and comments on the different cases of physical interests emanating from the results of this thesis are also presented in this section.

Chapter 2

BACKGROUND AND THEORY OF PROPAGATION IN SINGLE MODE FIBERS

Single mode fibers have been used in polarization-dependent applications and have also been the topic of several research over the past thirty years. Quite recently, interest has also grown in research on nonlinear polarization effects and its usefulness in single mode fiber applications. This chapter is intended to present a review of some of the past and current studies concerned with polarization in fibers. Also included in this chapter are definitions of key terms and fundamental concepts on single mode fibers as well as an analysis that describes the coupling between the modes of the fiber. It is the aim of this chapter to provide the background required for understanding the physical interpretation of what occurs when light propagates along a fiber without giving initially detailed rigorous mathematical derivations. Such an approach is intended to aid in understanding the remaining chapters without difficulty.

2.1 Historical Review of Polarization Phenomena in Single Mode Fibers

There has been a rapid expansion in the use of single mode optical fibers not only in optical telecommunication systems but also in the area of sensor applications. These technological advancement owe their success in part to a firm theoretical, experimental, and technical understanding of the basic underlying physics. The relevant fiber parameters, such as numerical aperture, index profile, core diameter, dispersion, attenuation, spot size, cut-off wavelength and polarization which control the physical behavior of the fiber structures need to be properly understood. Perhaps, more importantly, are the dictates of these parameters when the fiber is under a functional performance as it interacts with light. Many interesting features occur as the light propagates along the fiber and this has led to various applications. Since the focus of this work is on nonlinear polarization effects in single mode fibers, the discussion here is limited to only polarization features and their applications.

Several excellent books have been written to describe polarization phenomena in linear optics including some recently published [15, 16]. A number of other famous texts such as [17 – 19] have devoted significant attention to the subject of polarization dynamics. Nonlinear optics also covers a comprehensive monographic range and from among the well-known texts in this subject a few [20 – 23] are cited here. Even though nonlinear optics enjoys a wide coverage, one of the few texts devoted exclusively to polarization effects in nonlinear optics was published recently in 1998 [13]. Research in polarization phenomena in linear and nonlinear optics is enormous and very diverse. There is increasing interest in polarization effects in nonlinear optics and spectroscopy as evidenced by the number of research publications and the numerous exciting results produced in material science, chemistry, biology, and physics. However, since this work is concerned with single mode fibers (fibers that support only one transverse mode), the discussion to

follow will present a short historical review of research crucial for the development and understanding of the subject of this thesis.

Long before the advent of lasers, Wawilov and Lewshin in 1926 reported the observation of the first nonlinear optical effect of departure from the Beer-Lambert absorption law with light of high intensity. In 1950, twenty four years later, Wawilov suggested that nonlinear polarization effects should be seen in birefringence, dichroism and polarization rotatory power [13]. In 1964, Maker, Terhune and Savage demonstrated the self-interaction of a plane wave in a nonlinear isotropic medium and observed that for elliptically polarized light, the major axis of the ellipse rotates as a function of propagation length and that a nonlinear cubic crystal can exhibit an induced birefringence proportional to the light intensity [24]. This work stimulated further study of other nonlinear polarization phenomena such as nonlinear optical activity which was first predicted and described by Akhmanov and Zharikov in 1967 [25]. In this paper, they indicated that in a dichoric, gyrotropic, isotropic, nonlinear medium, there takes place a rotation of an initially linearly polarized incident wave that is proportional to the intensity of the light. In this case, light initially linearly polarized will become elliptically polarized with ellipticity increasing with intensity. Several papers [13] have provided theoretical analyses of the wave picture and of the different mechanisms of this effect. Nonlinear optical activity has also been intensively studied experimentally [80]. All of these authors studied the polarization dynamics using a straightforward method of calculating how the electric field varies as the wave propagates along the medium. In such an approach, an understanding of how the polarization evolves as the beam propagates is not immediately obvious from the complex slowly varying electric field amplitude approximation. However, several other authors use an alternative approach of the dynamical equation for Stokes parameters to describe the polarization changes of a wave propagating in a nonlinear medium. The use of Stokes parameters has an advantage of providing a rather straightforward analytical definition of different polarization states of light. Sala [26] and Gregori and Wabnitz [27] used Stokes parameters in studying the propagation of a plane

wave through a nonlinear medium in the presence of dc-field-induced birefringence. Tratnik and Sipe also considered the polarization dynamics of a pulse propagating through an arbitrary nonlinear medium using the full $SO(3)$ covariance of the Stokes parameters [28].

Analysis on polarization effects of isotropic media was also extended to optical fibers. Winful obtained exact solutions for the intensity dependent polarization state of a light wave in a birefringent optical fiber [29] and Daino et al analysed the evolution of the state of polarization along a nonlinear single-mode birefringent fiber using Stokes parameters and gave exact solutions by means of a Poincaré sphere representation. Other effects such as polarization instabilities [8 – 11, 30] and intensity discrimination in straight [12] and twisted [9, 29] birefringent optical fibers have been reported. In 1986, the polarization instability in a birefringent optical fiber was experimentally observed [10]. The nonlinear propagation of light pulse in optical fiber has been investigated both classically and quantum mechanically [31]. All of these studies have made immense contribution to the understanding of the concepts on polarization dynamics in materials of cubic nonlinearities.

A short review of research on polarization phenomena in linear optics is presented here for completeness. Two texts [15, 17] from a number of specialized books [16, 81] devoted to the description of light polarization in linear optics were referred to during this investigation. However, since this work deals specifically with fibers, much of the reference materials used to establish the concepts and develop the principles emanated from review articles. The analytical approach used in this work is based mainly on the unified formalism for polarization optics developed by Brown and Bak in 1995. The formalism utilized the Stokes-Mueller matrix equation with the Lorentz group to provide a framework for understanding complicated polarization phenomena in optical fibers. The formalism was applied successfully to modeling deterministic polarization phenomena occurring in a twisted single-mode fiber sensor helically wound around a vibrating cylindrical shell [32]. The formalism has also been applied to a nonuniform-core single mode

fiber [33]. The elegance of this formalism stems from the method used to deduce the matrix form that makes the analytical approach more transparent in knowing the nature of the effects on the polarization vector. The formalism also incorporates other popular approaches (namely, the Jones calculus, the Mueller calculus, and the coherency matrix approach) into a single unified formalism. Several other papers [34 – 55] were helpful in the development of the analysis for this investigation.

2.2 Concepts and Definitions

This section presents the concepts and underlying assumptions and defines the terminologies used in this thesis to avoid ambiguity and confusion.

The conventional single mode optical fibers may be considered as a cylindrical dielectric waveguide that consists of an inner core of radius smaller than the surrounding cladding. This geometry of the fiber allows a suitable use of the cylindrical coordinate system (r, ϕ, z) for a simplified analysis of the propagating fields along the z axis which coincides with the fiber's axis of symmetry. The dielectric cylinder which models the fiber permits total internal reflection at the cylindrical boundary with the cladding resulting in a standing wave across the core and a decaying field in the cladding [56].

A birefringent single mode fiber is one that propagates a fundamental mode with two distinct orthogonal polarizations at different speeds owing to the difference of refractive index for waves polarized along orthogonal directions, say x - and y - Cartesian coordinates axes, respectively. If the birefringence is very high the fibers are referred to as polarization maintaining fibers because they become capable of preserving the state of linear polarization over relatively long lengths. This polarization holding ability is derived from the high intrinsic birefringence introduced by core asymmetry or by applying an asymmetric stress distribution on the core. In the limit of zero intrinsic birefringence, the dominant mode of a conventional single mode fiber is composed of two degenerate

eigenmodes with equal propagation velocities. However, the high intrinsic birefringence of polarization preserving fibers removes the degeneracy of the two orthogonal components of the fundamental mode resulting in the two distinct eigenmodes with different propagation velocities.

A waveguide mode is a coherent distribution of light that is localized in the vicinity of the core by total internal reflection and that propagates along the fiber with a well-defined phase velocity. For a given waveguide mode, the electric and magnetic fields are given by

$$E(r, \phi, z, t) = \mathbf{E}(r, \phi) \exp[i(k_z z - \omega t)] \quad (2.1)$$

and

$$H(r, \phi, z, t) = \mathbf{H}(r, \phi) \exp[i(k_z z - \omega t)] \quad (2.2)$$

where ω is the radian frequency and k_z is the axial phase constant.

The fundamental mode supported by the fiber is called HE_{11} or LP_{01} modes [56]. More discussions on this dominant mode of the fiber will be presented in a later section.

The theory in this thesis, like in all electromagnetic field theory, begins with the use of Maxwell's equations to describe the fields propagating in the fiber. Generally, the number of variables in Maxwell's equations is greater than the number of equations, and therefore these equations alone are not sufficient for describing light propagation in a medium. There is a need for an additional relationship between the optical response of the medium and the wave fields. This additional relationship accounts for the material properties of the medium and could have the general form $\mathbf{P} = \mathbf{P}(\mathbf{E}, \mathbf{H})$. However, this relation reduces to the following functional for an optical fiber:

$$\mathbf{P} = \mathbf{P}(\mathbf{E}) \quad (2.3)$$

since the fiber is a nonmagnetic material. Such equations are referred to as constitutive equations. \mathbf{P} is the polarization response of the fiber. The polarization is induced in the fiber and is responsible for coupling the light to the fiber. The polarization acts as a

source term in Maxwell's wave equations. Solutions of the wave equations are obtained in terms of the propagating fields.

Also, the form of Maxwell's equations further simplifies since the fiber is a dielectric. There are no excess charges and external currents flowing in the fiber. Thus, terms representing the electric current and charge densities in Maxwell's equations are suppressed.

The specific form of the constitutive equations for linear and nonlinear optical response of the fiber are usually expressed in terms of susceptibility tensors. The susceptibility tensors relate components of the induced polarization vector to various components of the optical field vectors and have symmetry properties of the medium. As a result, they restrict the combinations of vector components of the various optical fields that can be used effectively. In some situations, the tensor properties are important only in determining which combinations of vector component can be used for the optical fields and the induced polarizations, and beyond that the optical susceptibilities can be treated as scalars. However, in this thesis which concern situations involving nonlinear optical processes that change the polarization vector of the optical wave, the tensor properties play a central role in the nonlinear interaction. The magnitudes of the susceptibilities are usually determined by measurement and in some cases calculated using various theories. They can also be estimated with varying degree of accuracy from products of the refractive indices at the various wavelengths involved [45]. Thus, the susceptibility characterizes and describes all the properties of the fiber and its knowledge permits one to know the linear and nonlinear response of the fiber.

The relation in Eq.(2.3) indicates implicitly that the induced polarization \mathbf{P} depends on space coordinates and on time. As such, Eq.(2.3) must obey the causality principle [13]. That is, at any given moment, the value of \mathbf{P} is determined by current and preceding values of the propagating fields but not by future excitations. It is this retrospective relationship between \mathbf{P} and \mathbf{E} that leads to the optical response dependence on the frequency of the wave. Similarly, the optical response is not necessarily local and therefore could depend on excitations not only at the point of observation but also

on the surrounding vicinity at earlier moments. Such nonlocality leads to the optical response dependence on the wave vector of the propagating light. This is the well-known phenomena of spatial dispersion.

In addition, for intense fields, the relationship between \mathbf{P} and \mathbf{E} could be such that an increase in the magnitude of \mathbf{E} results in a nonlinear change in \mathbf{P} . In such cases, a nonlinear constitutive equation becomes appropriate for the description of these optical effects, which are ultimately a matter of primary concern in this thesis.

It is worth noting that in linear optics, $\mathbf{P} \propto \mathbf{E}$, whereas in nonlinear optics, $\mathbf{P} \propto \mathbf{E}^n$, where $\{n \in \mathbb{Z} : n \geq 2\}$ where \mathbb{Z} is an integer. The upper index n , which is not necessarily an exponent since these are vector quantities, represent the order of the induced polarization with respect to the electric field strength. The higher order terms are assumed smaller than the preceding lower order terms so that the polarization response can be expressed mathematically as a series

$$\mathbf{P} = \epsilon_0 \left[\Psi^{(1)} \mathbf{E} + \Psi^{(2)} \mathbf{E}\mathbf{E} + \Psi^{(3)} \mathbf{E}\mathbf{E}\mathbf{E} + \dots \right] \quad (2.4)$$

where $\Psi^{(n)}$ is referred to as the response function related to the local and nonlocal susceptibility tensors of the medium. $\Psi^{(1)}$, $\Psi^{(2)}$, and $\Psi^{(3)}$ are respectively first, second, and third order response functions. ϵ_0 is the permittivity of free space and serves as the constant of proportionality. The first term on the right-hand side of Eq.(2.4) describes the linear optical response.

2.2.1 Constitutive Equations: The Linear Case

In this thesis, the fiber is assumed to respond instantaneously to an applied field so that dispersion is not a critical factor in the analysis. Furthermore, with this assumption, the polarization response of the fiber can be written as a convolution of the response

function

$$P_i^{(1)}(\mathbf{r}, t) = \sum_j \int_V d\mathbf{r}_1 \int_{-\infty}^t dt_1 \Psi_{ij}^{(1)}(\mathbf{r} - \mathbf{r}_1; t - t_1) E_j(\mathbf{r}_1, t_1) \quad (2.5)$$

In addition, the integral in Eq.(2.5) accounts for the nonlocality and causality of the fiber linear response to the input field. $\Psi_{ij}^{(1)}(\mathbf{r} - \mathbf{r}_1; t - t_1)$ which is a tensor of rank two describes the optical response at point \mathbf{r} and time t resulting from the electric field at a point \mathbf{r}_1 at an earlier time t_1 . The optical property of the fiber like any other medium depends crucially on how the function $\Psi_{ij}^{(1)}(\mathbf{r} - \mathbf{r}_1; t - t_1)$ depends on $\boldsymbol{\rho} = \mathbf{r} - \mathbf{r}_1$ and $\tau = t - t_1$. For example, if the response of the fiber at a particular location only depends on excitation at that location, the function $\Psi_{ij}^{(1)}(\boldsymbol{\rho}, \tau)$ is nonzero only at $\boldsymbol{\rho} = 0$, and the medium is said to have a local optical response. The indices i and j represent components of the fields in an arbitrary reference coordinate system.

It is further assumed that the light is strictly monochromatic. Then, with help of Fourier Transform, the electromagnetic wave of frequency ω can be written in terms of its spectral amplitude as $\mathbf{E}(\omega, \mathbf{r})$ and the corresponding optical response as $\mathbf{P}^{(1)}(\omega, \mathbf{r})$ in frequency domain as

$$\mathbf{E}(\mathbf{r}, t) = \mathbf{E}(\omega, \mathbf{r}) \exp(-i\omega t) + c.c. \quad (2.6)$$

and

$$\mathbf{P}^{(1)}(\mathbf{r}, t) = \mathbf{P}^{(1)}(\omega, \mathbf{r}) \exp(-i\omega t) + c.c. \quad (2.7)$$

so that Eq.(2.5) can be written as

$$P_i^{(1)}(\omega, \mathbf{r}) = \sum_j \int_V d\boldsymbol{\rho} \int_0^\infty d\tau \Psi_{ij}^{(1)}(\boldsymbol{\rho}, \tau) e^{i\omega\tau} E_j(\omega, \mathbf{r} - \boldsymbol{\rho}) \quad (2.8)$$

The notation *c.c.* indicates complex conjugate. The electric field can be expanded in Taylor Series about \mathbf{r} as follows

$$\mathbf{E}(\omega, \mathbf{r} - \boldsymbol{\rho}) = \mathbf{E}(\omega, \mathbf{r}) + \frac{\partial \mathbf{E}(\omega, \mathbf{r})}{\partial \mathbf{r}} \cdot (-\boldsymbol{\rho}) + \sum_i \sum_k \frac{\partial^2 \mathbf{E}(\omega, \mathbf{r})}{\partial r_i \partial r_k} (\rho_i \rho_k) + \dots \quad (2.9)$$

This expansion is necessary because $\Psi_{ij}^{(1)}(\mathbf{r} - \mathbf{r}_1; t - t_1)$ will normally have a maximum at $\rho = 0$ that is when $\mathbf{r} = \mathbf{r}_1$. The first term on the right-hand side of Eq.(2.9) is called the local approximation, the second is the first-order spatial dispersion approximation and the third are second-order spatial dispersion effects. In this work, second order effects will be neglected since the field amplitude is assumed to be a slowly varying function of r so that $\frac{\partial^2 \mathbf{E}(\omega, \mathbf{r})}{\partial r_i \partial r_k} \rho_i \rho_k \ll \frac{\partial \mathbf{E}(\omega, \mathbf{r})}{\partial r}(\rho)$. This approximation is suitable for the nonlinear consideration in this work since solitonic effects will not be considered. In expansion 2.9, i and k are dummy indices.

After substituting expansion (2.9) into Eq. (2.8) yields the following linear constitutive equation

$$P_i^1(\omega, \mathbf{r}) = \frac{1}{4\pi} \sum_j \chi_{ij}^{(1)}(\omega) E_j(\omega, \mathbf{r}) + \frac{1}{4\pi} \sum_j \sum_m \Gamma_{ijm}^{(1)}(\omega) \frac{\partial E_j(\omega, \mathbf{r})}{\partial r_m} \quad (2.10)$$

where

$$\chi_{ij}^{(1)}(\omega) = 4\pi \int_V d\rho \int_0^\infty d\tau \Psi_{ij}^{(1)}(\rho, \tau) e^{i\omega\tau} \quad (2.11)$$

is the material local susceptibility tensor and

$$\Gamma_{ijm}^{(1)}(\omega) = -4\pi \int_V d\rho \left[\rho_m \int_0^\infty d\tau \Psi_{ij}^{(1)}(\rho, \tau) e^{i\omega\tau} \right] \quad (2.12)$$

is the material nonlocality susceptibility tensor. It is worth noting that the local susceptibility can also be expressed in terms of the dielectric tensor as

$$\chi_{ij}^{(1)}(\omega) = \epsilon_{ij}(\omega) - \delta_{ij} \quad (2.13)$$

where δ_{ij} is the Kronecker delta symbol and $\epsilon_{ij}(\omega)$ is the material dielectric tensor. Henceforth, Einstein's summation convention for tensors, that is addition is done over repeated coordinate indices, will be used. Eq.(2.10) can then be written in a condensed

form as follows

$$P_i^1(\omega, \mathbf{r}) = \frac{1}{4\pi} \left\{ \chi_{ij}^{(1)}(\omega) E_j(\omega, \mathbf{r}) + \Gamma_{ijm}^{(1)}(\omega) \nabla_m E_j(\omega, \mathbf{r}) \right\} \quad (2.14)$$

or, in time domain as

$$P_i^1(\mathbf{r}, t) = \frac{1}{4\pi} \left\{ \chi_{ij}^{(1)}(\omega) E_j(\mathbf{r}, t) + \Gamma_{ijm}^{(1)}(\omega) \nabla_m E_j(\mathbf{r}, t) \right\} e^{-i\omega t} + c.c. \quad (2.15)$$

In equations (2.14) and (2.15), the symbol $\nabla = \partial/\partial r_m$ is the gradient operator.

An electromagnetic wave propagating with wave vector \mathbf{k} has a spectral amplitude $\mathbf{E}(\omega, \mathbf{r})$ that depends harmonically on the coordinate \mathbf{r} such that $\mathbf{E}(\omega, \mathbf{r}) = \mathbf{A} \exp\{i\mathbf{k} \cdot \mathbf{r}\}$. Then Eq.(2.14) takes the form

$$P_i^1(\omega, \mathbf{r}) = \frac{1}{4\pi} \left\{ \chi_{ij}^{(1)}(\omega) + ik_m \Gamma_{ijm}^{(1)}(\omega) \right\} A_j e^{i(\mathbf{k} \cdot \mathbf{r})} \quad (2.16)$$

The above constitutive equation (2.16), will be used widely in this thesis.

2.2.2 Constitutive Equations: The Nonlinear Case

The constitutive equations to describe nonlinear optical effects in a fiber are in terms of higher order expressions in the electric field strength of the propagating wave as indicated in Eq.(2.4). When the principles of causality and nonlocality are accounted for in a medium, the following equations are obtained:

$$P_i^2(\mathbf{r}, t) = \int_V d\rho_1 \int_V d\rho_2 \int_0^\infty d\tau_1 \int_0^\infty d\tau_2 \Psi_{ijk}^{(2)}(\rho_1, \tau_1; \rho_2, \tau_2) \times E_j(\mathbf{r} - \rho_1, t - \tau_1) E_k(\mathbf{r} - \rho_2, t - \tau_2) \quad (2.17)$$

Similarly, the third-order optical response, cubic in the electric field strength is given by

$$P_i^3(\omega, \mathbf{r}) = \sum_{p,q,r} \left\{ \begin{array}{l} \chi_{ijkl}^{(3)}(\omega_p + \omega_q + \omega_r; \omega_p, \omega_q, \omega_r) E_j(\omega_p, \mathbf{r}) E_k(\omega_q, \mathbf{r}) E_l(\omega_r, \mathbf{r}) \\ \Gamma_{ijklm}^{(3)}(\omega_p + \omega_q + \omega_r; \omega_p, \omega_q, \omega_r) + E_k(\omega_q, \mathbf{r}) E_l(\omega_r, \mathbf{r}) \nabla_m E_j(\omega_p, \mathbf{r}) \end{array} \right\} \quad (2.23)$$

where the third order local and nonlocal susceptibility tensors are given by

$$\chi_{ijkl}^{(3)}(\omega_p + \omega_q + \omega_r; \omega_p, \omega_q, \omega_r) = \left\{ \begin{array}{l} \int_V d\rho_1 \int_V d\rho_2 \int_V d\rho_3 \int_0^\infty d\tau_1 \int_0^\infty d\tau_2 \int_0^\infty d\tau_3 \\ \times \Psi_{ijkl}^{(3)}(\rho_1, \tau_1; \rho_2, \tau_2; \rho_3, \tau_3) \exp i(\omega_p \tau_1 + \omega_q \tau_2 + \omega_r \tau_3) \end{array} \right\} \quad (2.24)$$

and

$$\Gamma_{ijklm}^{(3)}(\omega_p + \omega_q + \omega_r; \omega_p, \omega_q, \omega_r) = \left\{ \begin{array}{l} -3 \int_V d\rho_1 \rho_{1n} \int_V d\rho_2 \int_V d\rho_3 \int_0^\infty d\tau_1 \int_0^\infty d\tau_2 \int_0^\infty d\tau_3 \\ \times \Psi_{ijkl}^{(3)}(\rho_1, \tau_1; \rho_2, \tau_2; \rho_3, \tau_3) \exp i(\omega_p \tau_1 + \omega_q \tau_2 + \omega_r \tau_3) \end{array} \right\} \quad (2.25)$$

The forms of the constitutive equations dictate some restraints on the susceptibility tensors. In addition, symmetry conditions of the medium also impose severe restrictions on the susceptibility tensors. These restrictions often result in relations between the susceptibility tensor components that can simplify the analysis of the optical effects of the medium under consideration. Knowledge of the symmetries aids in applying the constitutive relations correctly. It is desirable therefore, to identify the symmetries of the susceptibilities.

2.2.3 Symmetry Conditions for Susceptibility Tensors

General features of the optical response of a fiber can be analysed using the structure of the constitutive equations and the symmetry of the susceptibility tensors. This allows the symmetries of a medium such as an optical fiber to be related to the symmetries of the equation of motion describing the fields.

Symmetry occurs naturally because of regularity in nature. The conditions that a medium imposes on the observability of optical effects may be formulated as requirement on the optical susceptibility tensors. The lower the symmetry of a crystal, the wider the range of optical and nonlinear effects that can be observed. In a media with high symmetry, many optical effects are forbidden. Usually, the symmetry of a medium forces some elements of the susceptibility tensors to be zero and sets up relationships between others. The higher the symmetry of a medium, the smaller the number of nonzero elements and the more relationships there are between elements.

Before proceeding further, it is important to indicate that Eq.(2.20) and Eq.(2.23) are the most general forms of relations between an optical excitation and the response functions which are written in terms of optical susceptibilities. Henceforth, considerations will be given to important cases that specify light propagation in a fiber.

Reality Condition

The electric fields that propagate along a fiber have intensities that are real and the induced polarization fields are also physically measurable quantities. Thus, this imposes the following symmetry restrictions known as the reality condition or Hermiticity on the susceptibility tensors:

$$[\chi_{ij}^{(1)}(\omega)]^* = \chi_{ij}^{(1)}(-\omega) \quad (2.26)$$

and

$$[\Gamma_{ijm}^{(1)}(\omega)]^* = \Gamma_{ijm}^{(1)}(-\omega) \quad (2.27)$$

for the first order local and nonlocal linear responses. The relation which exist for second order local and nonlocal nonlinear responses are

$$[\chi_{ijk}^{(2)}(\omega_p + \omega_q; \omega_p, \omega_q)]^* = \chi_{ijk}^{(2)}(-\omega_p - \omega_q; -\omega_p, -\omega_q) \quad (2.28)$$

and

$$[\Gamma_{ijklm}^{(2)}(\omega_p + \omega_q; \omega_p, \omega_q)]^* = \Gamma_{ijklm}^{(2)}(-\omega_p - \omega_q; -\omega_p, -\omega_q) \quad (2.29)$$

and for the third order local and nonlocal nonlinear susceptibilities

$$[\chi_{ijkl}^{(3)}(\omega_p + \omega_q + \omega_r; \omega_p, \omega_q, \omega_r)]^* = \chi_{ijkl}^{(3)}(-\omega_p - \omega_q - \omega_r; -\omega_p, -\omega_q - \omega_r) \quad (2.30a)$$

and

$$[\Gamma_{ijklm}^{(3)}(\omega_p + \omega_q + \omega_r; \omega_p, \omega_q, \omega_r)]^* = \Gamma_{ijklm}^{(3)}(-\omega_p - \omega_q - \omega_r; -\omega_p, -\omega_q, -\omega_r) \quad (2.31)$$

The asterick symbol (*) in the above expressions indicates complex conjugation. Thus, the reality condition may be reasoned as follows: that simultaneous reversal of the signs of frequency arguments is equivalent to complex conjugation of the susceptibility tensors. It should also be observed that the reality condition permits negative frequencies.

Inversion Symmetry

An inversion is simply a reflection about the origin of a reference coordinate system. Polar vectors change sign upon inversion, that is, $\mathbf{E} = -\mathbf{E}$, $\mathbf{P} = -\mathbf{P}$, and $\mathbf{r} = -\mathbf{r}$. Tensors transform in the same manner as product of the coordinates. For example, $\chi_{xxy}^{(2)}$ upon inversion becomes $\chi_{(-x)(-x)(-y)}^{(2)} = -\chi_{xxy}^{(2)}$. A typical example for $\chi_{xyzx}^{(3)}$ upon inversion is $\chi_{(-x)(-y)(-z)(-x)}^{(3)} = \chi_{xyzx}^{(3)}$. Thus $\chi_{xyzx}^{(3)}$ is invariant under inversion. If a material is invariant under inversion symmetry it is called centrosymmetric. Furthermore, it can be shown that even-order susceptibility tensors are zero in centrosymmetric materials. Fused SiO₂ which is used to make optical fibers is a centrosymmetric crystal. Therefore, second order susceptibilities are henceforth neglected in this work.

Intrinsic Permutation Symmetry

This symmetry condition requires that simultaneous permutation of frequencies in the argument of the local susceptibility should not alter the optical response. This can be deduced from Eq.(2.23). The local response must be clearly independent of the order in which the spectral components $E_j(\omega_p, \mathbf{r})$, $E_k(\omega_q, \mathbf{r})$ and $E_l(\omega_r, \mathbf{r})$ appear in the equation. Therefore, the local third-order susceptibility does not change under a simultaneous permutation of the Cartesian indices j , k , and l . In other words, the indices except the first, can be interchanged if the corresponding frequencies are also interchanged. For example,

$$\begin{aligned} \chi_{ijkl}^{(3)}(\omega_p + \omega_q + \omega_r; \omega_p, \omega_q, \omega_r) &= \chi_{ikjl}^{(3)}(\omega_p + \omega_q + \omega_r; \omega_q, \omega_p, \omega_r) \\ &= \chi_{iljk}^{(3)}(\omega_p + \omega_q + \omega_r; \omega_r, \omega_p, \omega_q) \\ &= \chi_{ijlk}^{(3)}(\omega_p + \omega_q + \omega_r; \omega_p, \omega_r, \omega_q) \end{aligned} \quad (2.32)$$

If nonlocality is considered, the optical response depends not only on the spectral components of the fields but also on their gradients. The spectral component that is acted on by the gradient operator is distinguishable from other fields and is consequently not permutable with the other spectral components of the field. Therefore, the nonlocal contribution to the optical response is independent only of the order of the spectral components of the electric field having indices k and l in Eq.(2.23). Thus,

$$\Gamma_{ijklm}^{(3)}(\omega_p + \omega_q + \omega_r; \omega_p, \omega_q, \omega_r) = \Gamma_{ijlkm}^{(3)}(\omega_p + \omega_q + \omega_r; \omega_p, \omega_r, \omega_q) \quad (2.33)$$

It is important to note that this symmetry condition is not appropriate for first order susceptibility tensors because they depend on only one frequency.

Full Permutation Symmetry

The full permutation symmetry is an additional frequency permutation relation which may be deduced from energy conservation laws. It is applicable to absorption-less media in which the overall loss of energy of the propagating waves is negligible at optical frequencies far from resonance. In this case, one can interchange all the indices of the susceptibility tensors if the corresponding frequencies are also interchanged.

In order to fully understand the full permutation relation for $\chi_{ij}^{(1)}(\omega)$, it is important at this stage to introduce some of its properties. $\chi_{ij}^{(1)}(\omega)$ is a symmetric tensor of rank two and thus have nine elements which can be represented by a 3×3 matrix. In general, $\chi_{ij}^{(1)}(\omega)$ is complex with its imaginary part related to the absorption. If there is no absorption, then $\chi_{ij}^{(1)}(\omega)$ has real components implying that the matrix must be Hermitian. Therefore, for the first order local susceptibility, the following permutation relations hold

$$\chi_{ij}^{(1)}(\omega) = [\chi_{ji}^{(1)}(\omega)]^* \quad (2.34)$$

In the case of the first order nonlocal susceptibility $\Gamma_{ijm}^{(1)}(\omega)$, it is an antisymmetric tensor also of rank two with imaginary part related to absorption. Hence,

$$\Gamma_{ijm}^{(1)}(\omega) = -[\Gamma_{jim}^{(1)}(\omega)]^* \quad (2.35)$$

The absence of absorption imposes the following restraints on the cubic susceptibilities

$$\begin{aligned} \chi_{ijkl}^{(3)}(\omega_p + \omega_q + \omega_r; \omega_p, \omega_q, \omega_r) &= \chi_{jilk}^{(3)}(-\omega_p; -\omega_p - \omega_q - \omega_r, \omega_r, \omega_q) \\ &= \chi_{lijk}^{(3)}(-\omega_r; -\omega_p - \omega_q - \omega_r, \omega_p, \omega_q) \end{aligned} \quad (2.36)$$

and

$$\begin{aligned} & \Gamma_{ijklm}^{(3)}(\omega_p + \omega_q + \omega_r; \omega_p, \omega_q, \omega_r) + \Gamma_{jklim}^{(3)}(-\omega_p; \omega_q, \omega_r, -\omega_p - \omega_q - \omega_r) \quad (2.37) \\ & + \Gamma_{klijm}^{(3)}(-\omega_q; \omega_r, -\omega_p - \omega_q - \omega_r, \omega_p) + \Gamma_{lijkm}^{(3)}(-\omega_r; -\omega_p - \omega_q - \omega_r, \omega_p, \omega_q) \\ & = 0 \end{aligned}$$

Kleinman's Symmetry

This symmetry requirement holds for media that are dispersionless and lossless at all frequencies. In this case, one can interchange all indices without regard to the frequencies. That is, permutation of susceptibility indices are allowed without regard to the order of the frequencies. This implies that the susceptibility is independent of frequencies. This is possible under low frequency excitation, when the system is assumed to respond instantaneously to the applied field. For example,

$$\begin{aligned} \chi_{ijkl}^{(3)}(\omega_p + \omega_q + \omega_r; \omega_p, \omega_q, \omega_r) &= \chi_{klji}^{(3)}(\omega_p + \omega_q + \omega_r; \omega_p, \omega_q, \omega_r) \quad (2.38) \\ &= \chi_{ljik}^{(3)}(\omega_p + \omega_q + \omega_r; \omega_p, \omega_q, \omega_r) \end{aligned}$$

All of the above arguments have shown that the medium symmetry imposes a very serious restraint on the symmetry of the optical response.

2.2.4 Constitutive Equations for Optical Effects in a Single Mode Fiber

Suppose an electromagnetic wave of frequency ω propagates along a single mode fiber. Then, the optical response of the fiber can be expressed in terms of first and third order susceptibilities given in equations (2.10) and (2.23). It has already been established that a fiber possesses inversion symmetry and thus second order susceptibilities are negligible. Accordingly, since negative frequencies are admitted in frequency domain, the electric field associated with the light wave at the frequency ω has two complex-conjugated spectral components related by the reality condition $\mathbf{E}(\omega, \mathbf{r}) = [\mathbf{E}(-\omega, \mathbf{r})]^*$. This implies that the summation in Eq.(2.23) is taken over $\omega_p = \pm\omega$, $\omega_q = \pm\omega$ and $\omega_r = \pm\omega$. As a result the sum in Eq.(2.23) will have eight terms and the polarization response has spectral components at frequencies $\pm 3\omega$ and $\pm\omega$. Thus

$$\begin{aligned}
 \mathbf{P}_i^{(3)}(\omega, \mathbf{r}) = & \chi_{ijkl}^{(3)}(3\omega; \omega, \omega, \omega) E_j(\omega, \mathbf{r}) E_k(\omega, \mathbf{r}) E_l(\omega, \mathbf{r}) \\
 & + \Gamma_{ijklm}^{(3)}(3\omega; \omega, \omega, \omega) E_k(\omega, \mathbf{r}) E_l(\omega, \mathbf{r}) \nabla_m E_j(\omega, \mathbf{r}) \\
 & + 3\chi_{ijkl}^{(3)}(\omega; \omega, \omega, -\omega) E_j(\omega, \mathbf{r}) E_k(\omega, \mathbf{r}) E_l^*(\omega, \mathbf{r}) \\
 & + 2\Gamma_{ijklm}^{(3)}(\omega; \omega, \omega, -\omega) E_k(\omega, \mathbf{r}) E_l^*(\omega, \mathbf{r}) \nabla_m E_j(\omega, \mathbf{r}) \\
 & + \Gamma_{ijklm}^{(3)}(\omega; -\omega, \omega, \omega) E_k(\omega, \mathbf{r}) E_l(\omega, \mathbf{r}) \nabla_m E_j^*(\omega, \mathbf{r})
 \end{aligned} \tag{2.39}$$

Clearly, the light wave at frequency ω generates in the fiber an optical response oscillating at the frequency of the third optical harmonic and at the frequency of the incident wave. From Eq.(2.39), the equation for the spectral component of the optical response at the operating frequency ω can be written as

$$\begin{aligned} \mathbf{P}_i^{(3)}(\omega, \mathbf{r}) = & +3\chi_{ijkl}^{(3)}(\omega; \omega, \omega, -\omega) E_j(\omega, \mathbf{r}) E_k(\omega, \mathbf{r}) E_l^*(\omega, \mathbf{r}) \\ & +2\Gamma_{ijklm}^{(3)}(\omega; \omega, \omega, -\omega) E_k(\omega, \mathbf{r}) E_l^*(\omega, \mathbf{r}) \nabla_m E_j(\omega, \mathbf{r}) \\ & +\Gamma_{ijklm}^{(3)}(\omega; -\omega, \omega, \omega) E_k(\omega, \mathbf{r}) E_l(\omega, \mathbf{r}) \nabla_m E_j^*(\omega, \mathbf{r}) \end{aligned} \quad (2.40)$$

To obtain equations (2.39) and (2.40), intrinsic permutation relations were applied. The constitutive equation (2.40) describes the optical response of the fiber at the incident frequency when the incident electric field has an arbitrary coordinate dependence. In particular, this equation is suitable when there are several light waves of the same frequency propagating in different directions. However, this thesis considers a single light wave of frequency ω propagating along the axis of the fiber. Therefore, in this case, the spectral fields which depend harmonically on the coordinate z can be simply expressed as $\mathbf{E}(\omega, z) = \mathbf{A} \exp(ik_z z)$ so that Eq.(2.40) can be rewritten as

$$\mathbf{P}_i^{(3)}(\omega, \mathbf{r}) = \begin{bmatrix} 3\chi_{ijkl}^{(3)}(\omega; \omega, \omega, -\omega) + 2ik_z \Gamma_{ijklz}^{(3)}(\omega; \omega, \omega, -\omega) \\ -\Gamma_{ilkjz}^{(3)}(\omega; -\omega, \omega, \omega) \end{bmatrix} A_j A_k A_l^* e^{ik_z z} \quad (2.41)$$

In Eq.(2.41), the optical response depends on A_j and A_k , which are symmetrical with respect to permutation of the indices j and k . Therefore, only the part of the tensor $\Gamma_{ijklz}^{(3)}(\omega; \omega, \omega, -\omega)$ which is symmetrical with respect to the interchange of j and k will contribute to the second term on the right hand side of Eq.(2.41). Thus, the valid constitutive equation (2.41) may be rewritten in terms of the spectral component of the optical response as follows

$$\mathbf{P}_i^{(3)}(\omega, \mathbf{r}) = \left[3\chi_{ijkl}^{(3)}(\omega; \omega, \omega, -\omega) + 2ik_z \Gamma_{ijklz}^{(3)}(\omega; \omega, \omega, -\omega) \right] A_j A_k A_l^* e^{ik_z z} \quad (2.42)$$

2.3 Characteristics of Single Mode Fibers

Single-mode optical-fiber cables have very splendid characteristics such as wide bandwidth that is possible for multiplexing in an electrical domain, the possibility of wavelength division multiplexing, and a very low loss profile. Other characteristics such as flexibility, strength or durability, light weight, and radiation hardness are key components in application requirement for fibers. Many network topologies have been developed for optical transmission because of the suitability of these characteristics. This section gives a brief review of some of the fibers characteristics relevant to this work.

2.3.1 Refractive Index Profile

A single mode optical fiber is formed through a process called modified chemical vapor deposition (MCVD) as a glass thread usually made of silica doped with desired combination of germanium and fluorine [63]. There exists other fabrication methods such as outside vapor deposition (OVD) [64], and vapor-phase axial deposition (VAD) [65]. The inner layer of the fiber which is referred to as the core has an index of refraction that is larger than that of the surrounding cladding. This configuration is necessary to allow for the propagating wave to be kept within a confined region of the fiber. The cladding is normally quite thick so that fields are attenuated rapidly as the distance from the core-cladding interface increases (except at cutoff).

A key quantity used in describing one of the properties of a single mode fiber is the parameter V given in terms of the core radius a , core index n_1 and cladding index n_2 as

$$V = ka\sqrt{n_1^2 - n_2^2} \quad (2.43)$$

where $k = \omega/c = 2\pi/\lambda$ is the propagation constant of the input optical field in vacuum. Thus, V is proportional to the operating frequency if the indices are not significantly frequency dependent. V is also proportional to the size of the core. The remaining factor in Eq.(2.43), which measures the difference between the refractive indices of core and cladding is called the numerical aperture and abbreviated NA .

$$NA = \sqrt{n_1^2 - n_2^2} \quad (2.44)$$

The parameter V determines which modes can propagate along the fiber and how tightly bound they are to the core. A reasonable number of modes can propagate if V is reasonably small. For example, the dominant mode operation of a single mode fiber requires that $V < 2.4$ [56]. Thus, to maintain a reasonably small V , the numerical aperture must be very small also and this requires that the core and cladding index of refraction be quite close to each other. Therefore, the core and cladding glasses must be dissimilar, yet have nearly the same refractive indices n_1 and n_2 . In practice, this is achieved by introducing different concentrations of dopants for the same original type of glass to achieve the required difference in indices.

Since $n_1 \approx n_2$, it is convenient to define the relative difference

$$\Delta = \frac{n_1 - n_2}{n_2} \quad (2.45)$$

Then the quantity that determines the numerical aperture can be approximated by

$$n_1^2 - n_2^2 = (n_1 + n_2)(n_1 - n_2) \approx 2n_2^2\Delta \quad (2.46)$$

so that provided Δ is small, Eq.(2.43) can be rewritten as

$$V = kan_2\sqrt{2\Delta} \quad (2.47)$$

Since V depends on the relative magnitude of the core radius and on the operating

wavelength of the field, its value could still remain relatively large because a typical fiber has core diameter that are many wavelengths in diameters. For example, a fiber designed for operation at $\lambda = 0.8\mu m$ with core diameter of $2a = 50\mu m$ will have the parameter $V \approx 200NA$. Even when the core index is about $\frac{1}{2}\%$ greater than the cladding index, that is $\Delta = 0.005$, the parameter $V \approx 30$ (which is still fairly large) for a fiber with refractive index 1.5. When V exceeds 2.4048, more than one mode can propagate and share the available power. Therefore, to achieve single-mode operation, the core diameter has to be of the order of a few micrometers so that the product ka in Eq.(2.47) becomes reasonably small. Such fibers have now been developed with core radius made small enough to maintain $V < 2.4$ even for reasonable differences of refractive indices of the core and cladding. For example, a single mode fiber designed for operation at $\lambda = 1.3\mu m$ may have a core diameter of $8\mu m$, while the cladding diameter, which should be at least an order of magnitude thicker than the core, may be the standard $125\mu m$. It may have a numerical aperture of about $NA = 0.115$, so that it remains single-mode down to about $\lambda = \pi(2a/V)NA = 1.2\mu m$.

Evidently, fibers in general can allow the propagation of many guided modes even when the core and cladding have refractive indices that are quite close to each other. These modes which have spatial distributions that are solutions of the two-dimensional Helmholtz equation

$$\nabla^2 E_z + \gamma^2 E_z = 0 \quad (2.48)$$

also satisfies appropriate boundary conditions at the core and cladding interface. In addition, a fiber can support a continuum of unguided radiation modes. These radiation modes do not play an important role in the discussion on nonlinear effects as long as the fiber is assumed to have a perfect cylindrical geometry. However, radiation modes are crucial in problems involving the transfer of power between bounded and radiation modes. In Eq.(2.48), E_z is the axial component of the electric field amplitude and

$$\gamma^2 = k^2 n^2 - \beta^2 \quad (2.49)$$

where β is the axial phase constant in the fiber and n is the refractive index for a fiber of core radius $r = a$ given by

$$n = \begin{cases} n_1 & r \leq a \\ n_2 & r > a \end{cases} \quad (2.50)$$

Eq.(2.49) is usually referred to as a dispersion relation. It should be noted that the same relation as in Eq.(2.48) holds for the magnetic component of the propagating wave. Because of the cylindrical symmetry of the fiber it is convenient to express the wave equation (2.48) in cylindrical coordinates to obtain second-order nonconstant-coefficient ordinary differential equation whose solutions are the celebrated Bessel functions. The Bessel function is oscillatory and vanishes at infinitely many discrete points ℓ . These nulls generally are not evenly spaced like the nulls of the sinusoids but are evenly spaced by π for large arguments.

It has already been shown above in this section that a single mode fiber has core index of refraction n_1 that should slightly exceed that for the cladding n_2 , to get bound modes. The core being dense translates mathematically into the fact that $\beta < kn_1$ and that the cladding is less dense is expressed by $\beta > kn_2$ [56]. Thus, the phase constant β should take some value $kn_2 < \beta < kn_1$ so that rapidly decaying fields may be expected in the cladding but not in the core.

Therefore, it is reasonable to define the terms p and q : since $\beta < kn_1$ in the core, the difference of squares of these parameters be p^2 while, for the cladding, since $\beta > kn_2$, the difference is to be $-q^2$ so that

$$k^2 n_1^2 = \beta^2 + p^2 \quad k^2 n_2^2 = \beta^2 - q^2 \quad (2.51)$$

After eliminating β from Eq.(2.51), it can be shown that

$$V^2 = p^2 a^2 + q^2 a^2 \quad (2.52)$$

2.3.2 Fiber Modes

The waves that propagate along the fiber can be entirely expressed in terms of the axial fields E_z and H_z but the waves do not separate completely into transverse electric and magnetic (TM and TE) modes as they do for conducting waveguides or dielectric slab waveguides. This is due mainly to the nature of the fiber boundary condition and to the curvature of the boundary. The curvature of the core-cladding interface, together with the field continuity condition at the interface has the effect of mixing the transverse modes into what are referred to as hybrid modes. These hybrid modes have electric and magnetic fields both of which have axial components. Both axial fields are needed to satisfy all the conditions at the core-cladding interface.

Because of the circular geometry, the standing wave in the core is not sinusoidal but has the form of an oscillatory Bessel function $J_\ell(pa)$ and the decaying fields in the cladding are not exponential but follow a modified Bessel function $K_\ell(qa)$. Applying boundary condition that the tangential components of \mathbf{E} and \mathbf{H} must be continuous across the core-cladding interface requires that axial and transverse components are the same when $r = a$ is approached from inside or outside the core. The equality of these field components at $r = a$ leads to a characteristic equation whose solutions determine the propagation constant β for the fiber modes. The characteristic equation which is well known in the literature [56] is expressed in terms of $J_\ell(pa)$, $K_\ell(pa)$ and their derivatives. It has in general several solutions for each integer value of ℓ . When graphed, the characteristic equation has a curve with many branches because $J_\ell(pa)$ is oscillatory. Also, Eq.(2.52) plots simply as a circle of radius V which is proportional to the operating frequency since the refractive indices are considered to be frequency independent. As such, each branch of a plot of the characteristic equation corresponds to a possible mode of propagation attainable if the frequency is high enough for an intersection with the circle of radius V

to occur. To plot the characteristic equation conveniently, recursion relations are used to eliminate the derivative of the Bessel functions from the characteristic equation. The intersection of the branches with a typical circle of radius $r = V$ gives the number of modes propagating in the fiber.

It is customary to express the solution to the characteristic equation by $\beta_{\ell m}$ where both ℓ and m take up integer values. Each eigenvalue $\beta_{\ell m}$ corresponds to one mode which a fiber can support. It is well known [56] that there are two types of fiber modes, designated as $HE_{\ell m}$ and $EH_{\ell m}$. When $\ell = 0$, these modes are analogous to the transverse electric (TE) and transverse magnetic (TM) fields of planar waveguides since the axial component of the electric field or magnetic field vanishes. However, when $\ell > 0$, the fiber modes are hybrid and all six components of the electromagnetic field are nonzero.

Clearly, the number of modes supported by a fiber at a given wavelength depends on the design parameters, namely the core radius and the core-cladding index difference. Another important parameter for each mode is its cut-off frequency below which no real value of the phase constant β can be found. The waveguide dispersion relation of Eq.(2.49) can be rewritten as

$$\omega^2 = \omega_c^2 + \beta^2 v^2 \quad (2.53)$$

indicating that the operating frequency ω must exceed the cut-off frequency ω_c in order for the mode to propagate with phase constant β . The phase velocity at frequency ω above cut-off frequency is $v = \omega/\beta = c/n$. To obtain Eq.(2.53), the important relation $\gamma = \omega_c/v$ was used. Below cut-off frequency, $\omega < \omega_c$ and β is no longer real since β^2 becomes negative. This corresponds to oscillation (at frequency ω) without propagation but with attenuation in the direction away from the source. The wave gets weaker as the distance from the source increases and it is then said to be an evanescent mode, or to be “cut off” when the frequency is below ω_c . The cut-off frequency is obtained by the condition $q = 0$. The value of p when $q = 0$ for a given mode determines the cut-off frequency. Thus, the cut-off points correspond to pa at $qa = 0$ and from these the cut-off frequency for each mode is $pa = V$ at cut-off. This is obtained using Eq.(2.52) when

$qa \rightarrow 0$. As operating frequency increases, more and more intersections with branches of the characteristic curve are possible. Those branches that lie above the level $pa = V$ can have no intersection with the circle of radius V and are thus cut off. For $\ell = 1$, however, there is one branch that reaches down to the origin of the qa - pa plane, and there is intersection with the circle no matter how small its radius. This branch thus has no cut-off frequency and is designated as the HE_{11} mode. All other modes have cut-off frequency. Two branches emanate from each nonzero null of the $J_1(pa)$ Bessel function on the pa -axis; the corresponding modes are denoted HE_{1m} and EH_{1m} . For $\ell > 1$, the branches for the $HE_{\ell m}$ and $EH_{\ell m}$ modes emanate from separate cut-off points on the pa -axis (the axis for $qa = 0$, at cut-off). For $\ell = 0$, the exceptional transverse modes exist for the m th branch designated as TE_{0m} and TM_{0m} . Therefore for spiraling waves, $\ell \neq 0$, the modes are hybrid, with both axial field components E_z and H_z nonzero, designated by $HE_{\ell m}$ and $EH_{\ell m}$. The lowest value of pa that permits transverse modes to propagate is $pa = J_{01} = 2.4048$ and V must exceed this value for these modes to be above cut-off frequency. The procedure to determine the different values of V at which different modes reach cut-off is rather complicated and have been treated in many texts [56].

Since this thesis is mainly interested in single-mode fibers, the discussion is limited to the cut-off condition that allows the fiber to support only one mode. A single mode fiber supports only the HE_{11} mode that is also referred to as the fundamental mode. All other modes are "cut off" if the parameter $V < V_c$, where V_c is the smallest solution of $J_0(V_c) = 0$ or $V_c = 2.405$. The actual value of V_c is a critical design parameter and practical fibers are designed such that V is close to V_c .

The fundamental mode HE_{11} with corresponding field distribution $\mathbf{E}(r, \theta, z, t)$ has three nonzero components expressed in polar coordinates as E_r, E_θ, E_z or in cartesian coordinates as E_x, E_y, E_z . Among these, either E_x or E_y dominates. Therefore, the fundamental fiber mode is linearly polarized in either x or y direction depending on which of E_x or E_y dominates. In this respect, it can be concluded that a single mode fiber is strictly not single mode because it can support two modes of orthogonal

polarizations. The notation LP_{mn} is sometimes used to denote linearly polarized modes. In this notation, the dominant fiber mode HE_{11} corresponds to LP_{01} .

Under ideal conditions, the two orthogonally polarized modes of a single-mode fiber have the same propagation constant and are therefore degenerate. In a real fiber, however, irregularities such as geometrical asymmetries in the core diameter along the length of the fiber break the degeneracy thereby resulting in the random mixing of the two polarization components causing the polarization of the incident light to scramble as it propagates down the fiber.

2.3.3 Fiber Losses

Among the transmission characteristics of optical fiber, the most important is the attenuation of the power transmitted by the fiber [57]. Fiber loss depends on the wavelength of the light. Fig.(2.1) shows the loss spectrum of a single mode fiber. The fiber exhibits a minimum loss of about $0.2dB/km$ near $1.55\mu m$. The loss is considerably higher at shorter wavelengths reaching a level of $1 - 10dB/km$ in the visible regions.

The bound modes of a fiber propagate with attenuation due to losses. The attenuation arises from intrinsic material properties and from waveguide properties. In high-silica glasses, which are widely used to manufacture low-loss single mode fibers, the attenuation sources are due to absorption and Rayleigh scattering. The absorption loss is composed mainly of ultraviolet (UV) and infrared (IR) absorption tails of pure silica. The basic absorption is due to the electronic absorption band edge of the silica host materials at ultraviolet wavelength region and the molecular absorption edge of the silica host and its dopant at the infrared region.

In addition, impurity ions can also contribute to the absorption bands. The usual impurities that lead to absorption effects in the wavelength range of interest are the

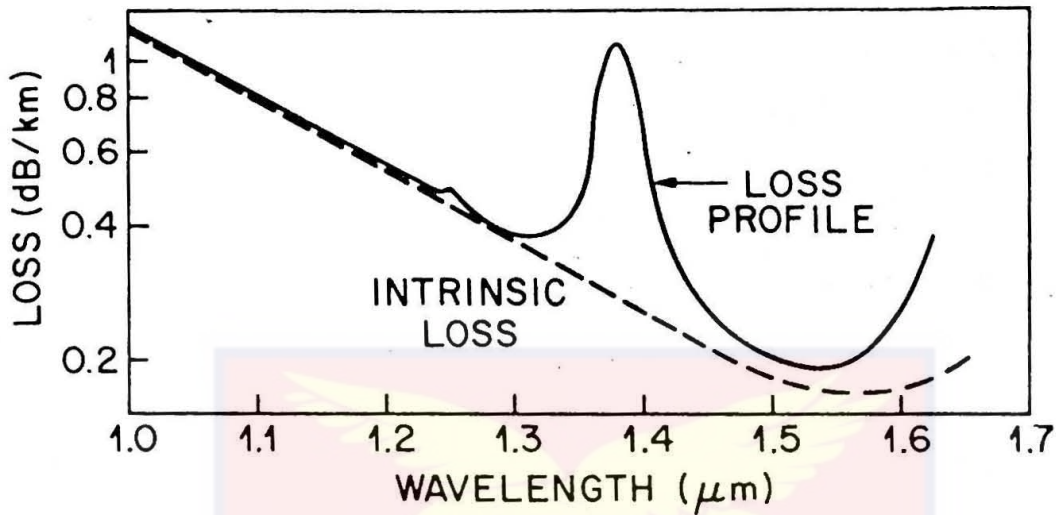


Figure 2-1: Measured loss profile of a single-mode fiber. Dashed curve represents the intrinsic loss profile resulting from Rayleigh scattering and absorption in pure silica (Ref.63).

sition metal ions (*Fe, Cu, Co, Mn*) and water in the form of the hydroxyl ion *OH*. The concentration of transition metals ions has been reduced to a negligible amount during the past decade. However, water thus remains practically the most important impurity affecting fiber losses. The ion has a fundamental vibrational absorption peak centered at $2.73\mu\text{m}$ which presents overtones responsible for the dominant peak in Fig.(2.1) near the $1.37\mu\text{m}$ and a smaller peak near the $1.23\mu\text{m}$. During the fabrication process, special precautions are taken through a very careful drying process to ensure an *OH*-impurity level of less than one part in hundred million.

The loss effects of dopants such as GeO_2 , P_2O_5 , *F*, and B_2O_3 which are incorporated into the silica to decrease the manufacturing temperature and to modify the refractive index profile have been studied. Early study has shown(57, 58) that GeO_2 has little effect on the *IR* absorption tail and more recently that care must be taken with fiber drawing temperature if a high GeO_2 content is used. The presence of P_2O_5 brings absorption peak at $3.8\mu\text{m}$ and $3.7\mu\text{m}$. It is also known that in obtaining ultra-low losses at $\lambda \geq 1.3\mu\text{m}$ requires that B_2O_3 not be present at radial distances smaller than five times the core

radius, and P_2O_5 should be kept out of the core.

The Rayleigh scattering loss which is due to microscopic inhomogeneities of material refractive index, varies as λ^{-4} and is dominant at short wavelengths. Rayleigh scattering is a fundamental loss mechanism arising from random density fluctuations frozen into the fused silica during manufacturing. Local fluctuations in the refractive index scatter the light in all directions. This loss is intrinsic to the fiber and sets the ultimate limit on the fiber loss. The intrinsic loss level is shown by a dashed line in Fig.(2-1). At $\lambda = 1.55\mu m$, the fiber loss is dominated by Rayleigh scattering.

Other factors that may contribute to losses due to fiber structure arise from power leakage, bending losses and boundary losses (scattering at the core-cladding boundary). The total loss of a fiber link in optical communication systems also includes splice loss that occurs at joints between fibers.

A measure of power loss during transmission of an optical signal inside the fiber can be expressed as

$$P_T = P_0 \exp(-\alpha L) \quad (2.54)$$

where α is the attenuation constant commonly referred to as fiber loss. P_0 is the initial power into the fiber of length L and P_T is the transmitted power. The fiber loss is customarily expressed in units of dB/km by using the relation [6]

$$\alpha_{dB} = -\frac{10}{L} \log \left(\frac{P_T}{P_0} \right) = 4.343\alpha \quad (2.55)$$

where the coefficient of α results from conversion of the logarithm of base 10 to the natural logarithm.

2.3.4 Dispersion in Single Mode Fibers

Fields propagating along an optical fiber are not only attenuated but also undergo some degree of distortion. Different frequency components in the spectrum of the signal are transmitted at different speeds and therefore arrive at the output at different times. The property of the fiber that makes different frequencies travel at different speeds is its dispersion

There are two major sources of dispersion in optical fibers. One is an inherent property of the glass and the other relates to the variety of waves that can travel along the fiber, each with its own speed of propagation. The former source of distortion can be mitigated by choosing a special operating frequency at which the inherent dispersion of the glass material is eliminated or minimized. The other cause for dispersive signal distortion can be dealt with by suitable design parameter.

An information-bearing signal is comprised of an entire spectrum of frequencies. How the spectrum is affected when the signal is conveyed is very important. If a fiber constitutive parameters μ , ϵ , and n are frequency dependent then the fiber is said to be dispersive. However, for narrow-band signals (i.e. slow modulation of a high-frequency carrier), the spectrum is confined to a relatively narrow range of frequencies and the information-bearing signals do not get distorted in a dispersive medium since they are transmitted at a speed different from that of any frequency component.

A practical light source is not precisely monochromatic and thus does not provide a pure single carrier frequency ω as it propagates along a media. When the light wave interacts with the bound electrons of a dielectric such as an optical fiber, the response of the fiber in general depends on the optical frequency. This property is referred to as chromatic dispersion and is manifested through the frequency dependence of the refractive index $n(\omega)$ and results in a spread of the propagating pulse. The origin of chromatic dispersion is related to the characteristic resonance frequencies at which a medium ab-

2.3.4 Dispersion in Single Mode Fibers

Fields propagating along an optical fiber are not only attenuated but also undergo some degree of distortion. Different frequency components in the spectrum of the signal are transmitted at different speeds and therefore arrive at the output at different times. The property of the fiber that makes different frequencies travel at different speeds is its dispersion

There are two major sources of dispersion in optical fibers. One is an inherent property of the glass and the other relates to the variety of waves that can travel along the fiber, each with its own speed of propagation. The former source of distortion can be mitigated by choosing a special operating frequency at which the inherent dispersion of the glass material is eliminated or minimized. The other cause for dispersive signal distortion can be dealt with by suitable design parameter.

An information-bearing signal is comprised of an entire spectrum of frequencies. How the spectrum is affected when the signal is conveyed is very important. If a fiber constitutive parameters μ , ϵ , and n are frequency dependent then the fiber is said to be dispersive. However, for narrow-band signals (i.e. slow modulation of a high-frequency carrier), the spectrum is confined to a relatively narrow range of frequencies and the information-bearing signals do not get distorted in a dispersive medium since they are transmitted at a speed different from that of any frequency component.

A practical light source is not precisely monochromatic and thus does not provide a pure single carrier frequency ω as it propagates along a media. When the light wave interacts with the bound electrons of a dielectric such as an optical fiber, the response of the fiber in general depends on the optical frequency. This property is referred to as chromatic dispersion and is manifested through the frequency dependence of the refractive index $n(\omega)$ and results in a spread of the propagating pulse. The origin of chromatic dispersion is related to the characteristic resonance frequencies at which a medium ab-

sorbs the electromagnetic radiation through oscillations of bound electrons. Even when nonlinear effects are not important, dispersion-induced pulse broadening can be detrimental for optical communication systems. In the nonlinear regime, the combination of dispersion and nonlinearity can result in the generation of special kinds of waves known as solitons that can propagate undistorted over long lengths of fiber.

The effects of fiber dispersion can be accounted for by expressing the propagation constant k in a Taylor series expansion about the center frequency ω_0 as follows:

$$k(\omega) = n(\omega) \frac{\omega}{c} = k_0 + (\omega - \omega_0) k'_{\omega=\omega_0} + \frac{1}{2} (\omega - \omega_0)^2 k''_{\omega=\omega_0} + \dots$$

where k' is related to the group velocity of the pulse envelope and k'' is the chromatic dispersion term responsible for pulse broadening. The primes indicate derivative with respect to ω . In silica glass, k'' vanishes at a wavelength of about $1.3\mu m$ and becomes negative for longer wavelength. This wavelength at which $k'' = 0$ is referred to as the zero-dispersion wavelength. However, it should be noted that operation at the zero-dispersion wavelength requires consideration of higher-order dispersive effects which can distort optical pulses both in the linear and nonlinear regimes [6]. In actual fibers, the zero-dispersion wavelength is shifted towards longer wavelengths because of the presence of dopants and because of fiber design parameters such as core radius and core-cladding index difference. This feature can be used to shift the zero-dispersion wavelength to the vicinity of $1.5\mu m$ where the fiber loss is a minimum. Such dispersion-shifted fibers [66] have applications in optical communications systems and are also useful for the study of many nonlinear effects whenever an experiment requires tailoring of the dispersion parameter.

2.4 Propagation in Single Mode Fibers - Coupled Mode Theory

The evolution of the fields along a fiber is analyzed using coupled-mode theory [39]. In a real single mode fiber, imperfections like bending, twisting, and squeezing all of which induce stress in the fiber and deformation in the core geometry would cause a split in the degeneracy of the phase velocity of the two modes. The two guided modes which contribute to this evolution are coupled due to the anisotropies resulting from these perturbations and imperfections which may be introduced either intentionally or randomly during the fabrication process. The effects of coupling are characterized by coupling coefficients which can be deduced from the details of the imperfections on the fiber.

Coupled-mode theory is a powerful method used to study changes in the propagation of light caused by perturbations of geometry or material properties. In this formalism, dielectric tensors represent the perturbations that change the polarization properties of the single mode fiber. The theory starts with the derivation of the coupled wave equations in terms of modes of an ideal waveguide. In this case, a “natural” frame has to be used to represent the basic modes of the unperturbed fiber and the dielectric tensor of the perturbation. Tang has shown [54] that there exists a “natural” frame in an unperturbed (isotropic) wave guide for an arbitrarily curved line in space, for which the solutions of the wave equation become orthogonal. This approach results in a simple expression for the coupling coefficients. The exact coupled mode theory for a real fiber is then applied to the problem of coupling between the simplified waveguide modes.

The coupled wave equations when integrated yield solutions describing the evolution of the transverse mode amplitudes. This evolution can be represented by a variety of graphic methods. Two useful representations are the Poincaré sphere [17, 67] and the phase plane [68, 69]. In particular, the Poincaré sphere representation provides a direct geometrical description of the evolution of polarization along a single mode fiber. The

birefringence effects on the fiber can be shown clearly from illustrations on the sphere. The phase plane representation also shows an evolution of the polarization state in a birefringent fiber

In subsequent chapters, the coupled mode theory is used to analyse the fields in a single mode fiber that is subjected to linear and nonlinear perturbative effects resulting from internal and external sources.



Chapter 3

POLARIZATION PHENOMENA IN SINGLE MODE OPTICAL FIBERS

3.1 Definition and Evolution of Polarization

Christian Huygen was the first to suggest that light was not a scalar quantity [15] and that the spatio-temporal fields of electromagnetic waves are vectors. The vectorial nature of light is called its polarization. Light consists of plane electromagnetic wave with their electric and magnetic field vectors perpendicular to the direction of propagation. If the direction of propagation is chosen to be the z-axis of a right-handed Cartesian coordinate frame, the optical field in free space is described by transverse components of its amplitudes and arbitrary phases.

Such a field can be considered a wave forming a narrow spectral band around the

central frequency ω expressed as

$$\mathbf{E}_{x,y}(z, t) = \mathbf{A}_{x,y}(z, t) e^{i(kz - \omega t)} + c.c. \quad (3.1)$$

The subscripts x and y refer to the field components in the X and Y directions. \mathbf{E}_x and \mathbf{E}_y are referred to as polarized or polarization components of the optical field. Here \mathbf{A} is the wave amplitude and k is the wave number. Such a wave represents a plane wave because its wavefront is seen as a plane to an observer facing the optical source; the vector \mathbf{E} oscillates in the XY plane perpendicular to the direction of propagation. Equation (3.1) suggests that anisotropy along the direction of propagation is small so that the wave remains generally transverse. The anisotropy results in different evolution rates for $A_x(z, t)$ and $A_y(z, t)$ with propagation distance z . This difference in the evolution rates of the field amplitudes results in a change in the light polarization state. It is assumed that for a wave with narrow spectral band, the amplitude changes insignificantly over the period of the wave [13]

$$\left| \frac{\partial A_{x,y}(z, t)}{\partial t} \right| \ll \omega |A_{x,y}(z, t)| \quad (3.2)$$

As the field propagates, the components $\mathbf{E}_x(z, t)$ and $\mathbf{E}_y(z, t)$ give rise to a resultant vector as this vector describes a locus of points in space over the distance of propagation.

If \mathbf{E}_x and \mathbf{E}_y oscillate in phase, so that the amplitude $A_x(z, t) = \alpha A_y(z, t)$ with α being a real constant, Eq.(3.1) represents the electric field of a linearly polarized light. An observer facing the source sees the oscillating vector tracing out a straight line in the XY plane. Thus, it is called linearly polarized. The wave vector \mathbf{k} and the vector \mathbf{E} are contained in a plane called the plane of polarization. If $A_y(z, t) = 0$, the \mathbf{E} vector oscillates along the X direction and is referred to as linearly polarized on axis. Also, if $A_x(z, t) = 0$, the wave will oscillate along the Y direction and is referred to as linearly polarized off axis. For the case where α is a complex number, there is a phase shift between \mathbf{E}_x and \mathbf{E}_y and the wave is said to have elliptical polarization. In this case,

an observer facing the wave source sees the end of the vector \mathbf{E} tracing an ellipse as it propagates. Light is considered circularly polarized when $\alpha = \pm i$ and an observer sees the vector \mathbf{E} trace out a circle. It is worth noting that linearly and circularly polarized light are specific cases of elliptical polarization. Circularly polarized light possess a sense of direction known as left-handed or right-handed. If $A_x(z, t) = i A_y(z, t)$, the wave is said to be left-handed circularly polarized (*LCP*) and an observer looking into the direction from which the light is advancing sees the end of the electric field vector trace out a circle in a counterclockwise direction. Furthermore, if $A_x(z, t) = -i A_y(z, t)$, the wave is right-handed circularly polarized (*RCP*) and an observer will see the end of the field vector trace out a circle in a clockwise direction. Right-handed elliptically polarized (*REP*) and left-handed elliptically (*LEP*) waves can be defined in a similar fashion.

The evolution of the polarization along single mode optical fibers under the influence of perturbations is next considered. The perturbations may be inherent resulting from imperfections and geometrical asymmetries of the fiber. External perturbations such as strains, twists and bends also lead to random variation in the polarization of the fields in the fiber. It is well known that under ideal conditions of perfect cylindrical geometry and isotropy, the fundamental fiber mode (HE_{11}) is doubly degenerate so that a mode excited with its polarization in one direction will not couple to the mode with the orthogonal polarization state. Thus, even a single mode fiber is not truly single mode since it can support two degenerate modes that are dominantly polarized in two orthogonal directions. In a real optical fiber, however, this degeneracy is split due to small departures from cylindrical geometry or small fluctuations in material anisotropy resulting in a mixing of the two polarization states by breaking the mode degeneracy. The mode-propagation constant k becomes slightly different for the two orthogonal components of the fundamental mode resulting in two distinct polarization eigenmodes with different propagation velocities. This property is referred to as birefringence and is defined by

$$k_i = \frac{2\pi}{\lambda} \delta n_p \quad (3.3)$$

where $\delta n_p = (n_x - n_y)$ is the phase index of refraction difference, n_x and n_y are the phase indices along the two orthogonal polarization states, and λ is the free space wavelength of the propagating light. The axis along which the effective mode index is smaller is called the fast axis since the group velocity is larger for light propagating in that direction and the axis with the larger phase index is called the slow axis because of the smaller group velocity for waves in that direction. In conventional single mode optical fibers, the birefringence is not constant along the fiber but changes randomly because of fluctuations in the core shape and stress-induced anisotropies. Thus, light launched into the fiber with linear polarization quickly reaches a state of arbitrary polarization. For some applications, it is desirable that the fibers transmit light without changing its state of polarization. Such fibers are called polarization-maintaining fibers. In polarization-maintaining fibers, a stable state of linear polarization can be maintained over relatively long lengths. This polarization handling ability is derived from the high intrinsic birefringence introduced intentionally in the fibers through design modifications in core asymmetry or applying an asymmetric stress distribution on the core. The use of polarization-maintaining fibers requires an identification of the slow and fast axes before the linearly polarized light is launched into the fiber. If the polarization axis of the incident light coincides with the slow or the fast axis, the polarization remains unchanged during propagation. If the polarization axis makes an angle of 45° to these axes, the polarization changes continuously along the fiber in a periodic manner [6]. The state of polarization of light will evolve from linear to elliptic, to circular, to elliptic, to linear but $\pi/2$ out of phase, to elliptic, to circular, to elliptic, and finally back to its original state as shown in Fig.(3.1). The period of this evolution of the polarization state is defined as the beatlength. It can be shown that for a given value of birefringence, the power between the two modes is exchanged periodically as they propagate inside the fiber with a period equal to its beatlength L_b defined by

$$L_b = \frac{2\pi}{k_i} = \frac{\lambda}{\delta n_p} \quad (3.4)$$

The beatlength is $\sim 1\text{cm}$ for a strongly birefringent fiber with $\delta n_p \sim 10^{-4}$.

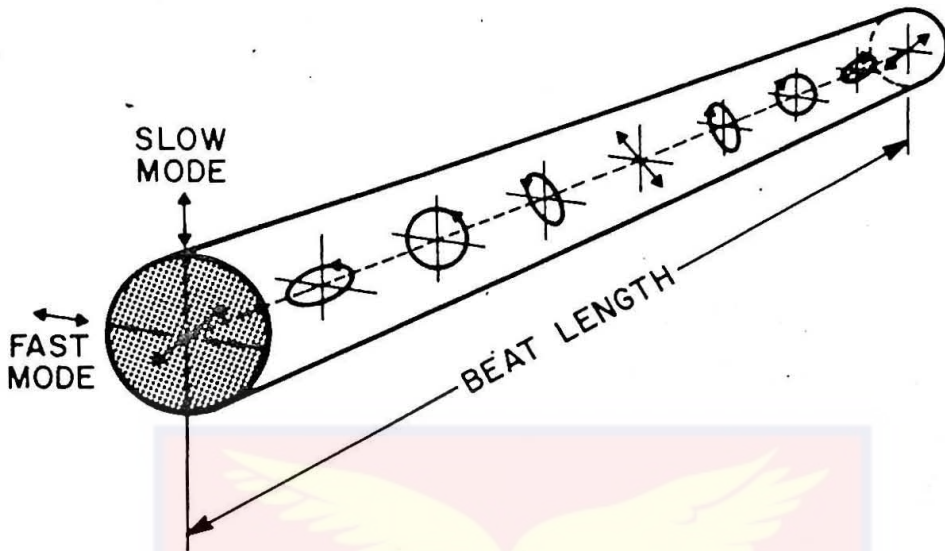


Figure 3-1: Evolution of the state of polarization along a birefringent fiber when the input beam is linearly polarized at 45° with respect to the slow axis.

A fiber with high linear birefringence will preserve the polarization state of a light beam whose electric-field vector is oriented along either principal axis of the fiber. In that case, the two principal axes are entirely equivalent. It is usually assumed that this equivalence also holds at high intensities and that an intense beam oriented along either axis will suffer no changes in its polarization, barring imperfections that cause scattering between the axes. It has been shown that an intensity-dependent refractive index leads to an instability in the polarization state of a light wave oriented along the fast axis of a birefringent medium. The slow axis remains a stable guiding center. Depending on the input intensity and polarization, the polarization ellipse can execute either oscillatory or rotatory motions about the slow axis in a manner analogous to the motion of a nonlinear pendulum [8]. These results have implications in fiber-optic devices and systems. The birefringence in a medium caused by an intensity-induced change in the refractive index of the medium, predicted prior to the advent of lasers, was one of the earliest nonlinear optical phenomena to be observed experimentally. This phenomena has since been and remains a topic of much interest and study given its practical importance in a variety of

applications including optical fiber communications.

Several analytical and numerical methods have been developed to study the polarization and its effects as the light propagates along a fiber. The evolution of the polarization state of a light beam during propagation can be represented by a variety of graphic methods. Two particularly useful representations in describing the polarization dynamics in a fiber are the Poincaré sphere and the phase plane. An analytical approach used to treat important polarization-related phenomena is the Jones matrix formalism. The Jones approach, even though powerful in the analysis of polarization effects, does not give quantities that are directly measurable. The unified formalism for polarization optics is another method developed to provide a means of understanding complicated polarization phenomena in optical media like fiber systems, devices and networks. The formalism utilizes Stokes-Mueller matrix equation with the Lorentz group in examining the dynamics of the polarization vector under the influence of birefringence and the effects of isotropic loss and diattenuation. The fiber is assumed to be isotropic with low internal linear birefringence. The Stokes-Mueller calculus is governed by an equation that has a sixteen element matrix \widehat{M} , which contains the information necessary to characterize the system and a four-parameter Stokes vector (S_0 and S_i) of the outgoing and incident light beams, respectively.

3.1.1 Stokes Parameters

The state of polarization of a wave is specified completely by a vector consisting of four physically real parameters. The four quantities comprise a column vector often written horizontally with curly brackets as $\{S_0, S_1, S_2, S_3\}$. The vector is referred to as Stokes vector and exists in a four-dimensional mathematical space. The four quantities that make up the elements of the Stokes vector are called Stokes parameters. The Stokes parameters are measurable quantities that describe the intensity and polarization of a beam of light. A beam may be polarized completely, partially or not at all and it may

be monochromatic or polychromatic. Stokes parameters have dimensions of intensity and each corresponds not to an instantaneous intensity but to a time-averaged intensity; the average being taken over a period long enough to permit practical measurement. The Stokes parameters are defined as follows: S_0 is the total intensity, S_1 is the excess intensity transmitted by the x-polarization eigenmode over the y-polarization eigenmode, S_2 is the excess intensity transmitted at 45° with respect to the x-polarization eigenmode over the intensity transmitted at 135° with respect to the x-polarization eigenmode, and S_3 is the excess intensity of right circular polarization over left circular polarization.

The Stokes parameters are related by

$$S_0^2 \geq S_1^2 + S_2^2 + S_3^2 = S^2 \quad (3.5)$$

where the equality holds for completely polarized purely monochromatic light and the inequality holds for partially polarized quasi-monochromatic light.

The degree of polarization of the light beam is given by

$$P = \frac{S}{S_0} = \frac{(S_1^2 + S_2^2 + S_3^2)^{\frac{1}{2}}}{S_0} \quad (3.6)$$

and a parameter that gives a measure of the relative amount of polarization in each can be expressed as

$$\%S_i = \left(\frac{S_i}{S_0}\right)^2 \quad (3.7)$$

Also, $P = 1$ for completely polarized light, $P = 0$ for unpolarized light and $0 < P < 1$ for partially polarized light.

If the Stokes parameters are known, the polarization azimuth Θ and the ellipticity angle η may be defined as follows

$$\tan 2\Theta = \frac{S_2}{S_1} \quad (3.8)$$

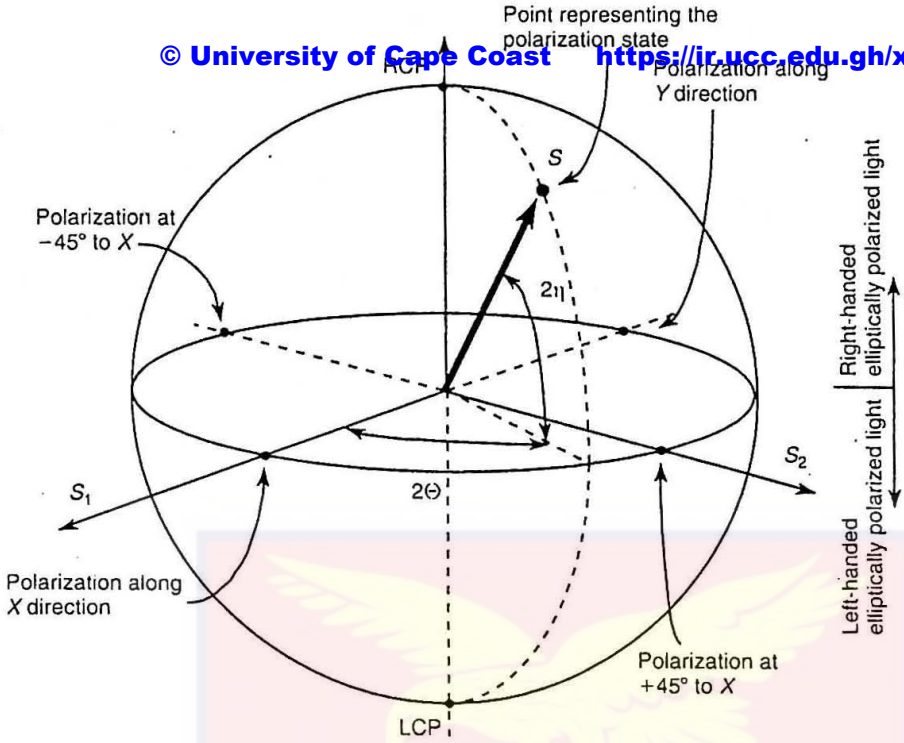


Figure 3-2: Illustration of the polarization state of a light wave on the Poincaré sphere.

and

$$\sin 2\eta = \frac{S_3}{S_0} \tag{3.9}$$

If the light intensity S_0 , the degree of polarization is $P = 1$, the polarization azimuth Θ and the ellipticity angle η are known, using equations (3.6), (3.8), and (3.9) one may obtain the Stokes parameters as follows

$$\begin{aligned} S_1 &= S_0 \cos 2\eta \cos 2\Theta \\ S_2 &= S_0 \cos 2\eta \sin 2\Theta \\ S_3 &= S_0 \sin 2\eta \end{aligned} \tag{3.10}$$

A particular polarization state may be represented as a point in a three dimensional Stokes coordinate space $\vec{S} = \{S_1, S_2, S_3\}$. The point lies on a sphere of radius S_0 . This sphere in Stokes space is known as the Poincaré sphere. An illustration of the polarization state of a light wave on the poincaré sphere is shown in Fig.(3.2).

3.1.2 Poincaré Sphere

The polarization state of a light wave can be represented as a point in a three dimensional Stokes coordinate space S_1, S_2 , and S_3 . The point lies on a sphere of radius $r = \sqrt{(S_1^2 + S_2^2 + S_3^2)}$. Another interesting feature of the Poincaré sphere is that the magnitude of interaction of a polarized beam with an optical medium corresponds to a rotation of the sphere. This sphere was first introduced in 1892 by Henri Poincaré who discovered that different polarization states may be represented on a sphere [13].

The radius of the Poincaré sphere is equal to S_0 for totally polarized light. The 'north' and 'south' poles of the sphere correspond to right and left circular polarizations (see Fig. 3.2). Linearly polarized light is represented by points along the equator with 'longitude' being twice the polarization azimuth Θ . The 'latitude' of the point will give twice the angle of ellipticity η of the wave. Points at opposite ends of a diameter, the 'antipodes' of the sphere are orthogonal polarizations [13]. If the light is partially polarized, the ratio of the Poincaré sphere radius to the Stokes parameter S_0 gives the degree of polarization.

3.1.3 Mueller Matrix

When an optical beam interacts with matter its polarization state is usually changed. The change in the polarization state may be due to a change in the amplitude, phase, or the direction of orthogonal field components of the optical beam. The Mueller matrix characterizes an optical device interposed in a polarized beam. The incident polarized beam interacts with the medium and a new set of Stokes parameters can be obtained for the emerging beam. The Mueller matrix is a 4×4 real matrix that describes the transformation of the state of polarization of the light beam as it interacts with an

optical system. The transformation is a simple matrix equation

$$\begin{bmatrix} S'_0 \\ S'_1 \\ S'_2 \\ S'_3 \end{bmatrix} = \begin{bmatrix} m_{00} & m_{01} & m_{02} & m_{03} \\ m_{10} & m_{11} & m_{12} & m_{13} \\ m_{20} & m_{21} & m_{22} & m_{23} \\ m_{30} & m_{31} & m_{32} & m_{33} \end{bmatrix} \begin{bmatrix} S_0 \\ S_1 \\ S_2 \\ S_3 \end{bmatrix} \quad (3.11)$$

where the primed Stokes parameters are for the output beam and the unprimed Stokes parameters represent the input beam. The matrix equation can be written more concisely in an operator form as

$$\vec{S}' = \widehat{M} \cdot \vec{S}_0 \quad (3.12)$$

where \vec{S}' and \vec{S}_0 are, respectively, the output and input Stokes four-vector and \widehat{M} is the Mueller matrix.

The Mueller matrix characterizes the optical system so that its effect on the state of polarization of a beam can be determined using the transformation given in the aforementioned Eq.(3.11). The sixteen unknown elements of the Mueller matrix can be determined by measuring the output polarization state, i.e. the output Stokes vector, of the light after it passes through the optical system from incident light sequentially polarized in four different polarization states, described by four independent Stokes vectors. The Mueller matrix \widehat{M} can be determined using the four pairs of input and output Stokes vectors [15]. If dichroism of the optical system is neglected, then $m_{00} = 1$ and the other Mueller matrix elements of the first row and first column are equal to zero. In this case, only three pairs of input and output Stokes vectors are necessary to determine \widehat{M} . In general, the 16 Mueller matrix elements depend on birefringence, dichroism and propagation length.

In Chapters 4 and 5 of this thesis, several Mueller matrices will be derived for various polarization effects in a single-mode fiber. The Mueller matrix calculus will be applied to a number of problems of interest in this study.

3.2 Stokes Parameters Equation of Motion

To derive the evolution equations for Stokes Parameters and illustrate their application to polarization effects in a medium starts with the use of Maxwell's wave equation.

$$\text{curl curl } \mathbf{E} + \frac{1}{c^2} \frac{\partial^2 \mathbf{D}}{\partial t^2} = 0 \quad (3.13)$$

where $\mathbf{D} = \mathbf{E} + 4\pi\mathbf{P}$ is the electric displacement vector and \mathbf{E} is the applied field. \mathbf{P} represents the polarization induced in the material by the propagating field. The induced polarization acts as a source term in the wave equation. Thus, Eq.(3.13) becomes

$$\nabla \times \nabla \times \mathbf{E} = -\frac{1}{c^2} \frac{\partial^2 (\mathbf{E} + 4\pi\mathbf{P})}{\partial t^2} \quad (3.14)$$

where $\nabla \times \nabla \times \mathbf{E} = \nabla(\nabla \cdot \mathbf{E}) - \nabla^2 \mathbf{E}$ is an identity from vector calculus. In linear optics, $(\nabla \cdot \mathbf{E}) = 0$ for isotropic source free media. In nonlinear optics, however, this term in general does not vanish even for isotropic materials due to the general relation between \mathbf{D} and \mathbf{E} .

The relationship between \mathbf{P} and \mathbf{E} could be nonlinear, that is, an increase in \mathbf{E} will lead to a disproportionate change in \mathbf{P} . The nonlinear optical response can be expressed as a Volterra series in the polarization vector.

$$\mathbf{P}_i(\mathbf{r}, t) = \mathbf{P}_i^1(\mathbf{r}, t) + \mathbf{P}_i^2(\mathbf{r}, t) + \mathbf{P}_i^3(\mathbf{r}, t) + \dots \quad (3.15)$$

The superscripts indicate the order of the term with respect to the electric field strength. The subscript $i = 1, 2$ indicates the transverse directions of the orthogonal field components. The first term on the right-hand side of Eq.(3.15) describes the linear optical response and increases proportionally with \mathbf{E} . The higher order terms describe the nonlinear response. In an optical fiber, $\mathbf{P}_i^2(t) = 0$ because the fiber is a centrosymmetric material. Thus, the third order polarization is the minimum nonvanishing nonlinear term

for a fiber. Equation (3.14) can now be written for the transverse fields as

$$\nabla_z^2 \mathbf{E}_i = \frac{1}{c^2} \frac{\partial^2 \mathbf{E}_i}{\partial t^2} + \frac{4\pi}{c^2} \frac{\partial^2 (\mathbf{P}_i^L + \mathbf{P}_i^{NL})}{\partial t^2} \quad (3.16)$$

where \mathbf{P}_i^L and \mathbf{P}_i^{NL} are respectively the linear and nonlinear induced polarizations. The wave equation (3.16) can be rewritten in frequency domain as follows:

$$\nabla_z^2 \tilde{\mathbf{E}}_i = -\frac{\omega^2}{c^2} (\tilde{\mathbf{E}}_i + 4\pi \tilde{\mathbf{P}}_i^L) \quad (3.17)$$

for the case where \mathbf{P}_i^{NL} is initially assumed to be zero. Furthermore, the linear response expressed in terms of the susceptibility and nonlocality tensors is given by

$$\mathbf{P}_i^L = P_i^1(\omega, \mathbf{r}) = \frac{1}{4\pi} \left\{ \left[\chi_{ij}^{(1)}(\omega) E_j(\omega, \mathbf{r}) + \Gamma_{ijm}^{(1)}(\omega) \nabla_m E_j(\omega, \mathbf{r}) \right] \right\} \quad (3.18)$$

For an electromagnetic wave propagating with wave vector \mathbf{k} , the spectral amplitude $\mathbf{E}(\omega, \mathbf{r})$ harmonically depends on the coordinate \mathbf{r} , so that $\mathbf{E}(\omega, \mathbf{r}) = \mathbf{A} \exp\{i\mathbf{k} \cdot \mathbf{r}\}$. Using Eq.(3.18), one can write Eq.(3.17) as

$$\nabla_z^2 \tilde{\mathbf{E}}_i = -\frac{\omega^2}{c^2} \left[(1 + \chi_{ij}^{(1)} + ik_m \Gamma_{ijm}^{(1)}) \tilde{\mathbf{E}}_j \right] \quad (3.19)$$

It is reasonable to assume that the Laplacian on the left of this equation contains second order derivative that is very much smaller than the first order derivative. In this case, the amplitude $\mathbf{A}(z, t)$ of the electric field of the wave is presumed a “slow” function of the propagation axis z . This approximation is known as the slowly-varying amplitude approximation and is valid whenever $\left| \frac{d^2 \mathbf{A}}{dz^2} \right| \ll k \left| \frac{d\mathbf{A}}{dz} \right| \ll k^2 \mathbf{A}$. Thus, it is also possible to write

$$\nabla_z^2 \tilde{\mathbf{E}}_i = \left(2ik \frac{dA_j}{dz} - k^2 A_j \right) e^{ikz} \quad (3.20)$$

Using these assumptions, the evolution equations which describe the transverse field amplitudes as they propagate along the coordinate axis z can be written in a compact

form as

$$\frac{dA_i}{dz} = \frac{i\omega}{2c} u_{ij} A_j \quad (3.21)$$

where $u_{ij} = \frac{1}{n} (\epsilon_{ij} + ik_m \Gamma_{ijm}^1 - n^2 \delta_{ij})$ is a tensor of rank two in two dimensional space representing the coupling due to the perturbations. The permittivity of the medium is denoted by $\epsilon_{ij} = 1 + \chi_{ij}^{(1)}$ while n indicates its refractive index. It is noted that Eq.(3.21) is a set of two differential equations for the field amplitudes known as the coupled mode equations.

In operator matrix form, u_{ij} may be regarded as a 2×2 matrix while A_i and A_j are column vectors in a two-dimensional vector space defined over the field of complex numbers. A rotation in this space transforms A_i and A_j into their linear combination. Therefore, the matrix u_{ij} must be unitary if the transformation is to leave the norm invariant [59]. This makes u_{ij} a member of the group $U(2)$, the group of all unitary matrices of order two and thus have a unique inverse such that $[u_{ij}]^{-1} = u_{ji}^*$. In this case, the determinant of the matrix u_{ij} equals ± 1 . Finally, it can be concluded that the matrix u_{ij} belongs to the group $SU(2)$, a subgroup of $U(2)$ which contains all unitary matrices of order two having determinant equal to $+1$. This stems from the fact that any unitary matrix may be expressed as an exponential of linear combination of traceless hermitian matrices. The three generators of $SU(2)$ can be chosen to be the Pauli spin matrices [59]

$$\sigma^{(1)} = \begin{pmatrix} 1 & 0 \\ 0 & -1 \end{pmatrix}, \quad \sigma^{(2)} = \begin{pmatrix} 0 & 1 \\ 1 & 0 \end{pmatrix}, \quad \sigma^{(3)} = \begin{pmatrix} 0 & -i \\ i & 0 \end{pmatrix} \quad (3.22)$$

which are a set of three independent traceless hermitian matrices of order 2 which obey the commutation relation $\sigma \times \sigma = 2i\sigma$. It is convenient to choose the set $[\sigma^{(0)}, \sigma^{(1)}, \sigma^{(2)}, \sigma^{(3)}]$ as the generator of $U(2)$ where $\sigma^{(0)}$ is a unit matrix of order 2. Therefore u_{ij} can be expanded in terms of the unit matrix and the Pauli matrices as follows

$$u_{ij} = \frac{1}{2} \Omega_{\alpha}^L \sigma_{ij}^{(\alpha)} \quad (3.23)$$

The summation is presumed over $\alpha = 0, \dots, 3$ and the expansion coefficients are

$$\Omega_{\alpha}^L = \sigma_{ji}^{(\alpha)} u_{ij} \quad (3.24)$$

With the use of Eq.(3.23), the coupled mode equation (3.21) takes the form

$$\frac{dA_i}{dz} = \frac{i\omega}{4c} \Omega_{\alpha}^L \sigma_{ij}^{(\alpha)} A_j \quad (3.25)$$

Stokes parameters may be defined in the following manner[13]

$$S_{\mu} \exp 2Im \{k\} z = A_j^* \sigma_{jk}^{(\mu)} A_k \quad (3.26)$$

With the use of Eq.(3.25) and its complex conjugate, the evolution equations for Stokes parameters can be written in the form

$$\frac{d}{dz} (S_{\mu} \exp 2Im \{k\} z) = \frac{i\omega}{4c} \left\{ \Omega_{\alpha}^L A_j^* \sigma_{ji}^{(\mu)} \sigma_{ik}^{(\alpha)} A_k - \Omega_{\alpha}^{L*} A_k^* \sigma_{kj}^{(\alpha)} \sigma_{ji}^{(\mu)} A_i \right\} \quad (3.27)$$

and making use of the fact that the Pauli matrices have the following property

$$\sigma_{ik}^{(\alpha)} \sigma_{kj}^{(\beta)} = \sigma_{ij}^{(0)} \delta_{\alpha\beta} + i e_{\alpha\beta\gamma} \sigma_{ij}^{(\gamma)} \quad (3.28)$$

and that they are additionally hermitian matrices, Eq.(3.27) can be written for the case $\mu = 0$ and $\alpha = 0, \dots, 3$ as

$$\frac{dS_0}{dz} = -\frac{\omega}{2c} Im \left[\left(4n + \Omega_0^L \right) S_0 + \left(\Omega^L \cdot \vec{S} \right) \right] \quad (3.29)$$

In Eq.(3.28), α, β and $\gamma = 1, 2,$ and $3,$ interchangeably. The term $e_{\alpha\beta\gamma}$ is the totally antisymmetric Levi-Civita tensor. For the specific case of $\mu = 1, 2, 3$ and $\alpha = 0, \dots, 3,$

equation (3.27) can be expressed for the components of the Stokes vector as

$$\frac{dS_\mu}{dz} = -\frac{\omega}{2c} Im \left[\left(4n + \Omega_0^L \right) S_\mu + \Omega^L S_0 + i \left(\Omega^L \times \vec{S} \right) \right] \quad (3.30)$$

Equations (3.29) and (3.30) are the evolution equations for Stokes parameters. The vector Ω^L with components $(\Omega_1^L, \Omega_2^L, \Omega_3^L)$ is defined in Stokes 3-vector space and depend only on the material parameters of the medium. These equations may be applied to media of arbitrary symmetry and low anisotropy along the direction of propagation. In fact, these equations work well when $\Delta n \ll n$, where Δn is the refractive index difference for the differently polarized eigenwaves of the medium [13].

If nonlinear induced polarization is now considered, Eq.(3.16) becomes

$$\nabla_z^2 \tilde{\mathbf{E}}_i = -\frac{\omega^2}{c^2} \left(\tilde{\mathbf{E}}_i + 4\pi \tilde{\mathbf{P}}_i^L + 4\pi \tilde{\mathbf{P}}_i^{NL} \right) \quad (3.31)$$

in frequency domain, where

$$\begin{aligned} \tilde{\mathbf{P}}_i^{NL} = & 3\chi_{ijkl}^{(3)}(\omega; \omega, \omega, -\omega) E_j(\omega, \mathbf{r}) E_k(\omega, \mathbf{r}) E_l^*(\omega, \mathbf{r}) \\ & + 2\Gamma_{ijklm}^{(3)}(\omega; \omega, \omega, -\omega) E_k(\omega, \mathbf{r}) E_l^*(\omega, \mathbf{r}) \nabla_m E_j(\omega, \mathbf{r}) \end{aligned} \quad (3.32)$$

is the induced polarization at the operating frequency ω .

Using the slowly varying amplitude approximation in (3.20) and Eq.(3.32), the evolution equations for the field amplitudes can now be expressed as

$$\frac{dA_i}{dz} = \frac{i\omega}{2c} \left[u_{ij} A_j + \gamma_{ijkl} A_j A_k A_l^* e^{-2Im\{k\}z} \right] \quad (3.33)$$

Here, $\gamma_{ijkl} = \frac{4\pi}{n} \left(3\chi_{ijkl}^{(3)} + ik_z \Gamma_{ijklz}^{(3)} \right)$ accounts for the third order local and nonlocal susceptibilities and u_{ij} as defined earlier. Expressed in terms of the Pauli matrices one can rewrite Eq.(3.23) as

$$u_{ij} = \frac{1}{2} v_\alpha \sigma_{ij}^{(\alpha)} \quad (3.34)$$

where $v_\alpha = \Omega_\alpha^L$ and

$$\gamma_{ijkl} = \frac{1}{4} w_{\alpha\beta} \sigma_{ij}^{(\alpha)} \sigma_{lk}^{(\beta)} \quad (3.35)$$

Then the expansion coefficients are therefore

$$v_\alpha = \sigma_{ji}^{(\alpha)} u_{ij} \quad (3.36)$$

and

$$w_{\alpha\beta} = \sigma_{ji}^{(\alpha)} \gamma_{ijkl} \sigma_{kl}^{(\beta)} \quad (3.37)$$

Resorting to (3.26), equation (3.33) can be written as

$$\frac{dA_i}{dz} = \frac{i\omega}{4c} \Omega_\alpha \sigma_{ij}^{(\alpha)} A_j \quad (3.38)$$

where

$$\Omega_\alpha = v_\alpha + \frac{1}{2} w_{\alpha\beta} S_\beta$$

is referred to as the nonlinear self-action four vector since itself is a function of the Stokes parameters and $\alpha = (0, 1, 2, 3)$. Using the same routine as was used to derive equations (3.29) and (3.30), a set of nonlinear differential equations structurally identical to (3.29) and (3.30) describing the evolution of Stokes parameter are obtained as follows

$$\frac{dS_0}{dz} = -\frac{\omega}{2c} \text{Im} \left[(4n + \Omega_0^L) S_0 + (\Omega_\alpha \cdot \vec{S}) \right] \quad (3.39)$$

and

$$\frac{dS_\mu}{dz} = -\frac{\omega}{2c} \text{Im} \left[(4n + \Omega_0^L) S_\mu + \Omega_\alpha S_0 + i (\Omega_\alpha \times \vec{S}) \right] \quad (3.40)$$

In the nonlinear case, therefore, Ω_α does not only depend on the material characteristics but also is a function of the Stokes parameters of the wave. The self action vector Ω_α coincides with the action vector Ω^L if nonlinearity is neglected. Therefore, the major

difference between linear and nonlinear media is that the propagation conditions are changed by the wave itself in a nonlinear media.

Such evolution equations may be utilized to obtain the polarization and describe its effects in an optical fiber. To do this, symmetry conditions need to be considered. Furthermore, low anisotropy along the direction of propagation will be assumed. This is reasonable because for a lossless fiber Eq.(3.30) implies a precession of the Stokes vector about Ω^L . Also, this assumption is necessary to allow for third order nonlinear anisotropy or induced anisotropies which will account for the dependence of Stokes parameters on the intensity of the light.

3.3 Polarization Ellipse

It was shown in section (3.1) that light is in general elliptically polarized and degenerates into linear and circular forms. The polarization ellipse has the form [13]

$$\frac{E_x^2}{E_{ox}^2} + \frac{E_y^2}{E_{oy}^2} - \frac{2E_x E_y \cos \delta}{E_{ox} E_{oy}} = \sin^2 \delta \quad (3.41)$$

where $\delta = \delta_x - \delta_y$ is the arbitrary phase while E_{ox} and E_{oy} are the maximum amplitudes. Close observation of Eq.(3.41) reveals that the product term $E_x E_y$ is not present in the standard form of an ellipse. This term indicates that the ellipse is actually rotated with respect to a principal axis, the X axis for example. The polarization state of an elliptically polarized wave may be specified completely by two parameters, the angle of rotation or polarization azimuth and an ellipticity angle [15]. This infers that there is a relationship between the parameters of the ellipse E_{ox} , E_{oy} , δ and the angle of rotation and ellipticity.

The polarization azimuth Θ is the angle measured between the X direction of the right-handed Cartesian frame and the major axis of the polarization ellipse. Θ may take on values between 0 and π . The ellipticity η , is defined as the angle between the main diagonal of a rectangular box enclosing the polarization ellipse and its major axis. The box have sides parallel to the major and minor axes of the ellipse. The angle is positive for (*REP*) and negative for (*LEP*). Therefore, the ellipticity angle varies from 0 to $\frac{\pi}{4}$ for (*REP*) and from 0 to $-\frac{\pi}{4}$ for (*LEP*) waves. Right and left circularly polarized waves correspond to $\eta = -\frac{\pi}{4}$ while $\eta = 0$ relates to linearly polarized wave. There are, however, shortcomings in characterizing an elliptically polarized state of a wave in terms of its azimuth and ellipticity. Since light waves have very high frequency, an experiment to trace out the electric field vector is impossible. Another limitation is that the polarization ellipse concept is applicable only to totally polarized light. It is not suitable for partially polarized light [13].

In section (3.2), the relationship between the parameters Θ and η to quantities that are directly measurable in an optical experiment was presented. The measurable parameters were the Stokes parameters.

3.3.1 Polarization Ellipse Plane Rotation

The plane of polarization rotates in some media as the light propagates through it. This effect named optical activity is a manifestation of the nonlocal optical response. It is a first-order spatial dispersion effect associated with the nonlocality tensor $\Gamma_{ijm}^{(1)}$. The rotation of the polarization plane takes place naturally and is sometimes called natural rotation [13].

From the same reference [13], it is also noted that for a lossless birefringent media, the rotation effect of the ellipse plane can be easily visualized in Stokes space. The effect

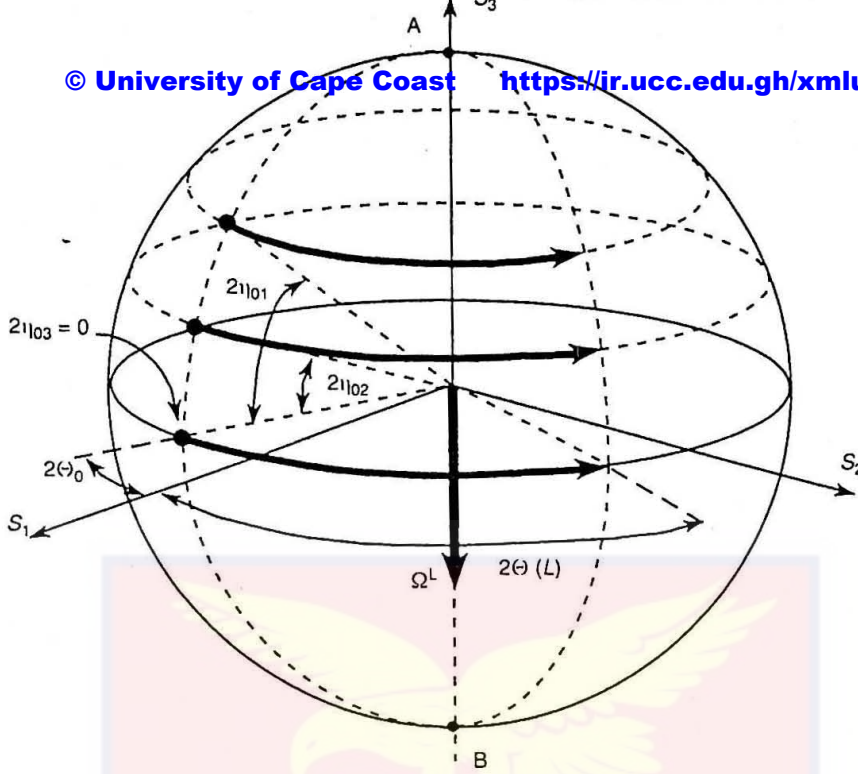


Figure 3-3: Poincaré's sphere representation of optical activity in a lossless birefringent fiber.

is a precession of the Stokes vector \vec{S} around vector Ω^L . The vector Ω^L in Stokes space is directed along the S_3 axis as shown in Fig.(3.1). The end of the Stokes vector of a propagating wave will trace out a horizontal circle on the Poincaré sphere and the azimuth Θ will steadily change along the direction of propagation. This illustrates optical activity. It is however worth noting that for natural rotation in lossless media, the end of the Stokes vector always remain on the same altitude, therefore the initial ellipticity angle does not change. For the specific case of a linearly polarized light, therefore, the plane of polarization rotates but the light remains linearly polarized. An elliptically polarized light will tend towards the right or left circular polarizations. The polarization states of the left and right-handed circularly polarized waves remain unchanged and are called eigenpolarization states. For a medium with small losses, a rotation of the ellipse plane suggests a rotation of both the azimuth and ellipticity. The azimuth rotation is proportional to the length of the medium where the proportionality constant indicates the specific polarization rotatory power. The azimuth rotates because of circular birefringence; the difference in refractive indices for left and right circularly polarized waves. The evolution

of ellipticity is due to circular dichroism, a difference in absorption coefficients for left and right-handed circularly polarized eigenwaves.

3.4 Polarization Mode Dispersion

Polarization mode dispersion (PMD) describes the change with frequency of the polarization of the field at the output of a fiber while the input polarization is held constant [51]. Beyond conventional chromatic dispersion which can be kept under control by suitable design, PMD is a limiting factor on the fibers bandwidth. It is a basic parameter required for estimation of birefringence-induced distortions in optical fiber systems [62]. The primary fiber properties which determine the PMD behavior of an optical cable are the linear and circular birefringence distributions along the fiber and mode-coupling parameter [82].

The evolution of the state of polarization of a lightwave as it propagates along the optical fiber can be mathematically expressed as

$$\frac{d \vec{S}(z, \omega)}{d\omega} = \vec{\delta\beta}(z, \omega) \times \vec{S}(z, \omega) \quad (3.42)$$

where $\vec{\delta\beta}$ is the differential group delay (DGD) vector and ω is the angular frequency of the source. z is the distance along the fiber. For long fiber lengths, the DGD becomes proportional to the frequency derivative of the magnitude of the birefringence vector [83]

$$\vec{\delta\beta}(z, \omega) = \frac{d\beta}{d\omega} \hat{\beta} z \quad (3.43)$$

$\hat{\beta}$ is a unit vector in the direction of the total birefringence. The magnitude of the total birefringence is

$$\beta = \sqrt{\beta_L^2 + (2\gamma - \beta_c)^2} \quad (3.44)$$

where β_L and β_c are respectively the linear and twist-induced circular components of the

total birefringence. γ is the twist rate of the fiber.

Using Eq.(3.44), one can express Eq.(3.43) as

$$\vec{\delta\beta}(z, \omega) = \left[\frac{\beta_L \beta'_L - (2\gamma - \beta_c) \beta'_c}{\sqrt{\beta_L^2 + (2\gamma - \beta_c)^2}} \right] \hat{\beta}_z \quad (3.45)$$

where $\beta'_L = d\beta_L/d\omega$ and $\beta'_c = d\beta_c/d\omega$. In this work, PMD is negligible since the fiber is assumed to be nondispersive. It is worth noting that PMD can be included if one considers, to first order, the dispersion of the fiber's stress-optic coefficient [83].



Chapter 4

POLARIZATION FORMALISM AND MODEL: THE LINEAR CASE

4.1 The Unified Formalism

If there are perturbations on a fiber resulting from length-dependent disturbances, the total dielectric function has the form

$$\epsilon = \epsilon_0(r, \phi) + \psi(r, \phi, z) \quad (4.1)$$

where ψ is the dielectric function of the perturbed fiber and $\epsilon_0(r, \phi)$ is the unperturbed dielectric function. r and ϕ are the polar parts of the cylindrical coordinates (r, ϕ, z) and z coincides with the fiber's axis of symmetry.

The electric field in the fiber can be represented as

$$E(r, \phi, z, t) = \sum_{\gamma=1}^2 a_{\gamma}(z) E_{\gamma}(r, \phi) \exp [i(k_{\gamma}z - \omega t)] \quad (4.2)$$

where $a_{\gamma}(z)$ are the field amplitudes containing the effects of the perturbations resulting from change of environment and various kinds of inhomogeneity in the fiber. k_{γ} is the propagation constant associated with each eigenmode. If there were no perturbations on the fiber, the coefficient $a_{\gamma}(z)$ of Eq.(4.2) would be a constant and in general a complex quantity. Using Maxwell's equations, along with (4.1) and (4.2) and the orthogonality conditions on the fields, (see Appendix A), the coupled-mode equations can be derived and written in operator notation as

$$\frac{da(z)}{dz} = i \hat{\mathbf{P}} \cdot a(z) \quad (4.3)$$

where $a(z)$ is a 2-dimensional column vector that represents the perturbed field amplitudes of the transverse fields and $\hat{\mathbf{P}}(z)$ is a 2×2 matrix operator that represents the coupling between the two polarization eigenmodes due to the perturbations. The coupling results in an evolution of the state of polarization as the light propagates in the fiber. In general, $\hat{\mathbf{P}}(z)$ is complex and has the form

$$\hat{\mathbf{P}}(z) = \hat{\mathbf{B}}(z) + i \hat{\mathbf{D}}(z) \quad (4.4)$$

where $\hat{\mathbf{B}}(z)$ is the birefringent operator that represents birefringent (phase) effects and $\hat{\mathbf{D}}(z)$ is the dichroic operator that represents dichroic (polarization dependent loss) effects. Both operators represent real quantities and are thus Hermitian [1].

Since only measurable quantities are of interest, the coherency matrix is used and is defined by an outer product as

$$\mathcal{I}(z) = a(z) a^{\dagger}(z) \quad (4.5)$$

The dagger symbol † which indicates the hermitian conjugate makes $a^\dagger(z)$ a row vector.

By taking the derivative of Eq.(4.5) with respect to the propagation length z , the following is obtained

$$\frac{d\mathcal{I}}{dz} = a(z) \frac{da^\dagger(z)}{dz} + \frac{da(z)}{dz} a^\dagger(z) \quad (4.6)$$

Substituting Eq.(4.3) and its hermitian conjugate into Eq.(4.6) yields the coherency equation of motion which can be expressed as

$$\frac{d\mathcal{I}}{dz} = i \left[\hat{\mathbf{P}}(z) \mathcal{I}(z) - \mathcal{I}(z) \hat{\mathbf{P}}^\dagger(z) \right] \quad (4.7)$$

Using Eq.(4.4) and the fact that $\hat{\mathbf{B}}(z)$ and $\hat{\mathbf{D}}(z)$ are hermitian, expression (4.7) can be rewritten as

$$\frac{d\mathcal{I}}{dz} = i \left[\hat{\mathbf{B}}(z), \mathcal{I}(z) \right] - \left\{ \hat{\mathbf{D}}(z), \mathcal{I}(z) \right\} \quad (4.8)$$

where $[B, \mathcal{I}] = B\mathcal{I} - \mathcal{I}B$ is called a commutator while $\{D, \mathcal{I}\} = D\mathcal{I} + \mathcal{I}D$ is called an anticommutator.

Since the operators in Eq.(4.5) are 2×2 and hermitian, they can be expanded in terms of the Pauli spin basis matrices and the unit matrix of order 2

$$\sigma_0 = \begin{pmatrix} 1 & 0 \\ 0 & 1 \end{pmatrix}, \quad \sigma_1 = \begin{pmatrix} 1 & 0 \\ 0 & -1 \end{pmatrix}, \quad \sigma_2 = \begin{pmatrix} 0 & 1 \\ 1 & 0 \end{pmatrix}, \quad \sigma_3 = \begin{pmatrix} 0 & -i \\ i & 0 \end{pmatrix} \quad (4.9)$$

These operators obey an algebra such that the multiplication property of the operators is

$$\sigma_l \sigma_m = \sigma_0 \delta_{lm} + i \sum_{n=1}^3 \epsilon_{lmn} \sigma_n \quad (4.10)$$

where δ_{lm} is the Kronecker delta symbol and ϵ_{lmn} is component lmn of the totally anti-symmetric tensor (with $\epsilon_{123} = +1$).

Using the Pauli spin matrices, the operators $\mathcal{I}(z)$, $\hat{\mathbf{B}}(z)$ and $\hat{\mathbf{D}}(z)$ can be expanded

as

$$\begin{aligned} \mathcal{I}(z) &= \frac{1}{2} \sum_{l=0}^3 S_l(z) \sigma_l \\ \hat{\mathbf{B}}(z) &= \frac{1}{2} \sum_{l=0}^3 \beta_l(z) \sigma_l \\ \hat{\mathbf{D}}(z) &= \frac{1}{2} \sum_{l=0}^3 d_l(z) \sigma_l \end{aligned} \quad (4.11)$$

where $S_i(z) = \{S_0, S_1, S_2, S_3\}$ is the 4-dimensional Stokes vector defined previously in section (3.2). β_0 represents the arbitrary phase of the fiber and $\vec{\beta} \equiv (\beta_1, \beta_2, \beta_3)$ is the birefringence in Stokes 3-vector representation. d_0 represents the arbitrary loss of the fiber and $\vec{d} \equiv (d_1, d_2, d_3)$ is the dichroism also in Stokes 3-vector representation.

Using Eq.(4.11) and the Pauli spin matrix algebra, the Stokes form of the coherency equation of motion (4.8) can be expressed as

$$\frac{dS_0}{dz} = -S_0(z) d_0(z) - \vec{\mathbf{S}}(z) \cdot \vec{\mathbf{d}}(z) \quad (4.12)$$

and

$$\frac{d\vec{\mathbf{S}}(z)}{dz} = \vec{\mathbf{S}}(z) \times \vec{\beta}(z) - S_0(z) \vec{\mathbf{d}}(z) - d_0(z) \vec{\mathbf{S}}(z) \quad (4.13)$$

where $\vec{\mathbf{S}}(z) = \{S_1, S_2, S_3\}$ is the 3-dimensional Stokes vector (see Appendix B). Note that equations (3.29) and (3.30) are identically equivalent to equations (4.12) and (4.13), respectively. However, equations (4.12) and (4.13) are expressed in vector notation whereas equations (3.29) and (3.30) are expressed in terms of components of the vectors.

The equations (4.12) and (4.13) can be rewritten in a more revealing Stokes 4-dimensional vector equation of motion as follows:

$$\frac{d}{dz} \begin{pmatrix} S_0 \\ S_1 \\ S_2 \\ S_3 \end{pmatrix} = \begin{pmatrix} -d_0 & -d_1 & -d_2 & -d_3 \\ -d_1 & -d_0 & \beta_3 & -\beta_2 \\ -d_2 & -\beta_3 & -d_0 & \beta_1 \\ -d_3 & \beta_2 & -\beta_1 & -d_0 \end{pmatrix} \begin{pmatrix} S_0 \\ S_1 \\ S_2 \\ S_3 \end{pmatrix} \quad (4.14)$$

The 4×4 matrix in equation (4.14) above exhibits Lorentz group symmetry which can

be exploited to expand the matrix by using a set of Lorentz group generators [1]. Consequently, the Stokes 4-dimensional equation of motion can be written in a compact operator form as

$$\frac{d\vec{\mathbf{S}}(z)}{dz} = \left\{ -d_0(z) \hat{\mathbf{I}} + \left(\vec{\mathbf{d}}(z) \cdot \hat{\mathbf{D}} \right) + \left(\vec{\beta}(z) \cdot \hat{\mathbf{B}} \right) \right\} \vec{\mathbf{S}}(z) \quad (4.15)$$

here $\vec{\mathbf{S}}(z)$ is the 4-dimensional Stokes vector and $\hat{\mathbf{I}}$ is the 4×4 unit matrix. The matrices $\hat{\mathbf{B}}$ and $\hat{\mathbf{D}}$ are the appropriate set of Lorentz generators given as follows [70]

$$\hat{\mathbf{D}}_1 = \begin{pmatrix} 0 & -1 & 0 & 0 \\ -1 & 0 & 0 & 0 \\ 0 & 0 & 0 & 0 \\ 0 & 0 & 0 & 0 \end{pmatrix}, \quad \hat{\mathbf{D}}_2 = \begin{pmatrix} 0 & 0 & -1 & 0 \\ 0 & 0 & 0 & 0 \\ -1 & 0 & 0 & 0 \\ 0 & 0 & 0 & 0 \end{pmatrix}$$

$$\hat{\mathbf{D}}_3 = \begin{pmatrix} 0 & 0 & 0 & -1 \\ 0 & 0 & 0 & 0 \\ 0 & 0 & 0 & 0 \\ -1 & 0 & 0 & 0 \end{pmatrix} \quad (4.16)$$

and

$$\hat{\mathbf{B}}_1 = \begin{pmatrix} 0 & 0 & 0 & 0 \\ 0 & 0 & 0 & 0 \\ 0 & 0 & 0 & 1 \\ 0 & 0 & -1 & 0 \end{pmatrix}, \quad \hat{\mathbf{B}}_2 = \begin{pmatrix} 0 & 0 & 0 & 0 \\ 0 & 0 & 0 & -1 \\ 0 & 0 & 0 & 0 \\ 0 & 1 & 0 & 0 \end{pmatrix}$$

$$\hat{\mathbf{B}}_3 = \begin{pmatrix} 0 & 0 & 0 & 0 \\ 0 & 0 & 1 & 0 \\ 0 & -1 & 0 & 0 \\ 0 & 0 & 0 & 0 \end{pmatrix} \quad (4.17)$$

The Lorentz generators in equations (4.16) and (4.17) obey an algebra given by the

following commutation relations [71]

$$\begin{aligned} [\hat{\mathbf{B}}_i, \hat{\mathbf{B}}_j] &= -\sum_k \epsilon_{ijk} \hat{\mathbf{B}}_k \\ [\hat{\mathbf{D}}_i, \hat{\mathbf{D}}_j] &= \sum_k \epsilon_{ijk} \hat{\mathbf{B}}_k \end{aligned} \tag{4.18}$$

and

$$[\hat{\mathbf{B}}_i, \hat{\mathbf{D}}_j] = -\sum_k \epsilon_{ijk} \hat{\mathbf{D}}_k$$

The formal solution to the Stokes 4-dimensional equation of motion (4.15) can be written as

$$\vec{\mathbf{S}}(d_0, \vec{\mathbf{d}}, \vec{\beta}, z) = \widehat{\mathbf{M}}(d_0, \vec{\mathbf{d}}, \vec{\beta}, z) \cdot \vec{\mathbf{S}}(0) \tag{4.19}$$

where $\vec{\mathbf{S}}(0) = \{S_{00}, S_{10}, S_{20}, S_{30}\}$ is the 4-dimensional input Stokes vector and the general Mueller matrix for arbitrary birefringence and dichroism expressed in terms of the Z-ordered exponential operators [72] is given by [1]

$$\widehat{\mathbf{M}}(d_0, \vec{\mathbf{d}}, \vec{\beta}, z) = \overleftarrow{Z} \exp \left\{ \begin{aligned} & -\int_0^z dz' \left[d_0(z') \hat{\mathbf{I}} \right] + \int_0^z dz' \left[\vec{\mathbf{d}}(z') \cdot \hat{\mathbf{D}} \right] \\ & + \int_0^z dz' \left[\vec{\beta}(z') \cdot \hat{\mathbf{B}} \right] \end{aligned} \right\} \tag{4.20}$$

The arrow pointing to the left above the Z in equation (4.20), indicates that the operators for the longer distances are ordered to the left.

For the case of arbitrary but uniform birefringence and dichroism, the general Mueller matrix in Eq.(4.20) after expanding and summing, takes the form

$$\widehat{\mathbf{M}}(d_0, \vec{\mathbf{d}}, \vec{\beta}, z) = \exp(-d_0 z) \exp \left[\left(\vec{\mathbf{d}}(z) \cdot \hat{\mathbf{D}} \right) z + \left(\vec{\beta}(z) \cdot \hat{\mathbf{B}} \right) z \right] \tag{4.21}$$

For the special case of only dichroism, Eq.(4.21) takes the form

$$\widehat{\mathbf{M}}(d_0, \vec{\mathbf{d}}, 0, z) = \exp(-d_0 z) \left\{ \begin{array}{l} \left[\hat{\mathbf{I}} - (\vec{\mathbf{e}}_d \cdot \hat{\mathbf{D}})^2 \right] + (\vec{\mathbf{e}}_d \cdot \hat{\mathbf{D}})^2 \cosh dz \\ + (\vec{\mathbf{e}}_d \cdot \hat{\mathbf{D}}) \sinh dz \end{array} \right\} \quad (4.22)$$

and for the case of pure birefringence Eq.(4.21) becomes

$$\widehat{\mathbf{M}}(0, 0, \vec{\beta}, z) = \left\{ \begin{array}{l} \left[\hat{\mathbf{I}} + (\vec{\mathbf{e}}_\beta \cdot \hat{\mathbf{B}})^2 \right] - (\vec{\mathbf{e}}_\beta \cdot \hat{\mathbf{B}})^2 \cos \beta z \\ + (\vec{\mathbf{e}}_\beta \cdot \hat{\mathbf{B}}) \sin \beta z \end{array} \right\} \quad (4.23)$$

With the use of a complex Lorentz 4×4 generator given by

$$\hat{\mathbf{P}} = \frac{1}{2} (\hat{\mathbf{B}} - i \hat{\mathbf{D}}) \quad (4.24)$$

the general Mueller matrix for arbitrary and uniform birefringence and dichroism given in Eq.(4.21) can be rewritten as

$$\widehat{\mathbf{M}}(d_0, \vec{\mathbf{d}}, \vec{\beta}, z) = \exp(-d_0 z) \exp \left[2 \operatorname{Re} (\vec{\mathbf{p}} \cdot \hat{\mathbf{P}}) z \right] \quad (4.25)$$

where

$$\vec{\mathbf{p}} = \vec{\beta} + i \vec{\mathbf{d}} = p_m \vec{\mathbf{e}}_p \quad (4.26)$$

is the Stokes 3-vector in complex form . With the use of Eq.(4.26)

$$p_m = (\vec{\mathbf{p}} \cdot \vec{\mathbf{p}})^{\frac{1}{2}} = N_p \exp \left[i \tan^{-1} \left(\frac{I_p}{R_p} \right) \right] \quad (4.27)$$

or

$$p_m = \left[(\beta_m^2 - d_m^2) + 2i (\vec{\beta} \cdot \vec{\mathbf{d}}) \right]^{\frac{1}{2}} = R_p + i I_p \quad (4.28)$$

where

$$R_p = \left[\frac{N_p^2 + (\beta_m^2 - d_m^2)}{2} \right]^{\frac{1}{2}} \quad (4.29)$$

and

$$I_p = \pm \left[\frac{N_p^2 - (\beta_m^2 - d_m^2)}{2} \right]^{\frac{1}{2}} \quad (4.30)$$

with

$$N_p = \left[(\beta_m^2 - d_m^2)^2 + 4(\vec{\beta} \cdot \vec{d})^2 \right]^{\frac{1}{4}} \quad (4.31)$$

Using equations (4.27) to (4.31) and some trigonometric identities, the Mueller matrix for arbitrary and uniform birefringence and dichroism (4.25) becomes

$$\widehat{\mathbf{M}}(d_0, \vec{d}, \vec{\beta}, z) = \exp(-d_0 z) \begin{pmatrix} \hat{\Phi}_+(\vec{e}_d, \vec{e}_\beta) \cosh(I_p z) + \hat{\Psi}_-(\vec{e}_d, \vec{e}_\beta) \sinh(I_p z) \\ \hat{\Phi}_-(\vec{e}_d, \vec{e}_\beta) \cos(R_p z) + \hat{\Psi}_+(\vec{e}_d, \vec{e}_\beta) \sin(R_p z) \end{pmatrix} \quad (4.32)$$

where

$$\hat{\Phi}_+(\vec{e}_d, \vec{e}_\beta) = \left\{ \begin{array}{l} \left(\frac{R_p}{N_p} \right)^2 \hat{\mathbf{I}} + \left(\frac{1}{N_p} \right)^2 \\ \times \left[(\vec{\beta} \cdot \hat{\mathbf{B}})^2 + (\vec{d} \cdot \hat{\mathbf{D}})^2 + (\vec{\beta} \times \vec{d}) \cdot \hat{\mathbf{D}} \right] \end{array} \right\} \quad (4.33)$$

$$\hat{\Phi}_-(\vec{e}_d, \vec{e}_\beta) = \left\{ \begin{array}{l} \left(\frac{I_p}{N_p} \right)^2 \hat{\mathbf{I}} - \left(\frac{1}{N_p} \right)^2 \\ \times \left[(\vec{\beta} \cdot \hat{\mathbf{B}})^2 + (\vec{d} \cdot \hat{\mathbf{D}})^2 + (\vec{\beta} \times \vec{d}) \cdot \hat{\mathbf{D}} \right] \end{array} \right\} \quad (4.34)$$

$$\hat{\Psi}_+(\vec{e}_d, \vec{e}_\beta) = \left\{ \begin{array}{l} \left(\frac{1}{N_p} \right)^2 R_p \left[(\vec{\beta} \cdot \hat{\mathbf{B}}) + (\vec{d} \cdot \hat{\mathbf{D}}) \right] \\ + \left(\frac{1}{N_p} \right)^2 I_p \left[(\vec{d} \cdot \hat{\mathbf{B}}) - (\vec{\beta} \cdot \hat{\mathbf{D}}) \right] \end{array} \right\} \quad (4.35)$$

and

$$\hat{\Psi}_-(\vec{e}_d, \vec{e}_\beta) = \left\{ \begin{array}{l} \left(\frac{1}{N_p} \right)^2 I_p \left[(\vec{\beta} \cdot \hat{\mathbf{B}}) + (\vec{d} \cdot \hat{\mathbf{D}}) \right] \\ - \left(\frac{1}{N_p} \right)^2 R_p \left[(\vec{d} \cdot \hat{\mathbf{B}}) - (\vec{\beta} \cdot \hat{\mathbf{D}}) \right] \end{array} \right\} \quad (4.36)$$

The minus sign in the scalar terms indicates dichroic loss. The matrices $\hat{\mathbf{D}}_{\sim} \equiv \left\{ \hat{\mathbf{D}}_{\sim 1}, \hat{\mathbf{D}}_{\sim 2}, \hat{\mathbf{D}}_{\sim 3} \right\}$

are new matrices associated with the mixing of the birefringence and dichroism effects when the birefringence and dichroism vectors are nonparallel. They obey the following relation

$$\hat{\mathcal{D}}_{\sim i} = -\eta \hat{\mathbf{D}}_i = \frac{1}{2} \sum_{r,s=1}^3 \epsilon_{irs} \left\{ \hat{\mathbf{B}}_r, \hat{\mathbf{D}}_s \right\} \quad (4.37)$$

The matrix $\eta = \text{diag}(-1, 1, 1, 1)$ in (4.37) is the metric matrix. The components of the $\hat{\mathcal{D}}_{\sim}$ matrices are thus defined as follows:

$$\hat{\mathcal{D}}_{\sim 1} = \begin{pmatrix} 0 & -1 & 0 & 0 \\ 1 & 0 & 0 & 0 \\ 0 & 0 & 0 & 0 \\ 0 & 0 & 0 & 0 \end{pmatrix}, \quad \hat{\mathcal{D}}_{\sim 2} = \begin{pmatrix} 0 & 0 & -1 & 0 \\ 0 & 0 & 0 & 0 \\ 1 & 0 & 0 & 0 \\ 0 & 0 & 0 & 0 \end{pmatrix}$$

$$\hat{\mathcal{D}}_{\sim 3} = \begin{pmatrix} 0 & 0 & 0 & -1 \\ 0 & 0 & 0 & 0 \\ 0 & 0 & 0 & 0 \\ 1 & 0 & 0 & 0 \end{pmatrix} \quad (4.38)$$

Note that in the limiting cases for very small dichroism or birefringence, the functional form of Eq.(4.32) for the Mueller matrix for arbitrary and uniform birefringence and dichroism reduces to the Mueller matrix for pure dichroism and pure birefringence given in equations (4.22) and (4.23).

In the following sections of this work, methods of the unified formalism will be used to obtain Mueller matrices for an optically active birefringent fiber with and without dichroism. Then, the elements of the Mueller matrices will be expressed in functional forms to provide a simple means for obtaining numerical solutions to the Stokes-Mueller equations that characterize the Stokes input and output parameters. The results obtained will be presented and discussed.

4.2 Polarization Formalism for an Optically Active Birefringent Fiber without Dichroism

In order to investigate the propagation of light in a birefringent fiber with optical activity and account for some of the interesting polarization effects which will emerge, it is important to initially consider the simple case of a fiber with negligible loss. Then, there is no dichroism and $Im(\Omega_\alpha^L) = 0$. Consequently, the action vector Ω_α^L is real and thus represents the birefringence of the fiber. In this case, Eq.(4.12) takes the form

$$\frac{dS_0(z)}{dz} = 0 \quad (4.39)$$

and the evolution equation for the Stokes 3-vector Eq.(4.13) becomes

$$\frac{d\vec{S}(z)}{dz} = -\frac{\omega}{2c} \left[\Omega_\alpha^L \times \vec{S}(z) \right] \quad (4.40)$$

Equation (4.40) represents a precession of the Stokes vector around Ω_α^L . Thus, a point on the Poincaré sphere representing the state of polarization moves along a circle whose center belongs to an axis which passes through the center of the sphere and is parallel to Ω_α^L (see Figure (1)). Therefore, the sphere rotates as a rigid body, and Ω_α^L evidently represents the angular velocity of a rotating sphere in an inertial frame.

Referring to the expansion given in Eq.(3.24), it is deduced that Ω_α^L accounts for small anisotropy in the dielectric tensor of the fiber. Thus, using Eq.(3.24), and assuming that there is no optical activity, the following components can be obtained for the special case

of a lossless birefringent fiber with small anisotropy along its length

$$\begin{aligned}\Omega_0 &= \frac{1}{n} (\epsilon_{11} + \epsilon_{33} - 2n^2) \\ \Omega_1 &= \frac{1}{n} (\Delta\epsilon \cos 2\phi) \\ \Omega_2 &= \frac{1}{n} (\Delta\epsilon \sin 2\phi) \\ \Omega_3 &= 0\end{aligned}\tag{4.41}$$

where $\Delta\epsilon = \epsilon_{11} - \epsilon_{33}$ and ϕ is the angle between the laboratory frame and the natural frame of the fiber. The second and third equations in (4.41) indicate that the linear birefringence relates to the anisotropy of the fiber.

For the case of an isotropic optically active fiber, the coupling term can be expressed with the use of the optical nonlocality tensor as follows [13]:

$$u_{ij} = i \frac{\omega}{c} \Gamma^a e_{ijz}\tag{4.42}$$

where Γ^a is the magnitude of the optical nonlocality and e_{ijz} is the Levi Civita antisymmetric tensor. Equation (4.42) can be used to obtain the following components of Ω_α^L for the case of an isotropic optically active fiber with negligible loss

$$\Omega_0^L = \Omega_1^L = \Omega_2^L = 0; \quad \Omega_3^L = -\frac{2\omega}{c} \Gamma^a\tag{4.43}$$

To investigate the light propagation in an optically active birefringent fiber and obtain some of the interesting polarization effects which may emerge, the vector Ω^L for such a fiber may be considered as an independent additive of the corresponding vectors for an optically active fiber and for a birefringent fiber. That is,

$$\Omega^L = \Omega_{opt}^L + \Omega_{bif}^L\tag{4.44}$$

Furthermore, in order to avoid initially tedious calculation, it is assumed that the fiber axes coincide with the laboratory frame so that $\phi = 0$. Using (4.41) and (4.43), equation (4.44) yields

$$\begin{aligned}\Omega_0 &= \frac{1}{n} (\epsilon_{11} + \epsilon_{33} - 2n^2) \\ \Omega_1 &= \frac{1}{n} \Delta\epsilon \\ \Omega_2 &= 0 \\ \Omega_3 &= -\frac{2\omega}{c} \Gamma^a\end{aligned}\tag{4.45}$$

Using the components for the 3-vector of Ω^L obtained in (4.45), equation (4.40) can be written as

$$\begin{aligned}\frac{dS_1}{dz} &= -2GS_2 \\ \frac{dS_2}{dz} &= 2GS_1 + 2\delta' S_3 \\ \frac{dS_3}{dz} &= -2\delta' S_2\end{aligned}\tag{4.46}$$

where $G = (\omega^2/2c^2) \Gamma^a$ is the fiber's optical rotatory power related to the circular birefringence and $\delta' = (\Delta\epsilon\omega/4cn)$ is a measure of the fiber's on-axis linear birefringence. The differential equations in (4.46) along with (4.39) represent the evolution of polarization as the light propagates along a lossless birefringent optically active fiber. It must be stressed here that a fiber generally does not exhibit optical activity. However, if small anisotropy along the fiber optical axis is assumed where no birefringence due to anisotropy of the dielectric tensor ϵ_{ij} is seen, optical activity is possible and therefore can be described using the equations derived in this section. Crystalline quartz SiO_2 is optically active along its optical axis [13].

The equations, (4.39) and (4.46), can be rewritten in the following matrix form

$$\frac{d}{dz} \begin{pmatrix} S_0 \\ S_1 \\ S_2 \\ S_3 \end{pmatrix} = \begin{pmatrix} 0 & 0 & 0 & 0 \\ 0 & 0 & -2G & 0 \\ 0 & 2G & 0 & 2\delta' \\ 0 & 0 & -2\delta' & 0 \end{pmatrix} \begin{pmatrix} S_0 \\ S_1 \\ S_2 \\ S_3 \end{pmatrix} \quad (4.47)$$

The solution to Eq.(4.47) is written simply as

$$\vec{S}_\alpha = \exp\left(\vec{\beta} \cdot \hat{\mathbf{B}}\right) z \cdot \vec{S}_{\alpha 0} \quad (4.48)$$

where $\vec{\beta} = \text{Re } \Omega^L$ is the birefringence three-vector and \vec{S}_α as well as $\vec{S}_{\alpha 0}$ represent the output and input Stokes 4 vectors, respectively. The exponential in Eq.(4.48) is immediately recognized as the Mueller matrix of the fiber [1]. Using the methods adopted from Brown's unified formalism, the exponential can be expanded in terms of the Lorentz generators $\hat{\mathbf{B}}$ as follows:

$$\begin{aligned} \widehat{\mathbf{M}}(0, 0, \vec{\beta}, z) &= \exp\left(\vec{\beta} \cdot \hat{\mathbf{B}}\right) z \\ &= \left[\hat{\mathbf{I}} + \left(\vec{e}_\beta \cdot \hat{\mathbf{B}}\right)^2 \right] - \left(\vec{e}_\beta \cdot \hat{\mathbf{B}}\right)^2 \cos \beta z + \left(\vec{e}_\beta \cdot \hat{\mathbf{B}}\right) \sin \beta z \end{aligned} \quad (4.49)$$

where $\beta = 2\sqrt{(\delta')^2 + G^2}$ is the magnitude of the birefringence and $\vec{e}_\beta = \cos 2\theta \vec{e}_1 + \sin 2\theta \vec{e}_3$ is a unit vector in the direction of the total birefringence. Then, the Mueller matrix for an optically active birefringent fiber without dichroism is given by (see Appendix C)

$$\widehat{\mathbf{M}}(0, 0, \vec{\beta}, z) = \begin{pmatrix} 1 & 0 & 0 & 0 \\ 0 & \cos^2 2\theta + \sin^2 2\theta \cos \beta z & -\sin 2\theta \sin \beta z & \cos 2\theta \sin 2\theta (\cos \beta z - 1) \\ 0 & \sin 2\theta \sin \beta z & \cos \beta z & \cos 2\theta \sin \beta z \\ 0 & \cos 2\theta \sin 2\theta (\cos \beta z - 1) & -\cos 2\theta \sin \beta z & \sin^2 2\theta + \cos^2 2\theta \cos \beta z \end{pmatrix} \quad (4.50)$$

Thus, the Stokes-Mueller equation can be expressed as

$$\begin{pmatrix} S_0 \\ S_1 \\ S_2 \\ S_3 \end{pmatrix} = \begin{pmatrix} 1 & 0 & 0 & 0 \\ 0 & \cos^2 2\theta + \sin^2 2\theta \cos \beta z & -\sin 2\theta \sin \beta z & \cos 2\theta \sin 2\theta (\cos \beta z - 1) \\ 0 & \sin 2\theta \sin \beta z & \cos \beta z & \cos 2\theta \sin \beta z \\ 0 & \cos 2\theta \sin 2\theta (\cos \beta z - 1) & -\cos 2\theta \sin \beta z & \sin^2 2\theta + \cos^2 2\theta \cos \beta z \end{pmatrix} \begin{pmatrix} S_{00} \\ S_{10} \\ S_{20} \\ S_{30} \end{pmatrix} \quad (4.51)$$

Now, in order to obtain a functional form of the output Stokes parameters, it is assumed that the input light is linearly polarized on axis so that $S_{00} = 1$, $S_{10} = S_{00} = 1$, and $S_{20} = S_{30} = 0$. The following functionals are obtained for a fiber of length $z = L$

$$\begin{aligned} S_0(L) &= S_{00} \\ S_1(L) &= \left[1 - \frac{G^2}{\mu^2} (1 - \cos 2\mu L) \right] S_{00} \\ S_2(L) &= \frac{G}{\mu} \sin 2\mu L S_{00} \\ S_3(L) &= -\frac{\delta' G}{\mu^2} (1 - \cos 2\mu L) S_{00} \end{aligned} \quad (4.52)$$

where $\mu = \sqrt{(\delta')^2 + G^2}$. Note that $\beta = 2\mu$.

Using the Stokes-Mueller equation (4.51), the results for various cases of input light polarization as a function of fiber length are presented in graphical figures. In all of these results, it is assumed that there is no polarization-dependent losses so that dichroism can be neglected and the light pulse propagates along the fiber without distortion or broadening barring other factors such as chromatic dispersion and nonlinear effects. In this case, the two principal states of polarization (PSP), that is, the polarization states for which the output polarization is independent of the optical frequency to first order are orthogonal and represent the slow and fast propagating pulses. Any other pulse can be decomposed in terms of these two PSP and will broaden during propagation [62].

It can be recalled that in obtaining Eq.(4.51), the fiber axis is assumed to coincide with

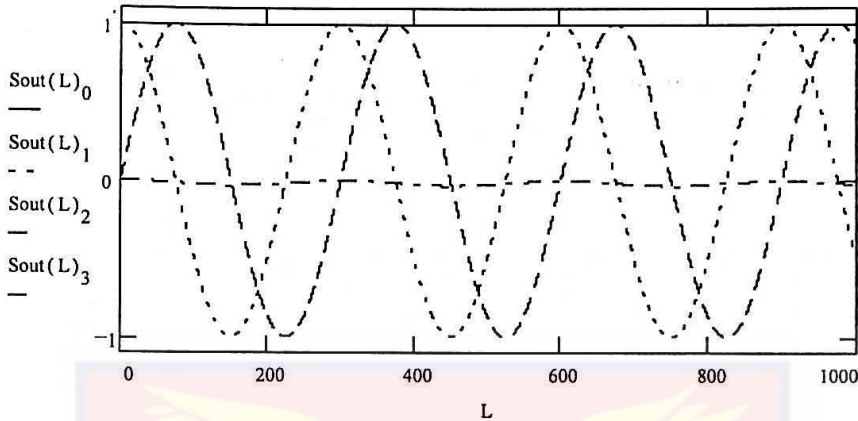


Figure 4-1: Variation in output Stokes parameters as a function of fiber length for linearly horizontally polarized input light. Circular birefringence present but linear birefringence off-axis not allowed.

the laboratory frame so that off-axis linear birefringence is not allowed but both linear on-axis and circular birefringence are present. Thus, for a given optical fiber trunk, this assumption amounts to neglecting bend-induced perturbations but considers that twist effects may be present along the length of the fiber and that perturbations intrinsic to the fiber resulting from material anisotropy or geometrical asymmetry or those external to the fiber such as thermal/mechanical stress may be induced in the fiber.

When the input light is linearly polarized on axis or off axis as shown, respectively, in Figs. (4-1) and (4-2), the output light for both cases is seen to be linearly polarized since S_3 is a null. For right circularly polarized input light, the output light is circularly polarized since S_1 and S_2 are both null intensities as shown in Fig.(4-3). If the light is initially elliptically polarized such that the orientation angle is 45° with respect to the principal axis and the ellipticity is 22.5° , inspection of Fig.(4-4) shows that the output beam emerges elliptically polarized.

It is interesting to observe the change in the output beam's behavior when the fiber is further assumed to have no circular birefringence. Then, in this case the fiber is straight with no bends and twists. Fig.(4-5) shows that the output light remains linearly polarized

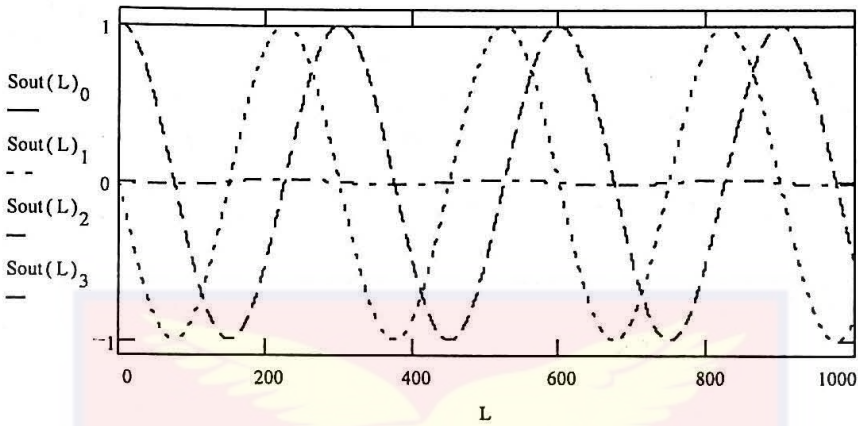


Figure 4-2: Variation in output Stokes parameters as a function of fiber length for linear $+45^\circ$ polarized input light. Circular birefringence assumed present but linear birefringence off-axis not allowed.

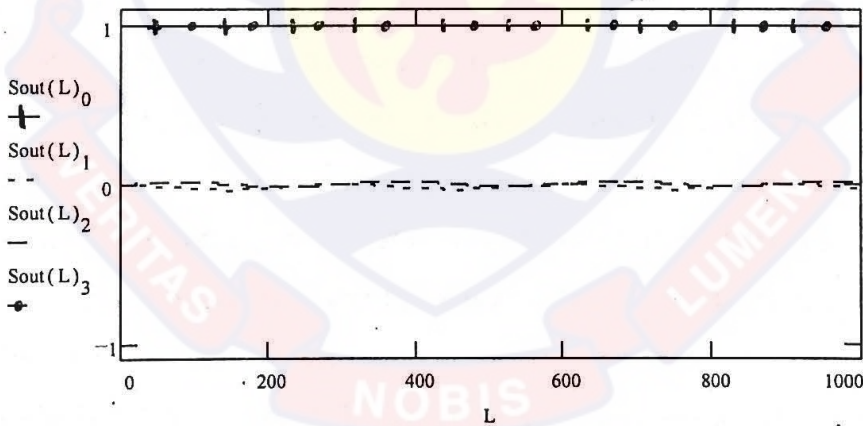


Figure 4-3: Output Stokes parameters as a function of fiber length for right circularly polarized input light. Circular birefringence present but linear birefringence off-axis not allowed.

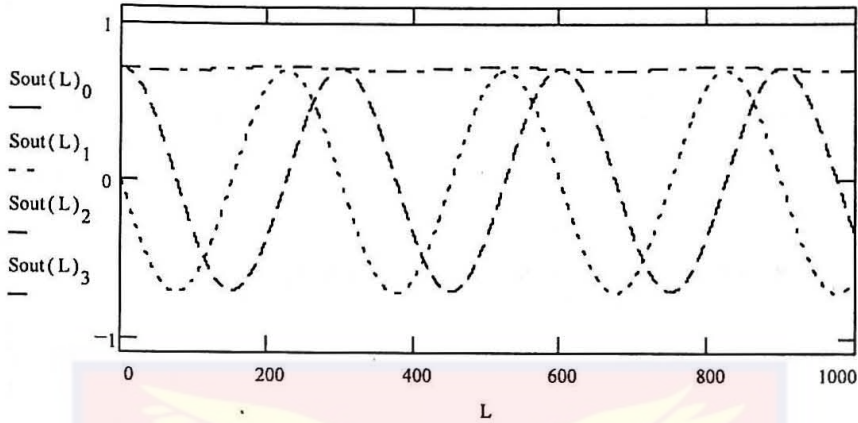


Figure 4-4: Variation in output Stokes parameters as a function of fiber length for elliptically polarized input light (45° azimuth and 22.5° ellipticity). Circular birefringence is present but linear birefringence off-axis not allowed.

on axis when the input polarization is off axis and for a light beam with polarization off axis, the output beam is off axis as shown in Fig.(4-6). It is shown in Figs.(4-7) and (4-8) that the output light maintains the same form of circular and elliptical polarizations when the input light is respectively circular and elliptical.

Comparing the results in Figs.(4-1) to (4-4) with Figs.(4-5) to (4-8), it is observed that the presence of circular birefringence induces a variation in the evolution of the polarization state for all cases of input polarization except for the case when the input light is right circularly polarized and the output beam remains unchanged. The change observed when circular birefringence is present can be attributed to the anisotropy introduced by twisting the fiber. The perturbation resulting from twisting the fiber causes the output polarization to change when the input light is either linear on-axis, off-axis, or elliptical. Right handed circular polarization is an eigenpolarization since the output states do not change for right circularly polarized input light.

To obtain the Mueller matrix in Eq.(4.50), it was assumed that the natural axis of the fiber coincided with the laboratory frame so that $\phi = 0$ and off-axis linear birefringence was not allowed. Suppose axes of fiber and lab frame do not coincide, then $\phi \neq 0$, and lin-

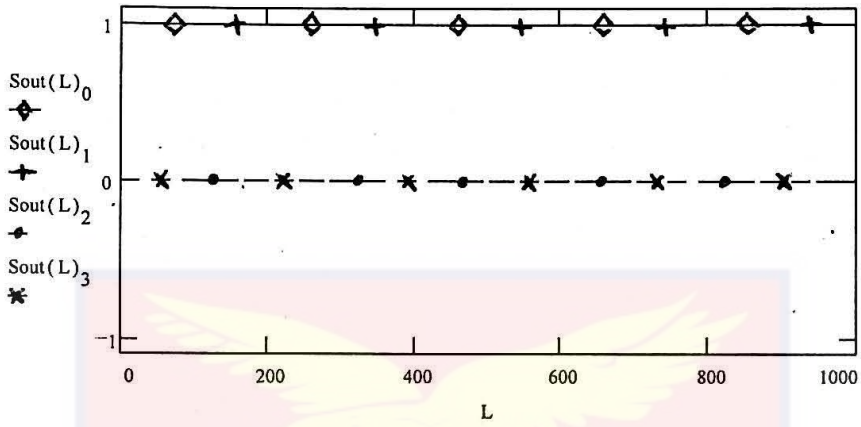


Figure 4-5: Output Stokes parameters as a function of fiber length for linearly horizontally polarized input light. Both circular and linear off-axis birefringence are absent.

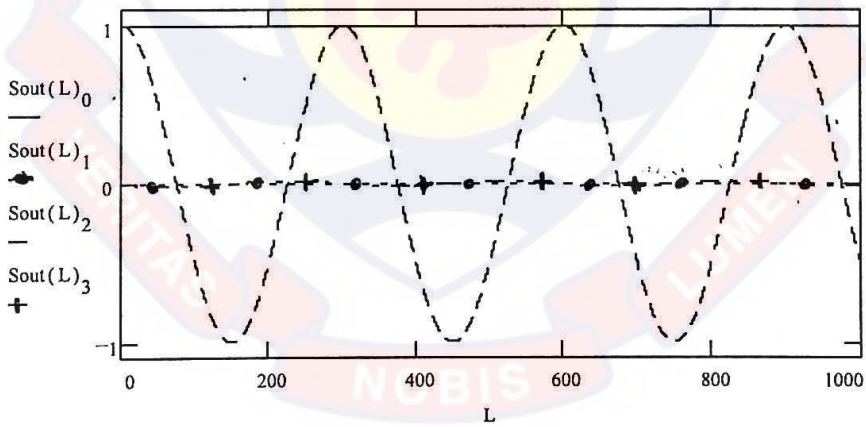


Figure 4-6: Output Stokes parameters as a function of fiber length for linear $+45^\circ$ polarized input light. Circular and linear birefringence off-axis are both absent.

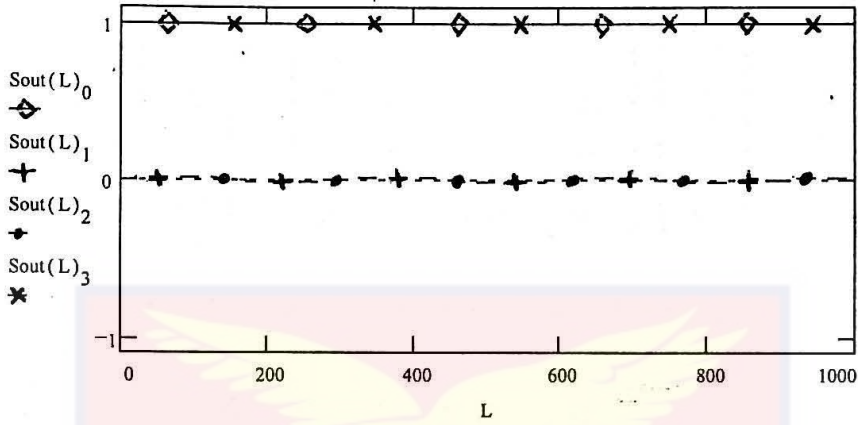


Figure 4-7: Output Stokes parameters as a function of fiber length for right circularly polarized input light. Circular birefringence and linear birefringence off-axis are both absent.

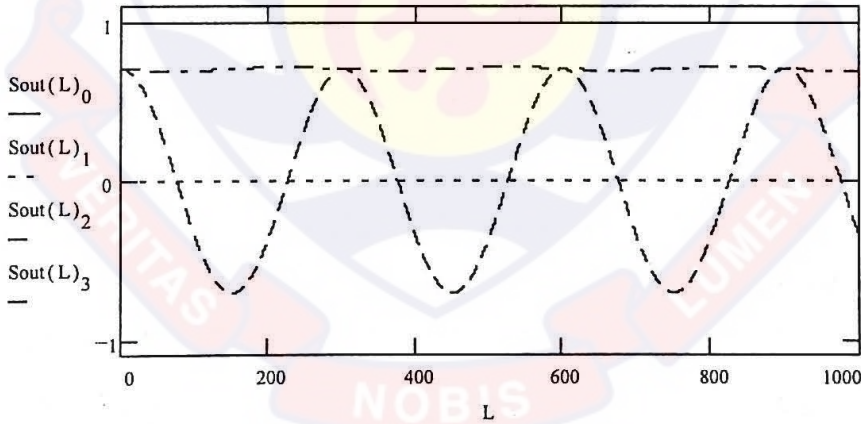


Figure 4-8: Variation in output Stokes parameters as a function of fiber length for elliptically polarized input light. (45° azimuth and 22.5° ellipticity). Circular and linear birefringence off-axis are both absent.

ear birefringence off axis is allowed, a more general Mueller matrix for pure birefringence can be obtained. In this case, the evolution equations will have the general form

$$\frac{d}{dz} \begin{pmatrix} S_0 \\ S_1 \\ S_2 \\ S_3 \end{pmatrix} = \begin{pmatrix} 0 & 0 & 0 & 0 \\ 0 & 0 & 2G & -2\gamma \\ 0 & -2G & 0 & 2\delta' \\ 0 & 2\gamma & -2\delta' & 0 \end{pmatrix} \begin{pmatrix} S_0 \\ S_1 \\ S_2 \\ S_3 \end{pmatrix} \quad (4.53)$$

and the Mueller matrix for the case of birefringence only becomes

$$\begin{aligned} \widehat{\mathbf{M}}(0, 0, \vec{\beta}, z) &= \exp(\vec{\beta} \cdot \hat{\mathbf{B}}) z \\ &= \left[\hat{\mathbf{I}} + (\vec{e}_\beta \cdot \hat{\mathbf{B}})^2 \right] - (\vec{e}_\beta \cdot \hat{\mathbf{B}})^2 \cos \beta z + (\vec{e}_\beta \cdot \hat{\mathbf{B}}) \sin \beta z \end{aligned} \quad (4.54)$$

where $\beta = 2\sqrt{(\delta')^2 + \gamma^2 + G^2}$ is the total birefringence and $\vec{e}_\beta = \cos 2\phi \cos 2\theta \vec{e}_1 + \sin 2\phi \cos 2\theta \vec{e}_2 + \sin 2\theta \vec{e}_3$ is a unit vector in the direction of $\vec{\beta}$. Again, using the unified formalism, the matrix can be expanded in terms of the exponential of the birefringence vector and the Lorentz generators to yield

$$\widehat{\mathbf{M}}(0, 0, \vec{\beta}, z) = \begin{pmatrix} 1 & 0 & 0 & 0 \\ 0 & C_\beta & S_{2\theta} S_\beta & -S_{2\phi} C_{2\theta} S_\beta \\ 0 & +C_{2\phi}^2 C_{2\theta}^2 (1 - C_\beta) & +C_{2\theta}^2 S_{2\phi} C_{2\phi} (1 - C_\beta) & +C_{2\phi} C_{2\theta} S_{2\theta} (1 - C_\beta) \\ 0 & -S_{2\theta} S_\beta & C_\beta & C_{2\phi} C_{2\theta} S_\beta \\ 0 & +C_{2\phi} C_{2\theta}^2 S_{2\phi} (1 - C_\beta) & +C_{2\theta}^2 S_{2\phi}^2 (1 - C_\beta) & +S_{2\phi} C_{2\theta} S_{2\theta} (1 - C_\beta) \\ 0 & S_{2\phi} C_{2\theta} S_\beta & -C_{2\phi} C_{2\theta} S_\beta & C_\beta \\ 0 & +C_{2\phi} C_{2\theta} S_{2\theta} (1 - C_\beta) & +S_{2\phi} C_{2\theta} S_{2\theta} (1 - C_\beta) & +S_{2\theta}^2 (1 - C_\beta) \end{pmatrix} \quad (4.55)$$

where $C_{2\phi} = \cos 2\phi$, $C_{2\theta} = \cos 2\theta$, $S_{2\theta} = \sin 2\theta$, $S_\beta = \sin \beta z$ and $C_\beta = \cos \beta z$.

With Eq.(4.55), the following functional form of the output Stokes parameters can

also be obtained for this case if the input light is linearly polarized on axis:

$$S_0(L) = S_{00}$$

$$S_1(L) = \left[\frac{(\delta')^2}{\nu^2} + \left(1 - \frac{(\delta')^2}{\nu^2} \right) \cos 2\nu L \right] S_{00}$$

$$S_2(L) = \left[-\frac{G}{\nu} \sin \beta L + \frac{\delta' \gamma}{\nu^2} (1 - \cos 2\nu L) \right] S_{00} \quad (4.56)$$

$$S_3(L) = \left[\frac{\gamma}{\nu} \sin \beta L + \frac{\delta' G}{\nu^2} (1 - \cos 2\nu L) \right] S_{00}$$

Where $\nu = \sqrt{(\delta')^2 + \gamma^2 + G^2}$. Note that when $\gamma \rightarrow 0$, then $\nu \rightarrow \mu$ as in the previous case of Eq.(4.52).

Hence, numerical results for several cases of input light polarization as a function of fiber length can be obtained for the special case in which linear birefringence off-axis is allowed but circular birefringence is assumed to be absent. The output polarization as a function of the fiber length for initially linearly horizontally polarized light, linear $+45^\circ$ polarized light, right circularly polarized light and elliptically polarized light with 45° orientation angle and 22.5° ellipticity are shown in Figs.(4-9) to (4-12).

It is observed from these figures that the beam emerging from the fiber has the same form for all cases as the input polarization. That is, for linearly polarized input light on-axis the output light is also shown to be linearly polarized on-axis and similarly for off-axis, circular, and elliptical input polarization.

When both linear off-axis and circular birefringence are considered to be present along the length of the fiber, it is seen from Figs.(4-13) to (4-16) that interesting effects may occur in the output polarization of the emerging light. Again, it is observed that circular birefringence introduces a variation in the polarization as the light propagates along the fiber. When circular birefringence is assumed absent the Stokes parameters remain constant for each input. However, when circular birefringence is present, the Stokes parameters are observed to vary with length depending on the input polarization.

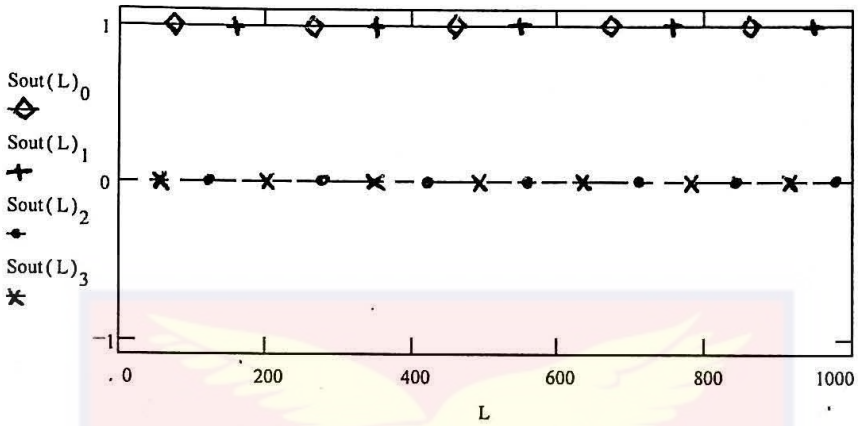


Figure 4-9: Output Stokes parameters as a function of fiber length for linearly horizontally polarized input light. Circular birefringence assumed absent and linear off-axis birefringence allowed.

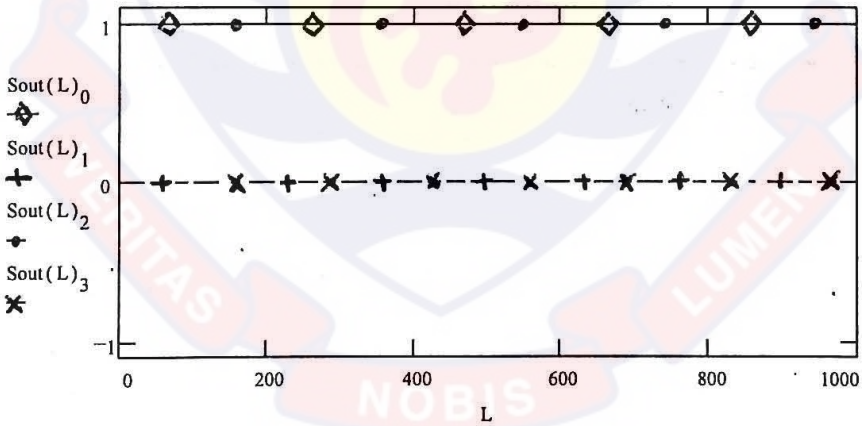


Figure 4-10: Output Stokes parameters as a function of fiber length for linear +45° polarized input light. Circular birefringence assumed absent and linear birefringence off-axis allowed.

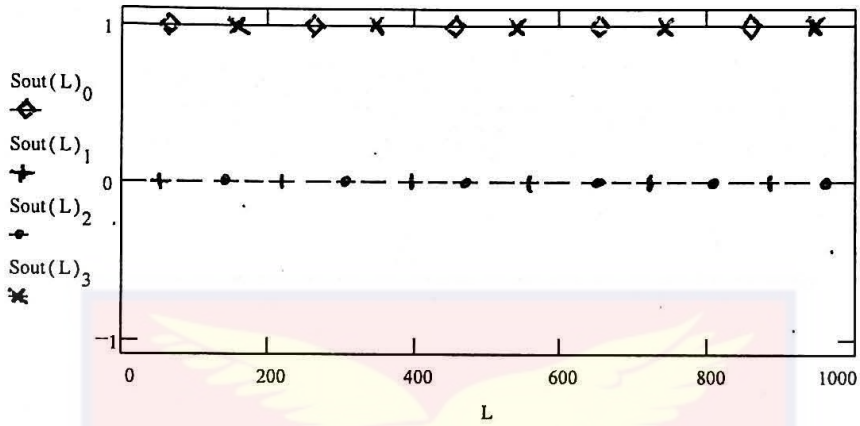


Figure 4-11: Output Stokes parameters as a function of fiber length for right circularly polarized input light. Circular birefringence is assumed absent and linear birefringence off-axis allowed.

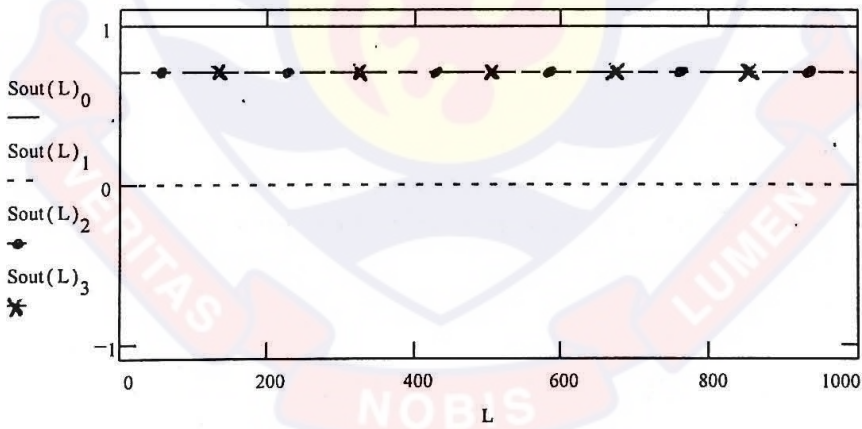


Figure 4-12: Output Stokes parameters as a function of fiber length for elliptically polarized input light (45° azimuth and 22.5° ellipticity). Circular birefringence is assumed absent and linear birefringence off-axis allowed.

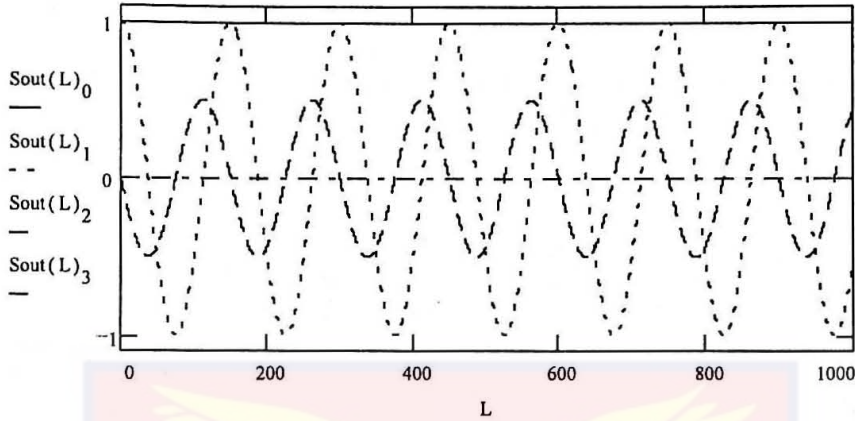


Figure 4-13: Variation in output Stokes parameters as a function of fiber length for linearly horizontally polarized input light. Circular birefringence assumed present and linear birefringence off-axis allowed.

4.3 Polarization Formalism for an Optically Active Birefringent Fiber with Dichroism

For the case of a lowloss isotropic fiber with optical activity, the evolution equations (4.12) and (4.13) take the form

$$\begin{aligned} \frac{dS_0}{dz} &= -2\text{Im}\{k\} S_0 + \frac{\omega^2}{c^2} \text{Im}\{\Gamma^a\} S_3 \\ \frac{dS_1}{dz} &= -2\text{Im}\{k\} S_1 - \frac{\omega^2}{c^2} \text{Re}\{\Gamma^a\} S_2 \\ \frac{dS_2}{dz} &= -2\text{Im}\{k\} S_2 - \frac{\omega^2}{c^2} \text{Re}\{\Gamma^a\} S_1 \end{aligned} \quad (4.57)$$

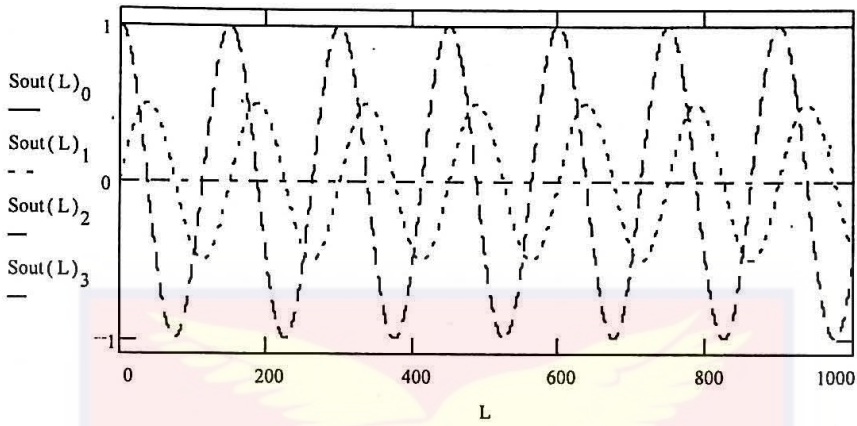


Figure 4-14: Variation in output Stokes parameters as a function of fiber length for linear $+45^\circ$ polarized input light. Circular birefringence present and linear birefringence off-axis allowed.

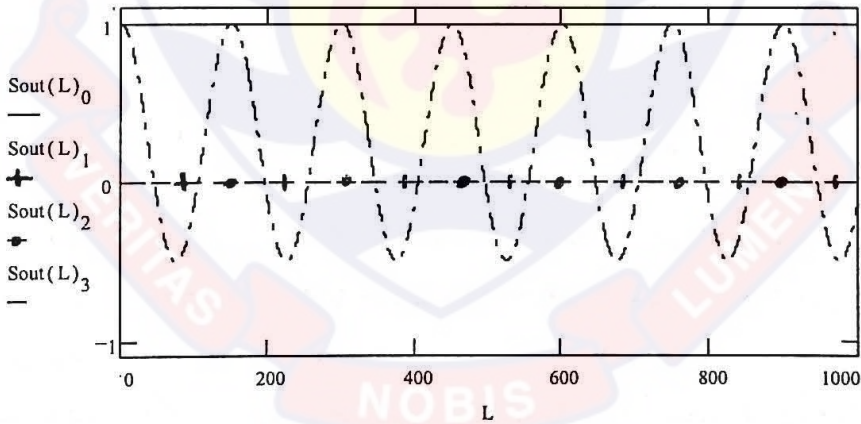


Figure 4-15: Variation in output Stokes parameters as a function of fiber length for right circularly polarized input light. Circular birefringence present and linear birefringence off-axis allowed.

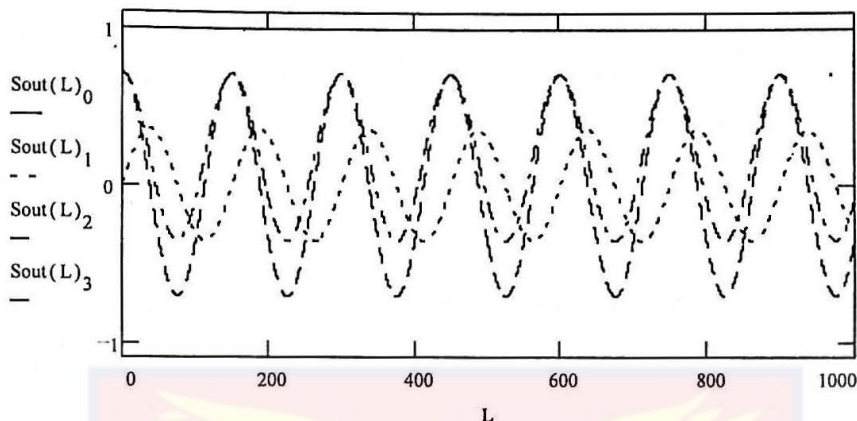


Figure 4-16: Variation in output Stokes parameters as a function of fiber length for elliptically polarized (45° azimuth and 22.5° ellipticity) input light. Circular birefringence assumed present and linear birefringence off-axis allowed.

$$\frac{dS_3}{dz} = -2Im\{k\} S_3 + \frac{\omega^2}{c^2} Im\{\Gamma^a\} S_0$$

The above equations can also be rewritten in matrix form as

$$\frac{d}{dz} \begin{pmatrix} S_0 \\ S_1 \\ S_2 \\ S_3 \end{pmatrix} = \begin{pmatrix} -2Im\{k\} & 0 & 0 & \frac{\omega^2}{c^2} Im\{\Gamma^a\} \\ 0 & -2Im\{k\} & -\frac{\omega^2}{c^2} Re\{\Gamma^a\} & 0 \\ 0 & \frac{\omega^2}{c^2} Re\{\Gamma^a\} & -2Im\{k\} & 0 \\ \frac{\omega^2}{c^2} Im\{\Gamma^a\} & 0 & 0 & -2Im\{k\} \end{pmatrix} \begin{pmatrix} S_0 \\ S_1 \\ S_2 \\ S_3 \end{pmatrix} \quad (4.58)$$

Inspection of Eq.(4.58) reveals that there is no linear birefringence and dichroism. The presence of circular birefringence and dichroism induces optical activity in the fiber. Circular birefringence gives the polarization azimuth rotation while circular dichroism controls the evolution of the ellipticity. These are manifestations of optical polarization phenomena. The Mueller matrix for circular birefringence only is

$$\begin{aligned} \widehat{M}(0, 0, \vec{\beta}, z) &= \exp \beta_3 (\vec{e}_3 \cdot \widehat{B}) z \\ &= \left[\widehat{I} + (\vec{e}_3 \cdot \widehat{B})^2 \right] - (\vec{e}_3 \cdot \widehat{B})^2 \cos \beta_3 z + (\vec{e}_3 \cdot \widehat{B}) \sin \beta_3 z \end{aligned} \quad (4.59)$$

and the Mueller matrix for circular dichroism only is

$$\widehat{\mathbf{M}}(d_0, \vec{d}, 0, z) = \exp d_3 (\vec{e}_3 \cdot \hat{\mathbf{D}}) z \\ = \left[\hat{\mathbf{I}} - (\vec{e}_3 \cdot \hat{\mathbf{D}})^2 \right] + (\vec{e}_3 \cdot \hat{\mathbf{D}})^2 \cosh d_3 z + (\vec{e}_3 \cdot \hat{\mathbf{D}}) \sinh d_3 z$$

Again, resorting to the use of the unified formalism, the Stokes-Mueller matrix equation for an isotropic optically active fiber with circular birefringence and dichroism can be expressed as

$$\begin{pmatrix} S_0 \\ S_1 \\ S_2 \\ S_3 \end{pmatrix} = e^{-2Im\{k\}z} \begin{pmatrix} C_h & 0 & 0 & S_h \\ 0 & C_\beta & -S_\beta & 0 \\ 0 & S_\beta & C_\beta & 0 \\ S_h & 0 & 0 & C_h \end{pmatrix} \begin{pmatrix} S_{00} \\ S_{10} \\ S_{20} \\ S_{30} \end{pmatrix} \quad (4.60)$$

where $C_h = \cosh\left(\frac{\omega^2}{c^2} Im\{\Gamma^a\}\right) z$ and $S_h = \sinh\left(\frac{\omega^2}{c^2} Im\{\Gamma^a\}\right) z$. Thus, equation (4.60) can be rewritten in the following explicit form

$$S_0(z) = e^{-2Im\{k\}z} \left[S_{00} \cosh\left(\frac{\omega^2}{c^2} Im\{\Gamma^a\}\right) z + S_{30} \sinh\left(\frac{\omega^2}{c^2} Im\{\Gamma^a\}\right) z \right] \\ S_1(z) = e^{-2Im\{k\}z} \left[S_{10} \cos\left(\frac{\omega^2}{c^2} Re\{\Gamma^a\}\right) z - S_{20} \sin\left(\frac{\omega^2}{c^2} Re\{\Gamma^a\}\right) z \right] \\ S_2(z) = e^{-2Im\{k\}z} \left[S_{20} \cos\left(\frac{\omega^2}{c^2} Re\{\Gamma^a\}\right) z + S_{10} \sin\left(\frac{\omega^2}{c^2} Re\{\Gamma^a\}\right) z \right] \quad (4.61) \\ S_3(z) = e^{-2Im\{k\}z} \left[S_{30} \cosh\left(\frac{\omega^2}{c^2} Im\{\Gamma^a\}\right) z + S_{00} \sinh\left(\frac{\omega^2}{c^2} Im\{\Gamma^a\}\right) z \right]$$

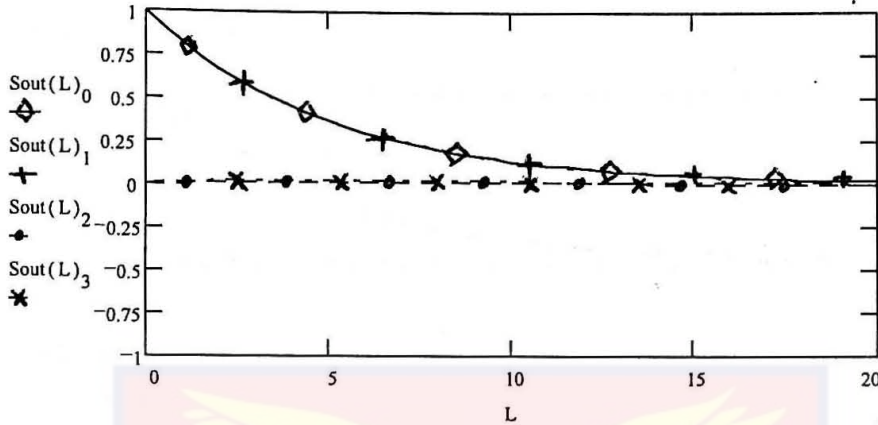


Figure 4-17: Output Stokes parameters for linearly horizontally polarized input light as a function of the fiber length. Circular birefringence and dichroism only are assumed present.

For the specific case of linearly polarized input light, the functional form can therefore be written as follows

$$\begin{aligned}
 S_0(L) &= e^{-\Delta L} (\cosh 2d_3 L) S_{00} \\
 S_1(L) &= e^{-\Delta L} (\cos 2\beta_3 L) S_{00} \\
 S_2(L) &= e^{-\Delta L} (\sin 2\beta_3 L) S_{00} \\
 S_3(L) &= e^{-\Delta L} (\sinh 2d_3 L) S_{00}
 \end{aligned}
 \tag{4.62}$$

where $\beta_3 = \omega^2/2c^2 \{Re\Gamma^a\}$ and $d_3 = \omega^2/2c^2 \{Im\Gamma^a\}$. Δ is the isotropic loss of the fiber.

The graphical results illustrating the change in the output Stokes parameters as the light propagates along the fiber for different input field polarization when linear birefringence and dichroism are absent are given in Figs.(4-17) to (4-20). The decreasing intensities observed in these diagrams are due to circular dichroism and isotropic loss in the fiber.

Now, for the case of a birefringent fiber with anisotropic dielectric tensor, without disregarding losses for the specific case when circular birefringence and dichroism are absent,

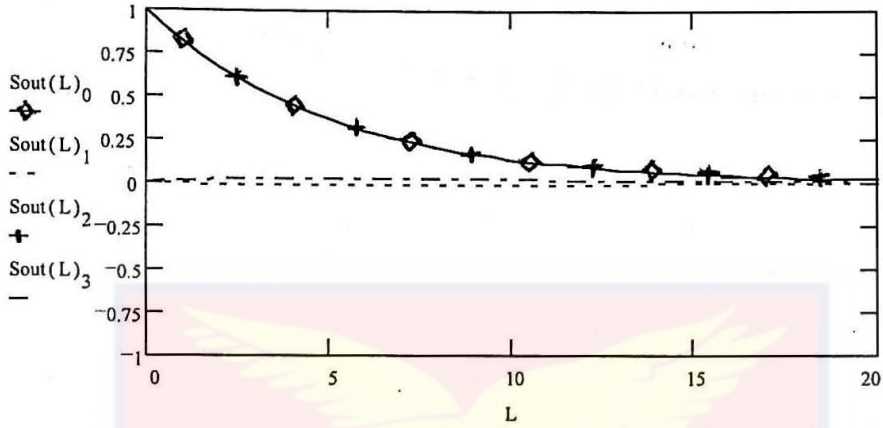


Figure 4-18: Output Stokes parameters for linearly $+45^\circ$ polarized input light as a function of the fiber length. Circular birefringence and dichroism only are assumed.

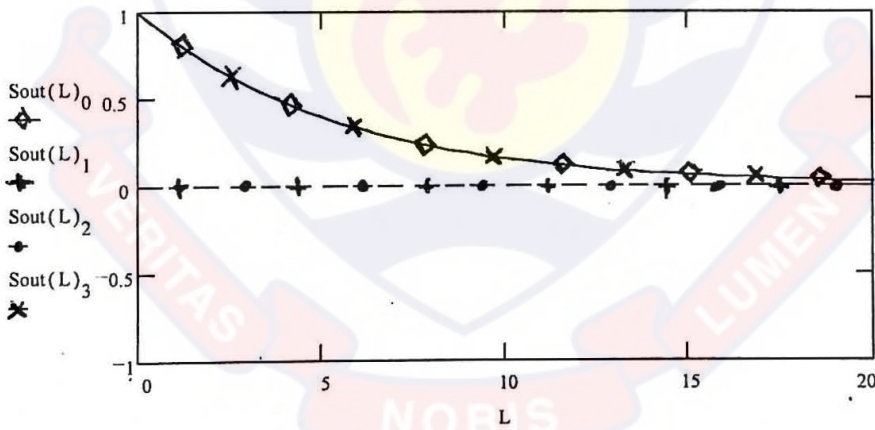


Figure 4-19: Variation in output Stokes parameters for right circularly polarized input light as a function of the fiber length. Circular birefringence and dichroism only are assumed present.

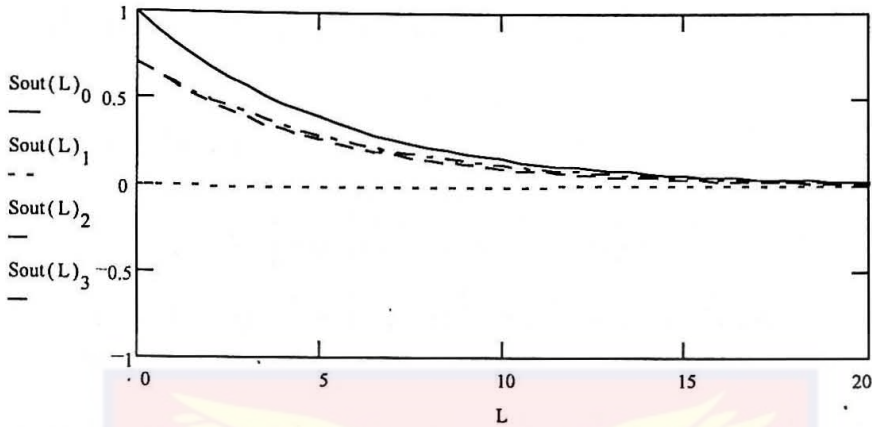


Figure 4-20: Output Stokes parameters for elliptically polarized (45° azimuth and 22.5° ellipticity) input light as a function of the fiber length. Circular birefringence and dichroism only are assumed present.

can also be analysed. Linear birefringence and dichroism account for small anisotropy and diattenuation effects in the fiber. Using Eq.(4.41), as well as equations (4.12) and (4.13) the following set of equations are obtained

$$\begin{aligned}
 \frac{dS_0}{dz} &= -\Delta S_0 - 2\delta'' \cos 2\phi S_1 - 2\delta'' \sin 2\phi S_2 \\
 \frac{dS_1}{dz} &= -\Delta S_1 - 2\delta'' \cos 2\phi S_0 - 2\delta' \sin 2\phi S_3 \\
 \frac{dS_2}{dz} &= -\Delta S_2 - 2\delta'' \sin 2\phi S_0 + 2\delta' \cos 2\phi S_3 \\
 \frac{dS_3}{dz} &= -\Delta S_3 - 2\delta' \cos 2\phi S_2 + 2\delta' \sin 2\phi S_1
 \end{aligned} \tag{4.63}$$

which can be rewritten in an equivalent form as

$$\frac{d}{dz} \begin{pmatrix} S_0 \\ S_1 \\ S_2 \\ S_3 \end{pmatrix} = \begin{pmatrix} -\Delta & -2\delta'' \cos 2\phi & -2\delta'' \sin 2\phi & 0 \\ -2\delta'' \cos 2\phi & -\Delta & 0 & -2\delta' \sin 2\phi \\ -2\delta'' \sin 2\phi & 0 & -\Delta & 2\delta' \cos 2\phi \\ 0 & 2\delta' \sin 2\phi & -2\delta' \cos 2\phi & -\Delta \end{pmatrix} \begin{pmatrix} S_0 \\ S_1 \\ S_2 \\ S_3 \end{pmatrix} \tag{4.64}$$

where $\Delta = \frac{\omega}{2c} \text{Im} \left\{ 2n + \frac{1}{n} (\epsilon_{11} + \epsilon_{33}) \right\}$, $\delta' = \text{Re} \{ \omega \Delta \epsilon / 4cn \}$ and $\delta'' = \text{Im} \{ \omega \Delta \epsilon / 4cn \}$. Note that Δ is the isotropic loss of the fiber, δ' and δ'' are its linear birefringence and dichroism, respectively.

The Mueller matrix for birefringence only becomes

$$\begin{aligned} \widehat{\mathbf{M}}(0, 0, \vec{\beta}, z) &= \exp(\vec{\beta} \cdot \hat{\mathbf{B}}) z \\ &= \left[\hat{\mathbf{I}} + (\vec{e}_\beta \cdot \hat{\mathbf{B}})^2 \right] - (\vec{e}_\beta \cdot \hat{\mathbf{B}})^2 \cos \beta z + (\vec{e}_\beta \cdot \hat{\mathbf{B}}) \sin \beta z \end{aligned} \quad (4.65)$$

where the unit vector is $\vec{e}_\beta = \cos 2\phi \vec{e}_1 + \sin 2\phi \vec{e}_2$. Equation (4.65), when expanded will yield

$$\widehat{\mathbf{M}}(0, 0, \vec{\beta}, z) = \begin{pmatrix} 1 & 0 & 0 & 0 \\ 0 & C_{2\phi}^2 + S_{2\phi}^2 C_\beta & S_{2\phi} C_{2\phi} (1 - C_\beta) & -S_{2\phi} S_\beta \\ 0 & S_{2\phi} C_{2\phi} (1 - C_\beta) & S_{2\phi}^2 + C_{2\phi}^2 C_\beta & C_{2\phi} S_\beta \\ 0 & S_{2\phi} S_\beta & -C_{2\phi} S_\beta & C_\beta \end{pmatrix} \quad (4.66)$$

and the Mueller matrix for only dichroism is

$$\begin{aligned} \widehat{\mathbf{M}}(d_0, \vec{\mathbf{d}}, 0, z) &= \exp(-d_0 z) \exp(\vec{\mathbf{d}} \cdot \hat{\mathbf{D}}) z \\ &= \left[\hat{\mathbf{I}} - (\vec{e}_d \cdot \hat{\mathbf{D}})^2 \right] + (\vec{e}_d \cdot \hat{\mathbf{D}})^2 \cosh d_m z + (\vec{e}_d \cdot \hat{\mathbf{D}}) \sinh d_m z \end{aligned} \quad (4.67)$$

Where the unit vector $\vec{e}_d = \cos 2\phi \vec{e}_1 + \sin 2\phi \vec{e}_2$. Equation (4.67) can also be expanded to obtain

$$\widehat{\mathbf{M}}(d_0, \vec{\mathbf{d}}, 0, z) = \begin{pmatrix} C_h & -C_{2\phi} S_h & -S_{2\phi} S_h & 0 \\ -C_{2\phi} S_h & S_{2\phi}^2 + C_{2\phi}^2 C_h & S_{2\phi} C_{2\phi} (C_h - 1) & 0 \\ -S_{2\phi} S_h & S_{2\phi} C_{2\phi} (C_h - 1) & C_{2\phi}^2 + S_{2\phi}^2 C_h & 0 \\ 0 & 0 & 0 & 1 \end{pmatrix} \quad (4.68)$$

The birefringence and dichroism occur simultaneously over the same optical path

and are thus parallel effects. Therefore the Mueller matrix for this case is a composite of the individual matrices due to only birefringence and only dichroism. The product of equations (4.66) and (4.68) with the appropriate order preserved yields the Mueller matrix for the system. Hence the Stokes-Mueller equation is

$$\begin{pmatrix} S_0 \\ S_1 \\ S_2 \\ S_3 \end{pmatrix} = e^{-\Delta z} \begin{pmatrix} C_h & -C_{2\phi}S_h & -S_{2\phi}S_h & 0 \\ -C_{2\phi}S_h & C_{2\phi}^2C_h + S_{2\phi}^2C_\beta & C_{2\phi}S_{2\phi}(C_h - C_\beta) & -S_{2\phi}S_\beta \\ -S_{2\phi}S_h & C_{2\phi}S_{2\phi}(C_h - C_\beta) & S_{2\phi}^2C_h + C_{2\phi}^2C_\beta & C_{2\phi}S_\beta \\ 0 & S_{2\phi}S_\beta & -C_{2\phi}S_\beta & C_\beta \end{pmatrix} \begin{pmatrix} S_{00} \\ S_{10} \\ S_{20} \\ S_{30} \end{pmatrix} \quad (4.69)$$

where $C_h = \cosh(2\delta'')z$, $S_h = \sinh(2\delta'')z$, $S_{2\phi} = \sin 2\phi$, $C_{2\phi} = \cos 2\phi$, $C_\beta = \cos(2\delta')z$, and $S_\beta = \sin(2\delta')z$.

For the case of linearly polarized input light, the functional form can be obtained using Eq.(4.69) as follows

$$\begin{aligned} S_0(L) &= e^{-\Delta L} [\cosh 2\delta''L - \cos 2\phi \sinh 2\delta''L] S_{00} \\ S_1(L) &= e^{-\Delta L} [-\cos 2\phi \sinh 2\delta''L + (\cos^2 2\phi \cosh 2\delta''L + \sin^2 2\phi \cos 2\delta' L)] S_{00} \\ S_2(L) &= e^{-\Delta L} [-\sin 2\phi \sinh 2\delta''L - \cos 2\phi \sin 2\phi (\cosh 2\delta''L - \cos 2\delta' L)] S_{00} \\ S_3(L) &= e^{-\Delta L} [\sin 2\phi \sin 2\delta' L] S_{00} \end{aligned} \quad (4.70)$$

For this case, it is noticed that the observed intensity depends on the orientation angle ϕ of the incident light.

Graphical results showing the variation in the Output Stokes parameters for different input polarization of a light beam propagating along a birefringent fiber having small losses are presented in Figs.(4-21) to (4-24). These results are for the specific case in which circular birefringence and dichroism are both assumed to be absent in the fiber. In general, the graphs show that the total intensity of the input laser light is dissipated by the fiber. This is due to attenuation by the fiber. In addition, it is also seen from these

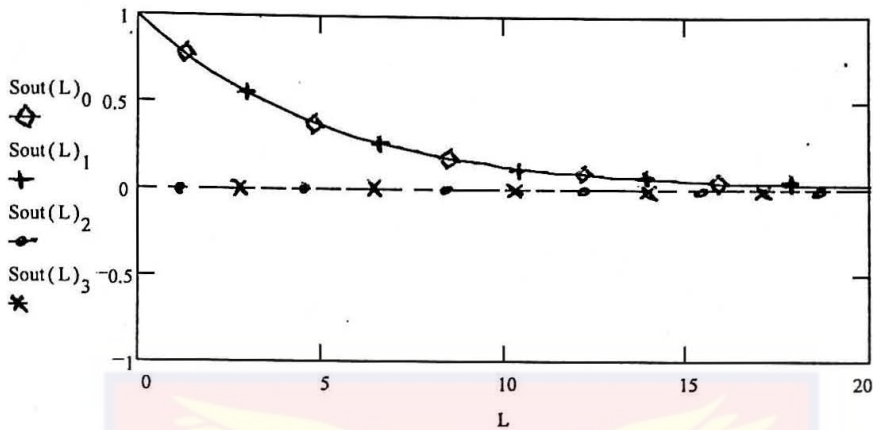


Figure 4-21: Output Stokes parameters for linearly horizontally polarized input light as a function of the fiber length. Circular birefringence and dichroism are assumed absent.

plots that the fiber depolarizes the propagating beam due to the polarization dependent losses accounted for by the presence of linear dichroism.

To obtain Eq.(4.69), effects due to circular birefringence and dichroism were not allowed. However, in order to generalize these results, this restriction must be removed. In Eq.(4.32), the general Mueller matrix for arbitrary birefringence and dichroism, the scalar terms $\{\Phi_+, \Psi_+, \Phi_-, \Psi_-\}$ may be rewritten in the following form

$$\Xi(\Phi_{\pm}, \Psi_{\pm}) = A \hat{\mathbf{I}} + (B \vec{\beta} - C \vec{\mathbf{d}}) \cdot \hat{\mathbf{B}} + (B \vec{\mathbf{d}} - C \vec{\beta}) \cdot \hat{\mathbf{D}} + D \left[(\vec{\beta} \cdot \hat{\mathbf{B}})^2 + (\vec{\mathbf{d}} \cdot \hat{\mathbf{D}})^2 + (\vec{\beta} \times \vec{\mathbf{d}}) \cdot \hat{\mathbf{D}} \right] \quad (4.71)$$

where

$$\begin{aligned} A &= \frac{1}{N_p} (R_p^2 \cosh I_p z + I_p^2 \cos R_p z) \\ B &= \frac{1}{N_p} (R_p \sin I_p z + I_p \sinh I_p z) \\ C &= \frac{1}{N_p} (R_p \sinh I_p z - I_p \sin R_p z) \end{aligned} \quad (4.72)$$

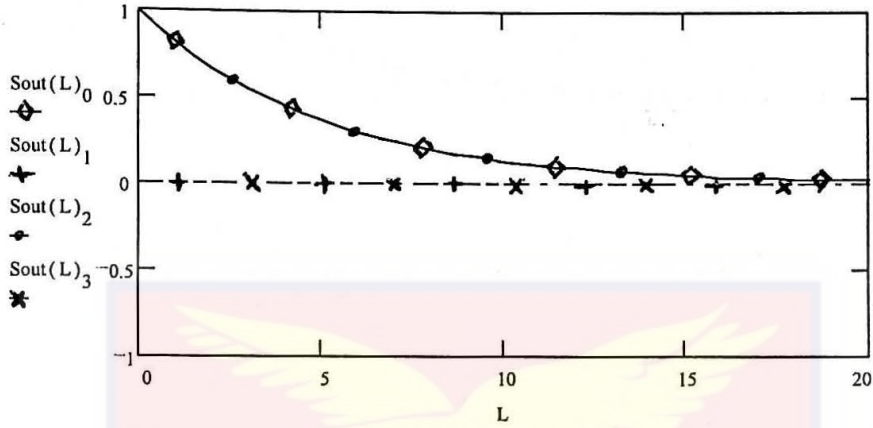


Figure 4-22: Output Stokes parameters for linear +45° polarized input light as a function of the fiber length. Circular birefringence and dichroism are assumed absent.

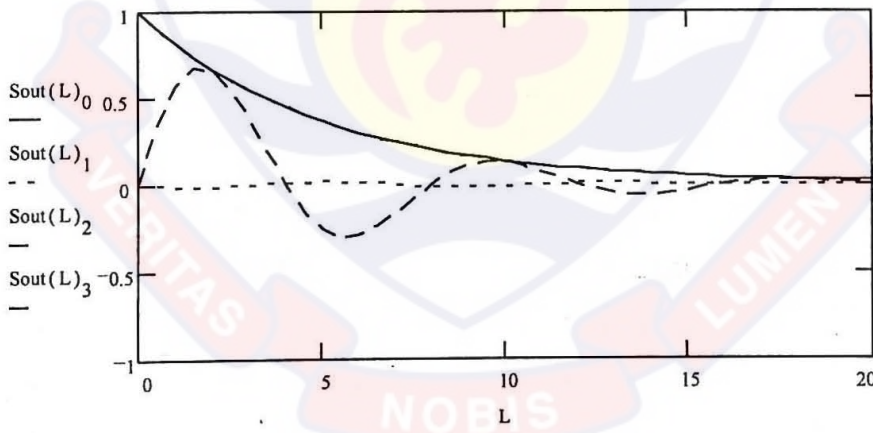


Figure 4-23: Variation in output Stokes parameters for right circularly polarized input light as a function of the fiber length. Circular birefringence and dichroism are assumed absent.

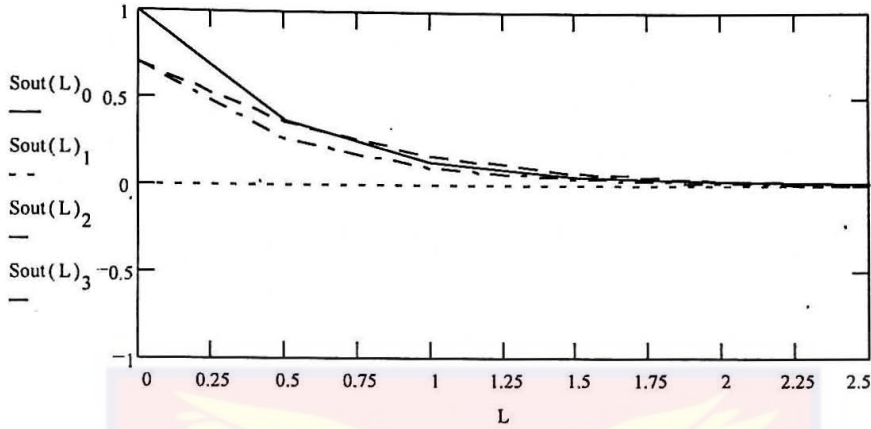


Figure 4-24: Output Stokes parameters for elliptically polarized (45° azimuth and 22.5° ellipticity) input light as a function of the fiber length. Circular birefringence and dichroism are assumed absent.

$$D = \frac{1}{N_p} (\cosh I_p z - \cos R_p z)$$

Therefore using equation (4.71), the expansion for the matrix represented by the scalar terms can be written more explicitly as

$$\Xi(\Phi_{\pm}, \Psi_{\pm}) = \begin{pmatrix} A + Dd^2 & -(Bd_1 + C\beta_1) & -(Bd_2 + C\beta_2) & -(Bd_3 + C\beta_3) \\ & -D\beta_2 d_3 & -D\beta_3 d_1 & -D\beta_1 d_2 \\ -(Bd_1 + C\beta_1) & A + & (B\beta_3 - Cd_3) & -(B\beta_2 - Cd_2) \\ +D\beta_2 d_3 & D(\beta_1^2 - \beta^2 - d_1^2) & +D(\beta_2\beta_1 + d_2d_1) & +D(\beta_3\beta_1 + d_3d_1) \\ -(Bd_2 + C\beta_2) & -(B\beta_3 - Cd_3) & A + & (B\beta_1 - Cd_1) \\ +D\beta_3 d_1 & +D(\beta_1\beta_2 + d_1d_2) & D(\beta_2^2 - \beta^2 - d_2^2) & +D(\beta_3\beta_2 + d_3d_2) \\ -(Bd_3 + C\beta_3) & (B\beta_2 - Cd_2) & -(B\beta_1 - Cd_1) & A + \\ +D\beta_1 d_2 & +D(\beta_3\beta_1 + d_3d_1) & +D(\beta_3\beta_2 + d_3d_2) & D(\beta_3^2 - \beta^2 - d_3^2) \end{pmatrix} \quad (4.73)$$

The matrix in Eq.(4.73) represents the most general case of birefringence and dichroism present in a fiber with an action-vector Ω having real and imaginary parts that are not necessarily parallel. Discussions on the results for specific cases of light polarization relating to this general case of both birefringence and dichroism present in the fiber will be presented in Chapter 6.



Chapter 5

POLARIZATION FORMALISM AND MODEL: THE NONLINEAR CASE

5.1 Evolution Equations For Stokes Parameters in Nonlinear Fiber

In this chapter, the nonlinear polarization effects in a single mode optical fiber are discussed and presented. The theoretical framework for describing the evolution of the polarization state of an intense light in the fiber is also discussed and key effects resulting from the propagation of such an intense light in the fiber are analysed theoretically. Numerical and graphical illustrations depicting these nonlinear polarization effects in the fiber will also be presented and discussed.

The self-action vector for a fiber with small nonlinearities may be expressed as follows

$$\Omega_{\alpha} = \Omega_{\alpha}^L + \Omega_{\alpha}^{NL} \quad (5.1)$$

where

$$\Omega_{\alpha}^L = \sigma_{ji}^{(\alpha)} u_{ij} = v_{\alpha} \quad (5.2)$$

is the linear action vector and

$$\Omega_{\alpha}^{NL} = \frac{1}{2} w_{\alpha\beta} S_{\beta} \quad (5.3)$$

is the nonlinear self-action vector where $w_{\alpha\beta} = \sigma_{ji}^{\alpha} \gamma_{ijkl} \sigma_{kl}^{\beta}$ is an expansion coefficient representing the material parameters responsible for the nonlinearities. These action vectors and tensors have already been defined in section (3.3). The tensors $u_{ij} = \frac{1}{2} v_{\alpha} \sigma_{ij}^{\alpha}$ and $\gamma_{ijkl} = \frac{1}{4} w_{\alpha\beta} \sigma_{ij}^{\alpha} \sigma_{lk}^{\beta}$ are restated here for clarity. Also, recall that $\gamma_{ijkl} = \frac{4\pi}{n} (\chi_{ijkl} + ik\Gamma_{ijklz})$.

To specify the evolution equations for an isotropic nonlinear optical fiber, the self-action vector Ω_{α} needs to be calculated. The linear part, Ω_{α}^L for an isotropic fiber has already been analysed in Chapter 4. The parameter $w_{\alpha\beta}$ responsible for the intensity-dependent effects of the fiber can be obtained provided proper consideration is made on the symmetry conditions of both the third order local and nonlocal susceptibilities.

In an isotropic medium, the nonlinear local susceptibility has 21 nonzero elements of which only 3 are independent [21]. This is due to the symmetry properties of an isotropic material. The nonzero elements are related by the equation

$$\chi_{ijkl}^{(3)} = \chi_{1122}^{(3)} \delta_{ij} \delta_{kl} + \chi_{1212}^{(3)} \delta_{ik} \delta_{jl} + \chi_{1221}^{(3)} \delta_{il} \delta_{jk} \quad (5.4)$$

where $1, 2 = x, y$ in Cartesian coordinates. To obtain Eq.(5.4), the invariance of $\chi_{ijkl}^{(3)}$ under reflection and rotation are utilized. A rotation of 45 degrees about the 3-axis (or z-axis) was the choice in the derivation. Equation (5.4) shows that the third-order local susceptibility has three independent elements for the general case in which the field frequencies are arbitrary.

To specialize this result to the study of nonlinear polarization effects in a fiber, there is a need to further characterize the third-order susceptibility tensor at the appropriate choice of the operating frequency given by $\chi_{ijkl}^{(3)}(\omega = \omega + \omega - \omega)$. Before this is done, it

is important to note that since the fields in the fiber are in the transverse directions, the number of nonzero elements reduce to eight as follows:

$$\begin{aligned}\chi_{1111}^{(3)} &= \chi_{2222}^{(3)} = \chi_{1122}^{(3)} + \chi_{1212}^{(3)} + \chi_{1221}^{(3)} \\ \chi_{1122}^{(3)} &= \chi_{2211}^{(3)} \\ \chi_{1212}^{(3)} &= \chi_{2121}^{(3)} \\ \chi_{1221}^{(3)} &= \chi_{2112}^{(3)}\end{aligned}\tag{5.5}$$

At this choice of frequency for $\chi_{ijkl}^{(3)}(\omega; \omega, \omega, -\omega)$, the intrinsic permutation symmetry requires that $\chi_{1122}^{(3)} = \chi_{1212}^{(3)}$ and the independent elements reduce to two. Furthermore, the electronic contribution to the susceptibility is dominant [21] so that $\chi_{1122}^{(3)} = \chi_{1221}^{(3)} = \frac{1}{3}\chi_{1111}^{(3)}$. Therefore, the nonlinear local response can now be given in terms of an effective nonlinear susceptibility as follows:

$$P_i(\omega) = D \sum_{j,k,l} \chi_{ijkl}(\omega; \omega, \omega, -\omega) E_j(\omega) E_k(\omega) E_l^*(\omega)\tag{5.6}$$

where the factor D in Eq.(5.6) accounts for degeneracy in the frequencies. $D = 3$ when two of the frequencies are equal as in this case. $D = 1$ if all the frequencies were the same and $D = 6$ if all frequencies were different. Thus, for a single-mode optical fiber, the nonlinear local response is characterized by the third order susceptibility tensor

$$\chi_{ijkl} = \chi_{ikjl} = 3\chi_{ijkl}^{(3)}(\omega, \omega, \omega, -\omega)\tag{5.7}$$

An isotropic nonlinear medium can be either gyrotropic or nongyrotropic depending on the value of the nonlocal susceptibility tensor. For gyrotropic isotropic media, the linear and nonlinear nonlocal optical responses are

$$\begin{aligned}\Gamma_{ijz}^{(1)} &= -\Gamma_{jiz}^{(1)} \\ \Gamma_{ijiz}^{(3)} &= \Gamma_{iijz}^{(3)} = -\Gamma_{jjiz}^{(3)} = -\Gamma_{jijz}^{(3)}\end{aligned}\tag{5.8}$$

$$\begin{aligned}\Gamma_{jjjiz}^{(3)} &= -\Gamma_{iiijs}^{(3)} = \Gamma_{jiiiz}^{(3)} + \Gamma_{ijjiz}^{(3)} + \Gamma_{iijiz}^{(3)} \\ \Gamma_{ijjjz}^{(3)} &= -\Gamma_{jiiiz}^{(3)} = \Gamma_{ijjiz}^{(3)} + \Gamma_{iijiz}^{(3)} + \Gamma_{iijiz}^{(3)}\end{aligned}$$

The nonlocality susceptibility which is symmetrical with respect to the permutation of the second and third indices is

$$\Gamma_{ijklz}^{(3)} = \Gamma_{ikjlz}^{(3)} = \Gamma_{ijklz}^{(3)}(\omega; \omega, \omega, -\omega) + \Gamma_{ikjlz}^{(3)}(\omega; \omega, \omega, -\omega) - \Gamma_{ilkjz}^{(3)}(\omega; \omega, \omega, -\omega) \quad (5.9)$$

However, in an isotropic nongyrotropic media, nonlocality is forbidden by symmetry and there are no nonlocal effects so that $\Gamma_{ijm}^{(1)} = \Gamma_{ijklm}^{(3)} = 0$. For isotropic materials, there are five different cubic crystal symmetry point groups: 23, $m\bar{3}$, 432, $\bar{4}3m$ and $m\bar{3}m$. Cubic crystals are optically isotropic and are considered completely isotropic for its optical property [60]. All cubic crystals have isotropic local susceptibility tensors $\chi_{ij}^{(1)} = (\epsilon - 1)\delta_{ij}$. ϵ is the dielectric permittivity of the medium. Therefore, without taking nonlocality into account, their linear optical properties are isotropic. Even within the first-order spatial dispersion approximation, the linear optical properties of crystals of $m\bar{3}$ and $m\bar{3}m$ point groups are indistinguishable from those of isotropic nongyrotropic media and thus these crystals show no nonlocal effects. Other cubic crystals, namely the 23 and 432 classes, show natural and nonlinear optical activity similar to that of isotropic gyrotropic media. It is also worthy to note that the crystals of $m\bar{3}$ and $m\bar{3}m$ classes possess inversion symmetry and are thus centrosymmetric. Crystals which belong to the $m\bar{3}$ class have 21 nonzero third order local susceptibility tensors of which 7 are independent and the $m\bar{3}m$ class have 21 nonzero third-order local susceptibility of which only 4 are independent. Quartz glass optical fibers belong to the $m\bar{3}m$ class of crystals and therefore do not exhibit nonlocal effects. In other words, optical fibers show no conventional natural nor nonlinear optical activity since $\Gamma_{ijz}^{(1)} = \Gamma_{ijklz}^{(3)} = 0$.

Therefore, the material parameter appropriate for light propagation along the longi-

tudinal axis of a single mode optical fiber can be expressed as

$$w_{\alpha\beta} = \frac{4\pi}{n} \left[\sigma_{ji}^{\alpha} \chi_{ijkl}^{(3)} \sigma_{kl}^{\beta} \right] \quad (5.10)$$

The parameters $w_{\alpha\beta}$ are responsible for the intensity-dependent part of the action vector Ω_{α} .

With the use of the relations in equation Eq.(5.10), the sixteen components for $w_{\alpha\beta}$ can be easily obtained as follows:

$$\begin{aligned} w_{00} &= \frac{12\pi}{n} \left\{ \sigma_{ji}^0 \left(\chi_{ijkl}^3 \right) \sigma_{kl}^0 \right\} = \frac{24\pi}{n} \left\{ \chi_{1111}^{(3)} + \chi_{1122}^{(3)} \right\} \\ w_{11} &= \frac{12\pi}{n} \left\{ \sigma_{ji}^1 \left(\chi_{ijkl}^3 \right) \sigma_{kl}^1 \right\} = \frac{24\pi}{n} \left\{ \chi_{1111}^{(3)} - \chi_{1122}^{(3)} \right\} \\ w_{22} &= \frac{12\pi}{n} \left\{ \sigma_{ji}^2 \left(\chi_{ijkl}^3 \right) \sigma_{kl}^2 \right\} = \frac{24\pi}{n} \left\{ \chi_{1122}^{(3)} + \chi_{1221}^{(3)} \right\} \\ w_{33} &= \frac{12\pi}{n} \left\{ \sigma_{ji}^3 \left(\chi_{ijkl}^3 \right) \sigma_{kl}^3 \right\} = \frac{24\pi}{n} \left\{ \chi_{1122}^{(3)} - \chi_{1221}^{(3)} \right\} \\ w_{01} &= w_{02} = w_{03} = w_{10} = 0 \\ w_{12} &= w_{13} = w_{20} = w_{21} = 0 \\ w_{23} &= w_{30} = w_{31} = w_{32} = 0 \end{aligned} \quad (5.11)$$

Hence the self-action vector Ω_{α} for light propagating along a fiber with small nonlinearities can now be obtained without much difficulty. For the case of a lossless fiber, all components of Ω_{α} are real. Therefore,

$$\Omega_0 = \frac{12\pi}{n} \left(\chi_{1111}^{(3)} + \chi_{1122}^{(3)} \right) S_0$$

$$\Omega_1 = \frac{12\pi}{n} \left(\chi_{1111}^{(3)} - \chi_{1122}^{(3)} \right) S_1$$

$$\Omega_2 = \frac{12\pi}{n} (\chi_{1122}^{(3)} + \chi_{1221}^{(3)}) S_2 \quad (5.12)$$

$$\Omega_3 = \frac{12\pi}{n} (\chi_{1122}^{(3)} - \chi_{1221}^{(3)}) S_3$$

Using the expressions in Eq.(5.12), the nonlinear evolution equations for

the Stokes parameters can now be written in the following form

$$\begin{aligned} \frac{dS_0}{dz} &= -\frac{6\pi\omega}{c} \text{Im} \left[\frac{2}{n} (\chi_{1111}^{(3)}) S_1^2 + \frac{1}{n} (\chi_{1111}^{(3)} + 2\chi_{1122}^{(3)} + \chi_{1221}^{(3)}) S_2^2 \right. \\ &\quad \left. + \frac{1}{n} (\chi_{1111}^{(3)} + 2\chi_{1122}^{(3)} - \chi_{1221}^{(3)}) S_3^2 \right] \\ \frac{dS_1}{dz} &= -\frac{12\pi\omega}{c} \left[\text{Im} \left\{ \frac{\chi_{1111}^{(3)}}{n} S_0 S_1 \right\} + \text{Re} \left\{ \frac{\chi_{1221}^{(3)}}{n} \right\} S_3 S_2 \right] \\ \frac{dS_2}{dz} &= -\frac{6\pi\omega}{c} \left[\text{Im} \left\{ \frac{1}{n} (\chi_{1111}^{(3)} + 2\chi_{1122}^{(3)} + \chi_{1221}^{(3)}) \right\} S_0 S_2 \right. \\ &\quad \left. + \text{Re} \left\{ \frac{1}{n} (2\chi_{1122}^{(3)} - \chi_{1111}^{(3)} - \chi_{1221}^{(3)}) \right\} S_1 S_3 \right] \\ \frac{dS_3}{dz} &= -\frac{6\pi\omega}{c} \left[\text{Im} \left\{ \frac{1}{n} (\chi_{1111}^{(3)} + 2\chi_{1122}^{(3)} - \chi_{1221}^{(3)}) \right\} S_0 S_3 \right. \\ &\quad \left. + \text{Re} \left\{ \frac{1}{n} (\chi_{1111}^{(3)} - 2\chi_{1122}^{(3)} - \chi_{1221}^{(3)}) \right\} S_1 S_2 \right] \end{aligned} \quad (5.13)$$

If the fiber is initially assumed to be lossless, then the refractive index n and cubic optical nonlinearity $\chi_{ijkl}^{(3)}$ are real and the expressions in Eq.(5.13) can now be written in the following simple form

$$\begin{aligned} \frac{dS_1}{dz} &= -\frac{12\pi\omega}{c} \left[\text{Re} \left\{ \frac{\chi_{1221}^{(3)}}{n} \right\} S_2 S_3 \right] \\ \frac{dS_2}{dz} &= \frac{12\pi\omega}{c} \left[\text{Re} \left\{ \frac{\chi_{1221}^{(3)}}{n} \right\} S_1 S_3 \right] \\ \frac{dS_3}{dz} &= 0 \\ \frac{dS_0}{dz} &= 0 \end{aligned} \quad (5.14)$$

It is noted that in obtaining Eq.(5.14), the fiber is also assumed to be isotropic.

It can be deduced readily from the last two expressions in Eq.(5.14), that S_0 and S_3 are constants and the wave ellipticity $\eta = \frac{1}{2} \sin^{-1} (S_3/S_0)$ does not change during propagation.

Consequently, the first two equations of (5.14) can now be written as

$$\frac{dS_1}{dz} = - \left[\frac{\omega}{c} \text{Re} \{ \chi^{eff} \} S_2 \right] \quad (5.15)$$

and

$$\frac{dS_2}{dz} = \frac{\omega}{c} \text{Re} \{ \chi^{eff} \} S_1 \quad (5.16)$$

where $\chi^{eff} = \left\{ \frac{12\pi}{n} \left(\chi_{1221}^{(3)} \right) S_0 \sin (2\eta) \right\}$. Equations (5.15) and (5.16) are two simple first order coupled differential equations which can now be solved in the usual way.

Thus, the solutions for Eq.(5.14) are

$$\begin{aligned} S_1(z) &= S_{10} \cos \left(\frac{\omega}{c} \text{Re} \{ \chi_0^{eff} \} z \right) - S_{20} \sin \left(\frac{\omega}{c} \text{Re} \{ \chi_0^{eff} \} z \right) \\ S_2(z) &= S_{20} \cos \left(\frac{\omega}{c} \text{Re} \{ \chi_0^{eff} \} z \right) + S_{10} \sin \left(\frac{\omega}{c} \text{Re} \{ \chi_0^{eff} \} z \right) \\ S_3(z) &= S_3(0) = S_{30} \\ S_0(z) &= S_0(0) = S_{00} \end{aligned} \quad (5.17)$$

where

$$\chi_0^{eff} = \left\{ \frac{12\pi}{n} \left(\chi_{1221}^{(3)} \right) S_{00} \sin (2\eta_0) \right\} \quad (5.18)$$

$S_{\alpha 0} = \{ S_{00}, S_{10}, S_{20}, S_{30} \}$ are the Stokes parameters for the input light and η_0 represents the initial angle of ellipticity. The expressions in Eq.(5.17) can be rewritten in matrix

form as follows:

$$\begin{pmatrix} S_0 \\ S_1 \\ S_2 \\ S_3 \end{pmatrix} = \begin{pmatrix} 1 & 0 & 0 & 0 \\ 0 & C_\Phi & -S_\Phi & 0 \\ 0 & S_\Phi & C_\Phi & 0 \\ 0 & 0 & 0 & 1 \end{pmatrix} \begin{pmatrix} S_{00} \\ S_{10} \\ S_{20} \\ S_{30} \end{pmatrix} \quad (5.19)$$

where $C_\Phi = \cos\left(\frac{\omega}{c} \text{Re}\{\chi_0^{eff}\}\right) z$ and $S_\Phi = \sin\left(\frac{\omega}{c} \text{Re}\{\chi_0^{eff}\}\right) z$. The 4×4 matrix in Eq.(5.19) is easily recognized as a Mueller matrix which contains terms that depend on the nonlinear perturbations of the fiber. It is worth noting that in order to obtain the Mueller matrix in Eq.(5.19), the fiber was assumed to be lossless so that the differential equations in Eq.(5.14) could be decoupled into Eqs. (5.15) and (5.16).

5.2 Nonlinear Polarization Effects

In Chapter 4, it was shown that anisotropy of the dielectric tensor led to birefringence in the fiber. If the fiber is assumed to be lossless and the initial polarization state of the light wave is linear and oriented along either principal axes of a highly birefringent fiber, the polarization state does not change as the light propagates through the fiber. However, if the initial state of the propagating wave is not linear or even if it is linear but off axis of a highly birefringent fiber, the polarization state will go from one elliptical polarization to the opposite handed elliptical polarization via a linearly polarized state and so on. This can be described by a precession of the Stokes vector around the birefringence vector so that from any initial position on the Poincaré sphere, the end of the Stokes vector of a propagating wave will trace out a vertical circle perpendicular to the birefringence vector. If losses are included and the birefringence is low or the fiber length is short, then for

linearly polarized incident wave there will be small changes in the polarization state of the light such that the change in azimuth $\Theta(L) - \Theta(0) \ll 1$ and the ellipticity $\eta(L) \ll 1$. A rotation of the polarization azimuth $\Theta(L) - \Theta(0)$ proportional to $Im\{(\Delta\epsilon/n)\}$ will occur due to the differential absorption of the two orthogonal linear eigenwaves. The propagation will yield ellipticity proportional to $Re\{(\Delta\epsilon/n)\}$ which is related to the differential refractive index of the eigenwaves.

The polarization phenomena described above is exhibited when nonlocality is neglected. That is, these polarization effects occur in the zero-order spatial dispersion approximation. Now when nonlocality is accounted for, optical activity is exemplified and the plane of polarization of the light rotates as the light propagates through the fiber. Such polarization effects appear in the first-order spatial dispersion approximation depicted by the linear nonlocality tensor $\Gamma_{ijz}^{(1)}$. Thus, it can be deduced that, the only reason for a change in the polarization of light propagating along an isotropic linear fiber is due to optical activity. To study the nonlinear effects, however, there is a need to account for the local and nonlocal nonlinearities, $\chi_{ijkl}^{(3)}$ and $\Gamma_{ijklz}^{(3)}$. These quantities have already been identified in equations (5.7) and (5.9). Consideration of these terms explains the dependence of the fiber on the intensity of the light wave. The main difference between a linear and nonlinear fiber, therefore, is that in a nonlinear fiber the susceptibilities depend on the light wave intensity and initial ellipticity. In what follows, several nonlinear polarization effects occurring in a fiber when local and nonlocal susceptibilities are considered will be analysed.

5.2.1 Nonlinear Anisotropic Effect

It is interesting to analyse the general case of a fiber without neglecting losses. Let the light be linearly polarized with polarization azimuth Θ_0 , then Stokes parameters can

be written as

$$S_{\alpha} = \{S_0, \cos 2\Theta_0, \sin 2\Theta_0, 0\} \quad (5.20)$$

It is reasonable to assume that only small polarization changes occur during propagation so that $\Theta(L) - \Theta_0 \ll \pi$ and $\eta(L) \ll \pi$. Then, using Eq.(5.13) yields the following formulae for the polarization azimuth and ellipticity of a light wave propagating along the optic axis of a lowloss birefringent fiber

$$\begin{pmatrix} \Theta(L) - \Theta_0 \\ \eta(L) \end{pmatrix} = \frac{8\pi^3 L}{\lambda c |1 + n|^2} \begin{pmatrix} Im \\ -Re \end{pmatrix} \left\{ \frac{\Delta\chi}{n} \right\} I \sin 4\Theta_0 \quad (5.21)$$

where L is the length of the fiber, I is the intensity of the light wave with wavelength λ approaching the fiber of core refractive index n from vacuum and

$$\Delta\chi = \chi_{1111}^{(3)} - 2\chi_{1122}^{(3)} - \chi_{1221}^{(3)} \quad (5.22)$$

Thus, it is seen from Eq.(5.21) that even when nonlocality is neglected, the orientation angle of the polarization ellipse of an initially linearly polarized light will rotate. The polarization azimuth of an intense light beam rotates even if the initial ellipticity of the light is zero. This is a nonlinear anisotropic polarization effect and its sign depends on the initial polarization azimuth Θ_0 . If $\sin 4\Theta_0 = 0$, i.e. the light is polarized along the [100] direction (fiber X-axis), the [010] direction (fiber Y-axis), the bisector [110] between X and Y, or perpendicular to this bisector, there will be no polarization change occurring. However, for any other initial polarization, the polarization state of the wave will change. If a fiber were lossless, the refractive index n and cubic optical nonlinearity $\chi_{ijkl}^{(3)}$ would be real. Then, the light will become elliptically polarized, but the main axis of the ellipse will retain its initial azimuth. This self-induced ellipticity will be proportional to the intensity and the length of the fiber. However, fibers have low losses and thus n or $\chi_{ijkl}^{(3)}$ is complex and the self-induced ellipticity will be accompanied by a rotation of the polarization azimuth.

The nonlinear anisotropic effects for small induced polarization azimuth rotation manifests itself in a way similar to nonlinear optical activity and early works [13] referred to it as (NLOA-II), a second type of nonlinear optical activity. Therefore, it can be concluded that the nonlinear anisotropic polarization effect reveals hidden anisotropy of third order local optical nonlinearity. This anisotropic effect is represented by $\Delta\chi = \chi_{1111}^{(3)} - 2\chi_{1122}^{(3)} - \chi_{1221}^{(3)}$. This combination of components of the cubic optical nonlinearity tensor is zero by symmetry if the fiber is considered totally isotropic. Self induced ellipticity due to nonlinear anisotropic effect has been observed in a range of highly transparent alkali-halid crystals of the $m3m$ point group.^[13] In these crystals, $Im\{\Delta\chi\} = 0$ in the visible range and no polarization azimuth rotation can take place. However, $Re\{\Delta\chi\}$ is not necessarily zero and according to Eq.(5.21), an initially linearly polarized light becomes elliptically polarized if $Re\{\Delta\chi\} \neq 0$. It is also worth noting here that the nonlinear anisotropic effect has very interesting spectroscopic applications for a fiber since it is sensitive to departures of the fibers crystal electronic structure from isotropy. Also, the anisotropic polarization effect is most pronounced along the cubic direction [001] which is the axis of propagation in the fiber.

5.2.2 Nonlinear Polarization Self-Ellipse Rotation

Another fundamental nonlinear polarization effect in a birefringent single mode optical fiber is that of polarization ellipse self-rotation. This effect was first observed by Maker, Terhune and Savage and presented in an experimental paper on nonlinear polarization effects [24]. Polarization ellipse can be easily deduced when the nonlocal susceptibilities (linear and nonlinear) are neglected but only if the light wave is initially elliptically polarized [13]. Then, the initial ellipticity $\eta_0 \neq 0$ and with the use of Eq.(5.18) it can be

shown that

$$\Theta^{ESR}(L) - \Theta_0 = \frac{32\pi^3 L}{\lambda c n |1 + n|^2} \text{Re} \{ \chi_{1221}^{(3)} \} S_{00} \sin(2\eta_0) \quad (5.23)$$

Eq.(5.23) indicates that the polarization azimuth rotates as the wave propagates along the length of the fiber. This effect is referred to as polarization ellipse self-rotation. The rotation requires an initial ellipticity η_0 which does not change during propagation so that $\eta(L) = \eta_0$. On the Poincaré sphere, this effect is represented by a point tracing out a horizontal arc above or below the equator [see Fig.(3-3)]. The length of the arc is proportional to the length of the fiber and increases with intensity and initial ellipticity. Depending on the sign of the initial ellipticity, the azimuth will be positive or negative. Clearly, Eq.(5.23) refers to a lossless fiber. However, for the general case in which losses in the fiber are accounted for, the imaginary part of $\chi_{1221}^{(3)}$ is considered and the azimuth is accompanied by an intensity-dependent change in the ellipticity of the light wave.

5.2.3 Polarization Instability

It has been shown in earlier sections that in optical fibers, the light waves are generally elliptically polarized and in the special case of a polarization maintaining fiber they are orthogonally linearly polarized. In linear optics, the polarization of the propagating wave is independent of the intensity of the light. In nonlinear optics, however, the refraction, absorption, and anisotropy of the fiber are all functions of the wave intensity. It has been shown [13] that when the input intensity or polarization of light undergoes a slow change, the output polarization is found to be a multivalued function containing both stable and unstable branches. The output polarization state depends on the prehistory of the excitation (polarization hysteresis). Given a particular combination of the parameters of the input field, the output polarization may oscillate in time or even change randomly with continuous frequency spectrum creating polarization chaos. Furthermore, whereas

in linear optics the polarization of the wave either oscillates along the direction of propagation or steadily tends towards one of the eigenpolarizations which remain unchanged, in nonlinear propagation, the polarization parameters along the propagation coordinate may change abruptly and can depend strongly and unpredictably on the initial conditions. This illustrates the phenomena of polarization instability and chaos which often appear in nonlinear interactions between two waves. But, simple examples of polarization instability can be seen in self-action effects. This section discusses how polarization instability develops for intense light in a birefringent single mode fiber.

Consider that light propagates along the symmetry axis of a nonlinear birefringent fiber having local optical response. Assuming that the X and Y Cartesian axes of the laboratory frame coincides with the major and minor axes of the fiber, the components of the self-action four vector can be expressed as

$$\begin{aligned}\Omega_0 &= \frac{48\pi}{n} \chi_{1122}^{(3)} S_0 \\ \Omega_1 &= \frac{\epsilon_{11} - \epsilon_{33}}{n} + \frac{24\pi}{n} \chi_{1122}^{(3)} S_1 \\ \Omega_2 &= \frac{24\pi}{n} \chi_{1122}^{(3)} S_2 \\ \Omega_3 &= 0\end{aligned}\tag{5.24}$$

In obtaining Eq.(5.24), small anisotropy is assumed along the direction of propagation and is accounted for in the dielectric tensor while the cubic nonlinearity is presumed isotropic. If losses are initially neglected, the nonlinear evolution equations become

$$\begin{aligned}\frac{dS_0}{dz} &= 0 \\ \frac{dS_1}{dz} &= - \left(\frac{12\pi\omega}{cn} \chi_{1122}^{(3)} \right) S_2 S_3 \\ \frac{dS_2}{dz} &= \frac{\omega}{2cn} \left(\epsilon_{11} - \epsilon_{33} + 24\pi \chi_{1122}^{(3)} S_1 \right) S_3\end{aligned}\tag{5.25}$$

and

$$\frac{dS_3}{dz} = - \left\{ \frac{\omega}{2cn} (\epsilon_{11} - \epsilon_{33}) \right\} S_2$$

The evolution equations can now be arranged into equations describing the polarization azimuth Θ and ellipticity angle η of the wave as follows:

$$\begin{aligned} \frac{d\Theta}{dz} &= \delta' \tan 2\eta \cos 2\Theta + \delta^{NL} \sin 2\eta \\ \frac{d\eta}{dz} &= -\delta' \sin 2\Theta \end{aligned} \quad (5.26)$$

where

$$\delta' = \frac{\omega}{4cn} (\epsilon_{11} - \epsilon_{33}) \quad (5.27)$$

and

$$\delta^{NL} = \frac{3\pi\omega\chi_{1122}^{(3)}S_{00}}{cn} \quad (5.28)$$

are measures of anisotropy and nonlinearity, respectively.

To analyse the stability of the eigenpolarizations with increasing wave intensity, there is a need to observe the development of small fluctuations $\Delta\Theta$ and $\Delta\eta$ in the polarization azimuth and ellipticity. If these small fluctuations lead to a drastic departure of the output polarization from the incident one, the polarization state is said to be unstable. To introduce an initial fluctuation of the light polarization azimuth $\Delta\Theta = \Theta - \Theta_0$ at $z = 0$, let the incident wave be linearly polarized close to the X direction but not strictly along it, then Eq.(5.26) takes the following simple form

$$\begin{aligned} \frac{d\Theta}{dz} &= 2(\delta' + \delta^{NL})\eta \\ \frac{d\eta}{dz} &= -2\delta'\Theta \end{aligned} \quad (5.29)$$

Differentiating the first of these equations with respect to z , and substituting $d\eta/dz$ from the second equation gives the following second-order differential equation for the

polarization azimuth

$$\frac{d^2\Theta}{dz^2} + 4\delta' (\delta' + \delta^{NL}) \Theta = 0 \quad (5.30)$$

The solution to Eq.(5.30) obviously depends on the sign of $\delta' (\delta' + \delta^{NL})$. In lossless media, $\chi_{1122}^{(3)}$ is real and as a rule positive. That is, δ^{NL} is real and positive. Therefore $\delta' (\delta' + \delta^{NL}) > 0$ for all values of δ' and δ^{NL} except when $-\delta^{NL} < \delta' < 0$. Thus, for $\delta' (\delta' + \delta^{NL}) > 0$, Eq.(5.30) has the following solution

$$\Theta = \Delta\Theta \cos \left[2\sqrt{\delta' (\delta' + \delta^{NL})} z \right] \quad (5.31)$$

In this case, the polarization azimuth oscillates within strict limits imposed by the initial fluctuation $\Delta\Theta$, and so linear polarization along the X direction is stable. When $\delta' (\delta' + \delta^{NL}) < 0$, the solution to Eq.(5.30) is

$$\Theta = \Delta\Theta \cosh \left[2\sqrt{\delta' (\delta' + \delta^{NL})} z \right] \quad (5.32)$$

For $z^2 \geq 1/|4\delta' (\delta' + \delta^{NL})|$,

$$\Theta = \frac{\Delta\Theta}{2} \exp \left[\sqrt{-\delta' (\delta' + \delta^{NL})} z \right] \quad (5.33)$$

Here, a small initial fluctuation $\Delta\Theta$ of the polarization azimuth will exponentially increase with propagation. Therefore, for $\delta' (\delta' + \delta^{NL}) < 0$, linear polarization along the X direction is unstable. The condition $\delta' (\delta' + \delta^{NL}) < 0$ for polarization instability can be expressed in terms of material parameters. This condition is achieved if

$$\chi_{1122}^{(3)} S_{00} > \frac{\epsilon_{33} - \epsilon_{11}}{24\pi} > 0 \quad (5.34)$$

Therefore, polarization instability requires ϵ_{11} to be smaller than ϵ_{33} , that is, the refractive index for a wave polarized along the X direction, $n_x = \epsilon_{11}^{1/2}$, should be smaller than the refractive index $n_y = \epsilon_{33}^{1/2}$ for a wave polarized along the Y direction. Only

the eigenpolarization with the smaller refractive index can be unstable. Note that the left-hand-side of the inequality (5.34) also imposes a condition on the light intensity. Polarization instability occurs if $24\pi\chi_{1122}^{(3)}S_{00} > \epsilon_{33} - \epsilon_{11}$ or in terms of the threshold light intensity I_0 ,

$$I > I_0 = \frac{cn(n_y - n_x)(1 + n)^2}{96\pi^2\chi_{1122}^{(3)}} \quad (5.35)$$

This is polarization instability for the intensity of a wave approaching a crystal with core refractive coefficient n from a vacuum. Reflection losses at the boundary is taken into account in this expression. If the intensity exceeds the threshold value in Eq.(5.35) a small fluctuation of the incident polarization state will lead to a very considerable change in the output polarization. Depending on the sign of the initial fluctuation, the wave will become right or left elliptically polarized.

Polarization instability in a birefringent media was purely academic when Sala first drew attention to the trigger behavior of the polarization of light in a birefringent crystal [26]. The intensity threshold for polarization instability is easily achieved in optical fibers with small birefringence. Quartz glass optical fibers typically have nonlinearities of $\chi_{1122}^{(3)} \simeq 10^{-15}$ esu. For a fiber with birefringence of $n_y - n_x \simeq 10^{-7}$ and $n \simeq 1.5$ the polarization instability threshold intensity is about $I_0 = 10^{17}$ erg/cm², which is equivalent to $I_0 = 10$ GW/cm². With a fiber core of $5\mu m$ diameter, the threshold power required for the observation of polarization instability is of the order of several kilowatts. A number of works, both theoretical and experimental have been published [2, 7, 8, 13] on this problem. A similar effect of polarization instability occurs with circularly polarized light in a birefringent media. When light intensity exceeds a threshold value, circular polarization becomes unstable. Infact, polarization instability was first seen in a birefringent fiber with circularly polarized light in 1986 [10].

Polarization instability can also be seen along the direction of propagation in a fiber. This type of instability does not require the intensity to exceed a threshold value but rather develops as an exponential instability. If the initial polarization state is linear, at

an angle Θ_0 to the X direction in the natural coordinate frame, then

$$\mathbf{S} = S_{00} (\cos 2\Theta_0, \sin 2\Theta_0, 0) \quad (5.36)$$

and for a lossless fiber, the formula in Eq.(5.13) may be written as

$$\begin{aligned} \frac{dS_0}{dz} &= 0 \\ \frac{dS_1}{dz} &= -\frac{12\pi\omega}{cn} \chi_{1122}^{(3)} S_2 S_3 \\ \frac{dS_2}{dz} &= \frac{6\omega}{cn} (2\chi_{1122}^{(3)} + \Delta\chi) S_1 S_3 \\ \frac{dS_3}{dz} &= -\frac{6\pi\omega}{cn} (\Delta\chi) S_1 S_2 \end{aligned} \quad (5.37)$$

where $\Delta\chi = \chi_{1111}^{(3)} - 3\chi_{1122}^{(3)}$. Note that in this case, $\Delta\chi \neq 0$; it is zero by symmetry in isotropic media and thus shows the difference between the nonlinearity tensor in isotropic media and a cubic media like an optical fiber. These evolution equations may be rearranged directly into equations for the polarization azimuth Θ and ellipticity η as follows

$$\begin{aligned} \frac{d\Theta}{dz} &= \frac{1}{2} (2\delta^{NL} + \delta_a^{NL} \cos^2 2\Theta) \sin 2\eta \\ \frac{d\eta}{dz} &= -\frac{1}{4} \delta_a^{NL} \sin 4\Theta \cos 2\eta \end{aligned} \quad (5.38)$$

where

$$\delta^{NL} = \frac{6\pi\omega}{cn} \chi_{1122}^{(3)}$$

and

$$\delta_a^{NL} = \frac{6\pi\omega}{cn} \Delta\chi$$

From Eq.(5.38), it follows that polarizations which exactly satisfy the conditions $\sin 4\Theta = 0$ and $\eta = 0$ will not change since the right-hand sides of the evolution equations become

zero. To obtain the instability of these polarizations a small fluctuation $\Delta\Theta$ is introduced in the polarization azimuth of the incident wave allowing $\Delta\Theta(0) = \Delta\Theta + \Theta_0$ with $\sin 4\Theta_0 = 0$ and $\eta(0) = 0$. In this case, Eq.(5.38) may be written in simplified form for $\Theta - \Theta_0 \ll \pi$ and $\eta \ll \pi$ as follows:

$$\begin{aligned} \frac{d\Theta}{dz} &= (2\delta^{NL} + \delta_a^{NL} \cos^2 2\Theta_0) \eta \\ \frac{d\eta}{dz} &= -\delta_a^{NL} \cos 4\Theta_0 \end{aligned} \quad (5.39)$$

Solving Eq.(5.39) yields

$$\Theta = \theta_0 + \Delta\Theta \cos \sqrt{\mu z} \quad (5.40)$$

and

$$\eta = \frac{\Delta\Theta \sqrt{\mu}}{2\delta^{NL} + \delta_a^{NL} \cos^2 2\Theta_0} \sin \sqrt{\mu z} \quad (5.41)$$

where

$$\mu = (2\delta^{NL} + \delta_a^{NL} \cos^2 2\Theta_0) \delta_a^{NL} \cos 4\Theta_0 \quad (5.42)$$

The character of these solutions depends on the sign of μ . For positive μ , the polarization azimuth and ellipticity will oscillate within strict limits imposed by the initial fluctuation $\Delta\Theta$, and the incident linear polarization will be stable. For negative μ , the solution will become exponential in nature: $\cos(\mu^{1/2}z) = \cosh(|\mu^{1/2}|z) \simeq \frac{1}{2} \exp(|\mu^{1/2}|z)$. Therefore for $\mu < 0$ and $|\mu^{1/2}|z \gg 1$, the output polarization will depart exponentially from the input one. For small anisotropy, $\Delta\chi < |\chi_{1122}|$, and therefore $|\delta^{NL}| \ll |\delta_a^{NL}|$. Since the nonlinearity is often positive, that is $\chi_{1122} > 0$ and $\delta^{NL} > 0$, the term in the brackets in the first equation of (5.38) is positive. Therefore, the sign μ and the stability of the polarization state will depend on the sign of $\delta_a^{NL} \cos^2 2\Theta_0$, that is, on the sign of $\Delta\chi \cos 4\Theta_0$. For

$$\Delta\chi \cos 4\Theta_0 < 0$$

the initial linear polarization corresponding to $\sin 4\Theta_0 = 0$ is unstable. If, however,

$$\Delta\chi \cos 4\Theta_0 > 0$$

the linear polarization corresponding to $\sin 4\Theta_0 = 0$ is stable.

It is now appropriate to present the general solutions to the system of coupled nonlinear differential equations expressed in Eq.(5.25) which will describe the characteristics of an intense light wave propagating in an optical fiber with small losses and anisotropy. The anisotropy will be accounted for in the dielectric tensor and the nonlinear susceptibility tensor components are presumed to be strictly real and isotropic. The approach of [26] was used in this work to obtain a closed-form solution to these nonlinear differential equations. Firstly, it is noted that Eq.(5.25) can be rewritten as

$$\begin{aligned} \frac{dS_0}{dz} &= 0 \\ \frac{dS_1}{dz} &= -R_1 S_2 S_3 \\ \frac{dS_2}{dz} &= R_0 S_3 + R_1 S_1 S_3 \\ \frac{dS_3}{dz} &= -R_0 S_2 \end{aligned} \tag{5.43}$$

where $R_0 = \omega\Delta\epsilon/2nc$ and $R_1 = 12\pi\omega\chi_{1122}^{(3)}/nc$. With the use of the second and third equations in Eq.(5.25), S_2 can be eliminated to obtain

$$\frac{d}{dz} (2R_0 S_1 - R_1 S_3^2) = 0 \tag{5.44}$$

which when integrated will yield

$$2R_0 (S_1 - S_{10}) = R_1 (S_3^2 - S_{30}^2) \tag{5.45}$$

It is immediately seen from Eq.(5.45) that only one of the stokes parameters is indepen-

dent. Furthermore, S_1 can also be eliminated by squaring the last equation of Eq.(5.43) and considering that the light is completely polarized so that

$$S_1^2 + S_2^2 + S_3^2 = 1 \tag{5.46}$$

then one obtains

$$\left(\frac{dS_3}{dz}\right)^2 = -B_1 S_3^4 - B_2 S_3^2 + B_3 \tag{5.47}$$

where

$$\begin{aligned} B_1 &= \frac{1}{4}R_1^2 \\ B_2 &= R_0^2 + R_1 \left(R_0 S_{10} - \frac{1}{2}R_1 S_{30}^2 \right) \\ B_3 &= R_0^2 - \left(R_0 S_{10} - \frac{1}{2}R_1 S_{30}^2 \right) \end{aligned} \tag{5.48}$$

Equation (5.47) can be re-expressed as

$$\left(\frac{dS_3}{dz}\right)^2 = -B_1 (S_3^2 - \alpha_1) (S_3^2 - \alpha_2) \tag{5.49}$$

where

$$\alpha_{1,2} = \frac{-B_2 \pm \sqrt{B_2^2 + 4B_1 B_3}}{2B_1} \tag{5.50}$$

are the roots of Eq.(5.47). Hence, Eq.(5.49) can now be expressed as

$$\sqrt{B_1} \int_0^z dz = \pm \int_y^b \frac{dS_3}{\sqrt{(S_3^2 + a^2)(b^2 - S_3^2)}} \tag{5.51}$$

where $a^2 = -\alpha_2$ and $b^2 = \alpha_1$. Solutions to Eq.(5.51) are in the form of elliptic functions [61] and are given as (see Appendix D)

$$S_3 = \pm \sqrt{\alpha_1} \operatorname{cn} \left(\sqrt{B_1 (\alpha_1 - \alpha_2)} z + C ; k \right) \tag{5.52}$$

where C is a constant and $k = \sqrt{(\alpha_1/\alpha_1 - \alpha_2)}$ is the modulus. Equation (5.52) can be written more compactly as

$$S_3 = \frac{2pkf}{r} \text{cn}(R_0fz + C; k) \quad (5.53)$$

where $r = R_1/R_0$ and $f = [(1 + rS_{10})^2 - r^2S_{20}^2]^{\frac{1}{4}}$. Also, $p = \pm 1 = \text{sgn}(S_{30})$ with the sign function defined as $\text{sgn}(x) = 1$ for $x \geq 0$ and $\text{sgn}(x) = -1$ for $x < 0$. The solutions for S_2 and S_1 are obtained as follows (see Appendix D)

$$S_2 = \frac{2pkf^2}{r} [\text{sn}(R_0fz + C; k)] \text{dn}(R_0fz + C; k) \quad (5.54)$$

and

$$S_1 = \frac{f^2}{r} \left\{ 1 - 2m [\text{sn}^2(R_0fz + C; k)] \right\} - 1 \quad (5.55)$$

These solutions describe the characteristics of an arbitrarily intense beam propagating along a low-loss optical fiber. The solutions are both general since no restrictions are placed on the relative strength of the optical fields and are exact since the set of coupled nonlinear equations are solved in terms of known transcendental functions. These results contain those for self induced ellipse rotation and the linearly polarized optical Kerr effect [26].

It is seen from Eq.(5.53), Eq.(5.54) and Eq.(5.55) that the output Stokes parameters are dependent on the Jacobian modulus k which in turn depends on the initial values of the Stokes parameters as well as the nonlinear susceptibility tensor and the anisotropic dielectric tensor. Therefore, in order to describe the propagation characteristics of the optical beam for different initial polarization states, it is important to deduce a relationship between k and the ratio r which is a relative measure of the anisotropy and the cubic nonlinear susceptibility of the fiber. Thus, using the definition of k as well as Eq.(5.50)

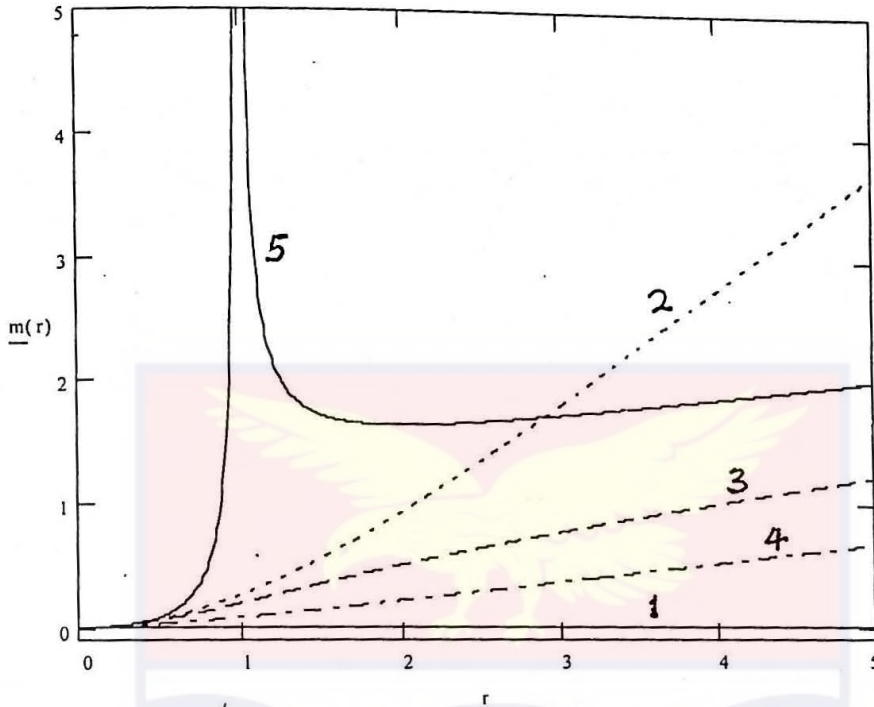


Figure 5-1: Jacobian parameter m as a function of the ratio r for initial polarization states S_{10} , S_{20} , and S_{30} of (1) 1, 0, 0; (2) 0, 0.3, 1; (3) 0, 0.71, 0.71; (4) 1, 0, 0.8; (5) -1, 0, 0.8.

and Eq.(5.48), one obtains the following expression

$$m = \frac{1}{2} + \frac{r^2 S_{30}^2 - 2(1 + rS_{10})}{4\sqrt{[(1 + rS_{10})^2 + r^2 S_{20}^2]}} \quad (5.56)$$

where the Jacobian parameter $m = k^2$ has been used.

With the use of Eq.(5.56), therefore, one can obtain the variation of the parameter m with r for different initial polarization states [see Fig.(5-1)]. It is noted that similar results were obtained in [26].

Fig.(5-1) shows, for five different initial polarization states, the values of r for which m is defined. It is seen that $m \geq 0$ for all values of $r \geq 0$. It can also be deduced from the figure that there is a value of r for which m is not defined. This special case occurs when $S_{20} = 0$, $S_{10} < 0$, and $r = 1$. In particular, examples 4 and 5 of this figure illustrate

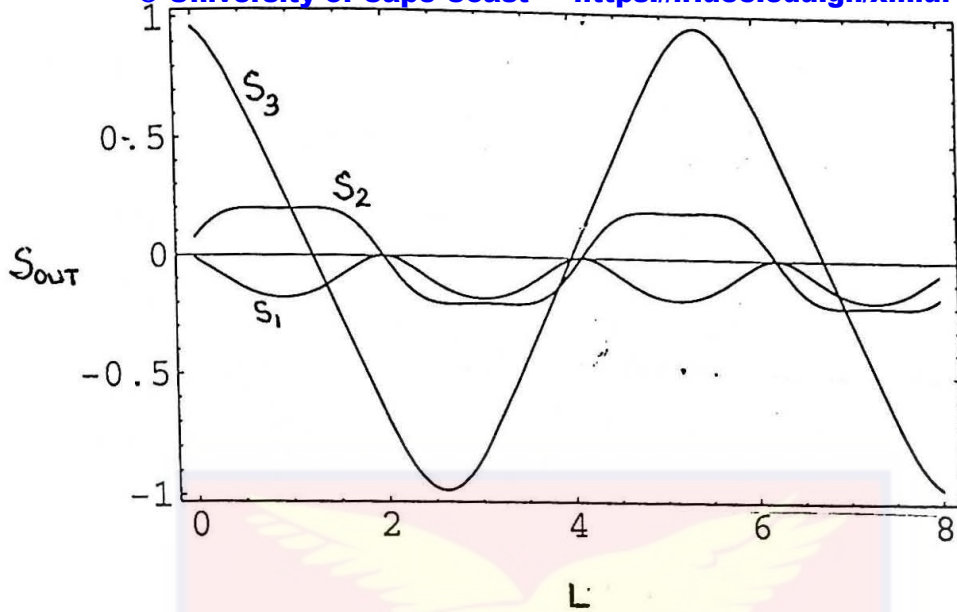


Figure 5-2: Variation of Stokes parameters as a function of fiber length for the initial polarization state $S_{10} = 0$, $S_{20} = 0.71$, and $S_{30} = 0.71$. The dependence of $m(r)$ for this initial state is given by curve 3. In this figure $r = 2.3$ and $m = 0.58$.

the two-cases where $S_{20} = 0$ but the radically different $m(r)$ dependence for example 5 results from simply changing the sign of S_{10} which physically indicates a 90° rotation of the initial polarization ellipse.

Thus, one can now obtain numerical solutions for the variation in the Stokes parameters using Eq.(5.53), Eq.(5.54) and Eq.(5.55) with knowledge of the $m(r)$ values obtained from along a curve of Fig.(5-1). Typical results obtained for propagation characteristics of the light beam for various values of the ratio r are illustrated in Figs.(5-2) to (5-5). For an input light with initial polarization state $S_{10} = 0$, $S_{20} = 0.71$, and $S_{30} = 0.71$ corresponding to a right elliptically polarized beam with 45° azimuthal angle and 22.5° ellipticity, Figs.(5-2) and (5-3) show, respectively for $r = 2.3$ and $r = 4$, the variations in the Stokes parameters as a function of fiber length. Another set of interesting results for an input light with initial polarization state $S_{10} = 0$, $S_{20} = 0.3$, and $S_{30} = 1$ corresponding to a right elliptically polarized beam with 45° azimuthal angle and 37° ellipticity are shown in Figs.(5-4) and (5-5) for $r = 2.3$ and $r = 4$, respectively.

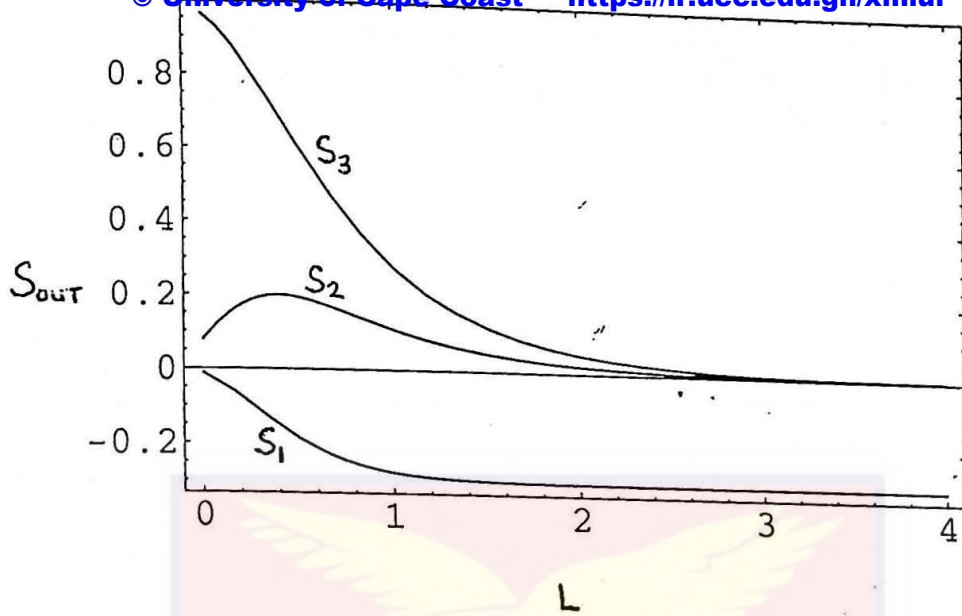


Figure 5-3: Variation of Stokes parameters as a function of fiber length for the initial polarization state $S_{10} = 0$, $S_{20} = 0.71$, and $S_{30} = 0.71$. The dependence of $m(r)$ for this initial state is given by curve 3. In this figure $r = 4$ and $m = 1$.

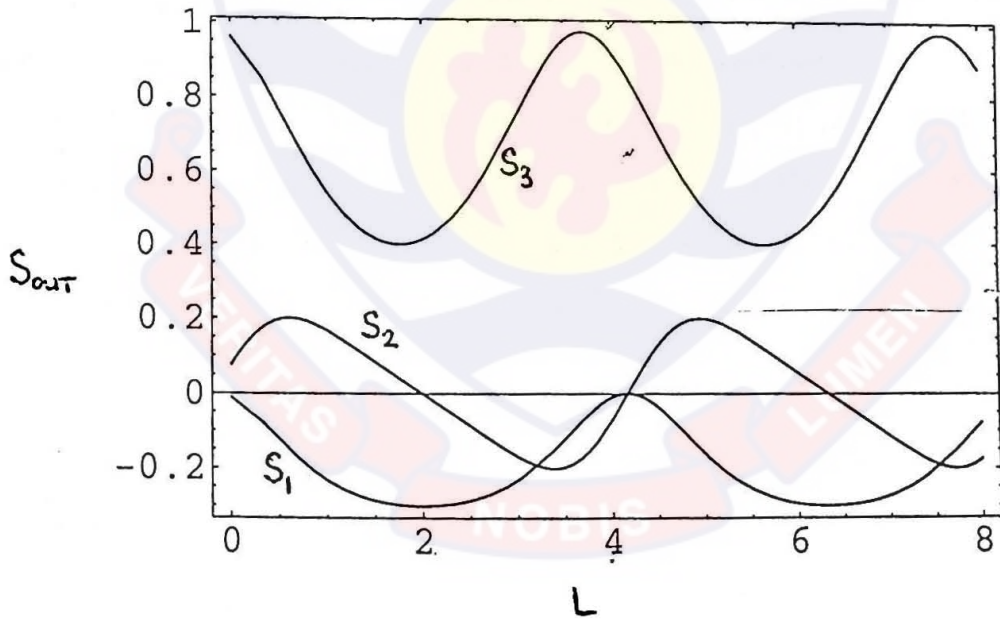


Figure 5-4: Variation of Stokes parameters as a function of fiber length for the initial polarization state $S_{10} = 0$, $S_{20} = 0.3$, and $S_{30} = 1$. The dependence of $m(r)$ for this initial state is given by curve 2. In this figure $r = 2.3$ and $m = 1.2$.

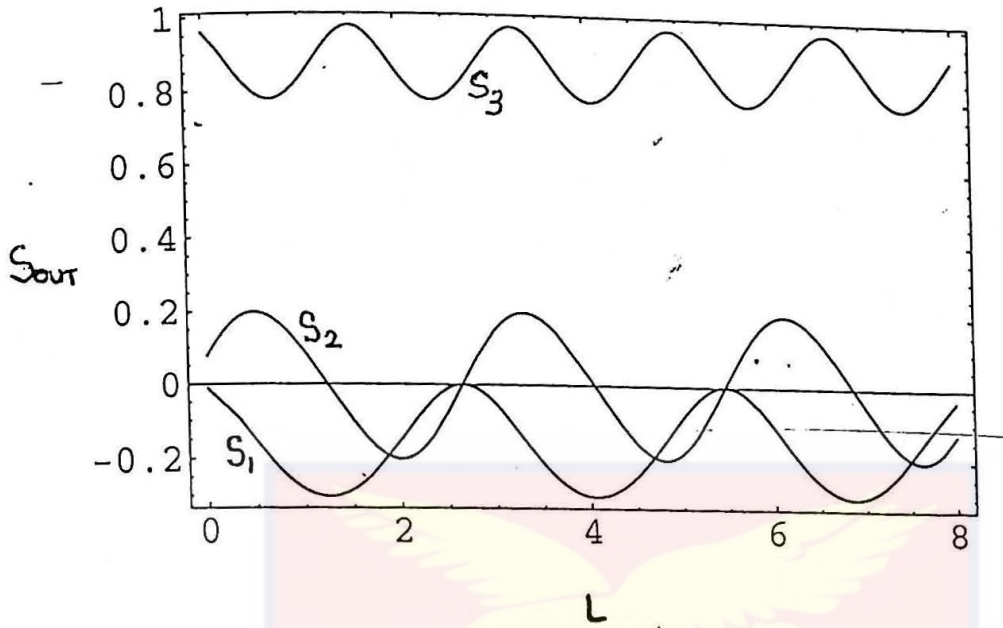


Figure 5-5: Variation of Stokes parameters as a function of fiber length for the initial polarization state $S_{10} = 0$, $S_{20} = 0.3$, and $S_{30} = 1$. The dependence of $m(r)$ for this initial state is given by curve 2. In this figure $r = 4$ and $m = 2.7$.

It is observed from these figures that the solutions are periodic for the output Stokes parameters having $0 \leq m < 1$ and $m > 1$. However, the case of $m = 1$ is special. The polarization tends asymptotically to a final state instead of varying periodically as in the other cases when $m \neq 1$. Fig.(5-3) shows this aperiodic behavior when $m = 1$ for the same initial polarization state as Fig.(5-2). The final state in the example of Fig.(5-3) corresponds to a linearly polarized optical beam.

5.2.4 Nonlinear Optical Activity

Nonlinear optical activity (NLOA) was first predicted in 1967 [25]. It is a nonlinear analog of the conventional optical activity (OA) mentioned earlier in Chapter 4. This effect is easily identified if the incident light wave is linearly polarized [13]. Then in such

a case, the polarization azimuth becomes a function of the medium length expressed as

$$\Theta(L) = \Theta_0 + \Theta^{OA}(L) + \Theta^{NLOA}(L) \quad (5.57)$$

where

$$\Theta^{OA}(L) = \frac{2\pi^2 L}{\lambda^2} \text{Re}\{\Gamma^a\} \quad (5.58)$$

and

$$\Theta^{NLOA}(L) = \frac{64\pi^4 L}{c\lambda^2(1+n)^2} \text{Re}\{\Gamma_{2111}^3\} S_{00} \quad (5.59)$$

S_{00} is the intensity of the incident light with wavelength λ propagating in an optical medium with negligible loss of refractive index n . The angles here are measured in radians. $\Theta^{OA}(L)$ describes the polarization plane rotation due to natural optical activity and $\Theta^{NLOA}(L)$ gives the polarization azimuth rotation due to intensity-dependent, nonlinear optical activity. From above, the nonlinear optical activity is simply an additive to the natural optical rotation proportional to $\text{Re}\{\Gamma_{2111}^3\}$. If losses in the medium are considered, then $\text{Im}\{\Gamma_{2111}^3\} \neq 0$ due to fast electronic mechanisms and light initially linearly polarized will become elliptically polarized, with ellipticity increasing with intensity. This phenomena is analogous to circular dichroism in linear fiber optics where linearly polarized light becomes elliptically polarized in an optically active fiber when $\text{Im}\{\Gamma^a\} \neq 0$ as discussed in Section (4.2). Nonlinear optical activity has its origin from two fundamental sources. Intensity-dependent optical activity can be due to thermal mechanism of nonlinearity as observed in an experiment using SiO_2 in which the *NLOA* resulted from heating of the crystal by an intense laser pulse [13]. *NLOA* has also been intensively studied experimentally with effort concentrated on the search for the fast electronic mechanism nonlinear optical activity. The *NLOA* can be represented on the Poincaré sphere by an arc parallel to the equator indicating that the light does not change its ellipticity but the azimuth changes steadily. The length of the arc is proportional to the length of the fiber. The arc consists of two segments: one is due to natural activity and the other is due to nonlinear optical activity. The length due to *NLOA* increases

with intensity.

It must be emphasized that even though nonlocality vanishes in optical fibers due to symmetry requirements, an intensity-dependent optical activity due to thermal effects of nonlinearity can be observed [13].



Chapter 6

DISCUSSION OF RESULTS

Expressions describing the linear polarization effects in a birefringent single mode optical fiber were obtained analytically within the framework of the unified formalism for polarization optics. Using the methods of this formalism, several Mueller matrices which characterize the interaction of a beam with an optical fiber were calculated so that the effects on the polarization of the light could be determined. The matrices obtained were as follows: (1) Mueller matrix for an optically active birefringent fiber without dichroism for the specific case in which circular birefringence was present but linear birefringence off-axis was assumed absent, (2) Mueller matrix for an optically active birefringent fiber without dichroism for the specific case in which circular birefringence is present but linear birefringence off-axis was assumed present, (3) Mueller matrix for an optically active birefringent fiber without dichroism for the specific case in which circular birefringence is assumed absent but linear birefringence off-axis was assumed present, (4) Mueller matrix for an optically active birefringent fiber with losses for the specific case in which only circular birefringence and dichroism were assumed present in the optical fiber, (5) Mueller matrix for an optically active birefringent fiber with losses for the specific case in which only circular birefringence and dichroism were assumed absent in the optical fiber, and (6) general Mueller matrix for an optically active birefringent fiber with different sources of birefringence and dichroism present for the case in which the birefringence and

dichroism vectors were not necessarily parallel.

The elements of each matrix were expressed in terms of their functional forms to facilitate the simulation of models that would determine the polarization behavior of the light as a function of the fiber length with negligible nonlinear effects assumed. Several results for different input polarization states were obtained and illustrated in Figs.(4-1) through (4-24). These solutions can be divided into two classes according to whether the fiber was assumed to have losses or not. When there were no dichroism, the output Stokes parameters were seen to be either periodic or to have a constant value see Figs.(4-1) to (4-16). It was observed from comparing Figs.(4-1) to (4-4) with Figs.(4-5) to (4-8) that the presence of circular birefringence, which is related to introducing twists in a fiber, induces a change in the polarization state of the light as it evolves along the fiber for linear and elliptically polarized input light. This variation in the polarization can be attributed to the linear anisotropy as a result of twisting the fiber. Thus, the perturbation which results from twisting the fiber causes the polarization state to change when the input light is either linear on-axis, off-axis or elliptical. It is further seen from Figs.(4-3) and (4-7) that when the input light is circularly polarized, the output beam polarization states do not vary as in the other cases. It can therefore be deduced that in the presence of optical activity, circular polarization becomes an eigenpolarization. Furthermore, in the examples where the polarization states are found to be periodic, the Stokes parameters are observed to have the same periods. See Figs.(4-1), (4-2), and (4-4) as well as Figs.(4-6) and (4-8).

However, the results were dramatically different when dichroism was assumed to be present in the optical fiber as shown in Figs.(4-17) to (4-24). These solutions show that the intensity of the input light is dissipated by the fiber. This is due to the presence of losses in the fiber. They showed the changes that occur in the output Stokes parameters as the light propagates along an optical fiber assumed to have small losses for different input polarization states. All of these results show a characteristic exponential decrease in the total intensity of the propagating light wave. The various sources of losses in

the fiber causes the beam's intensity to rapidly attenuate as it traverses along the fiber so that the optical fields become attenuated with distance. A particularly interesting result occurs as shown in Fig.(4-23) for the output polarization of the propagating light when the input light is right circularly polarized and circular birefringence and dichroism are assumed absent. In this case, the polarization of the output beam changes from circular to elliptical and back to circular. Note the damped oscillatory form of the Stokes parameter S_2 whose magnitude and period of oscillation tend to decrease with length.

It is also interesting to observe the behavior of the output Stokes parameters as a function of the orientation angle of the polarization ellipse. It was observed that for linearly polarized input light as a function of orientation angle, the output was seen to be linear and the presence of optical activity introduces a variation in the polarization states. When the input light was elliptically polarized, the output light was found to also be elliptical. However, for circularly polarized input light, the output light was circularly polarized but independent of orientation angle. Figs.(6-1) and (6-2) show the polarization change for an elliptically polarized input light as a function of orientation angle. Fig.(6-1) shows the variation when circular birefringence is not present while Fig.(6-2) depicts the change when circular birefringence is present.

In all of the results discussed thus far, the incident light was regarded to be at low optical intensity and the fiber response was considered linear so that the output Stokes parameters would be independent of the incident light. However, when the incident radiation is high enough, the response of the fiber is expected to change qualitatively from its behavior at low intensity giving rise to nonlinear optical effects. Hence, in this case, the output Stokes parameters would depend on the intensity of the incident light. In other words, the output Stokes parameters will have a dependence on the input Stokes parameters.

Fig.(5-1) showed the Jacobian parameter m as a function of the ratio r for five different initial polarization states. The term $r \sim \chi_{1122}^{(3)}/\Delta\epsilon$ is the relative measure of the nonlinearity (induced birefringence proportional to the intensity) and the linear anisotropy

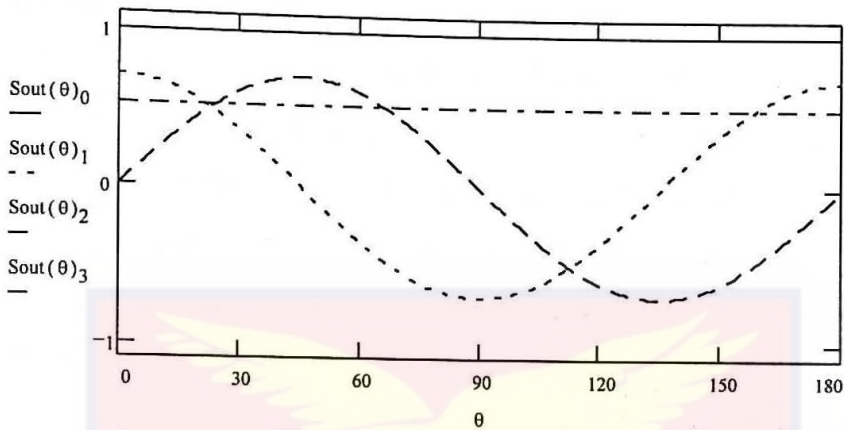


Figure 6-1: Variation in output Stokes parameters as a function of orientation angle for elliptically polarized (45° azimuth and 22.5° ellipticity) input light. Circular birefringence is assumed absent.

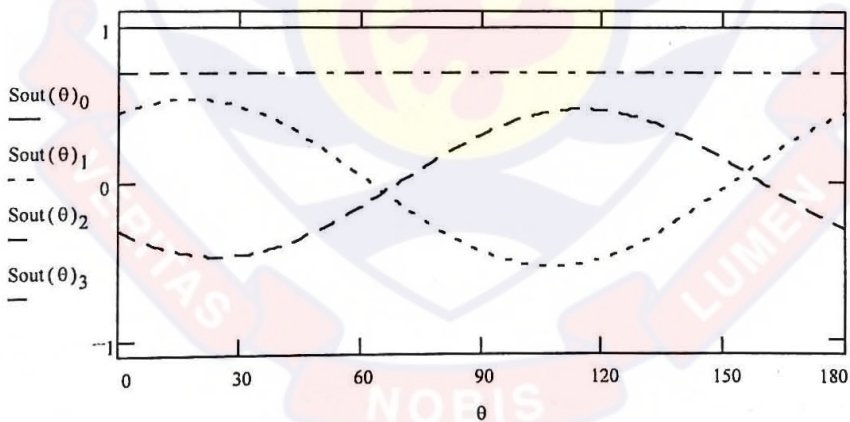


Figure 6-2: Variation in output Stokes parameters as a function of orientation angle for elliptically polarized (45° azimuth and 22.5° ellipticity) input light. Circular birefringence is assumed present.

(linear dielectric tensor). r is dimensionless since $\chi_{1122}^{(3)}$ is a contracted tensor of rank zero and the difference $\Delta\epsilon$ is an ordinary number. It may be assumed without loss of generality that $r \geq 0$ even though in some materials the denominator $\Delta\epsilon$ can be negative. Thus, the assumption that r may be taken as positive with no loss of generality holds in this case because the difference in refractive indices for the eigenpolarization is $\delta n_p \simeq \Delta\epsilon/2n$ and for a birefringent fiber $\delta n_p > 0$. It follows from Eq.(5.53) through Eq.(5.55) that the propagation characteristics of the optical beam depend critically upon the Jacobian parameter m which in turn is dependent on the initial values of the Stokes parameters and the ratio r according to Eq.(5.56). Also note from Eq.(5.56), that m is undefined when $S_{20} = 0$, $S_{10} < 0$, and $r = -1/S_{10}$. Fig.(5-1) showed the variation of the parameter m with r for five different initial polarization states. In particular, examples 1 and 4 in that figure illustrate the two cases where $S_{20} = 0$ for $S_{10} < 0$ and $S_{10} > 0$ respectively. Curve 5 illustrates the $m(r)$ dependency when the initial polarization ellipse is rotated by $\pi/2$. Curves 2, 3, and 4 show that m is strictly monotonically increasing function of r . However, curve 5 shows that when the input light is linearly polarized on axis $m = 0$ for $r \geq 0$. When $m = 0$, the Jacobian elliptic functions degenerate to their trigonometric counterparts (cosine and sine functions) indicating the limiting case when nonlinearities are not considered. Thus, when $m = 0$, the output Stokes parameters will have behavior as shown previously in Figs.(4-1) through (4-24) for the different input polarization states.

Fig.(5-2) showed the variation of Stokes parameters as a function of fiber length for an input light with initial polarization state $S_{10} = 0$, $S_{20} = 0.71$, and $S_{30} = 0.71$ corresponding to a right elliptically polarized beam with azimuth 45° and ellipticity 22.5° . The dependence of m for this initial state is given by curve 3. This figure illustrates the propagation characteristics in the case where $r = 2.3$ and $m = 0.58$. The output Stokes parameters are seen to be doubly periodic and to have different periods.

Fig.(5-3) showed a qualitatively different behavior for the same input polarization as in Fig.(5-2) except that the propagation characteristics are for the case $r = 4$ and $m = 1$.

This would represent a high input power for a birefringent optical fiber. The polarization is seen to be aperiodic and that it tends asymptotically to a linearly polarized final state in this example.

Figs.(5-4) and (5-5) indicate, respectively for $r = 2.3$ and $r = 4$, another set of results for an input light with initial polarization state $S_{10} = 0$, $S_{20} = 0.3$, and $S_{30} = 1$ corresponding to a right elliptically polarized beam with 45° azimuth and 37° ellipticity. The $m(r)$ dependence for this initial state is given by curve 2. In these figures, the output Stokes parameters are observed to vary periodically. It is also noticed from these figures that as r increases from 2.3 to 4, the periods of the Stokes parameters also increase. This implies that the output polarization state at $z = L$ is dependent on the beam's intensity. Thus, it can be deduced from these examples that the state of a beam propagating along a birefringent single mode fiber depend on the initial polarization as well as the intensity of the input light in a complicated way.

It was also of interest to investigate if there are any significant changes in the Jacobian parameter m when a parameter such as the ellipticity of the polarization ellipse undergoes a change. It was observed in this work that for the unique polarization state in which the orientation angle is 90° but the initial Stokes parameter is such that $S_{10} = -0.5$, $S_{20} = 0$, and $S_{30} = 0.3$, the value of r for which m is undefined is shifted to larger r values as shown in Fig.(6-3). In this example, $r = 2$. Recall that in Fig.(5-1) $m(r)$ was undefined at $r = 1$ for $S_{10} = -1$, $S_{20} = 0$, and $S_{30} = 0.8$. Thus when an intense elliptically polarized beam which propagates along a birefringent optical fiber undergoes a change in both the shape and orientation, the critical input intensity at which the light-induced birefringence cancels the existing fiber birefringence will increase.

Furthermore, one recalls from Fig.(5-1) that when the input light was linearly polarized along the principal axis of the fiber, the output polarization was observed to remain linear; $m = 0$ for $r > 0$. However, Fig.(6-1) shows that when the input light is linearly polarized off-axis, that is the input polarization is 45° to the principal axis of the birefringent fiber, $m \neq 0$ for $r > 0$. This indicates that the output polarization become intensity

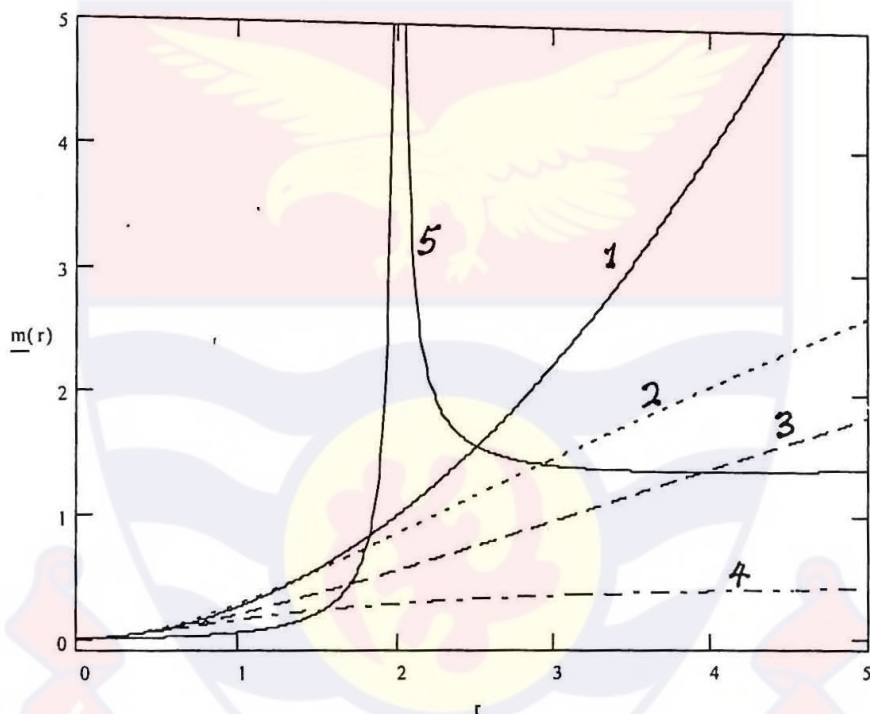


Figure 6-3: Jacobian parameter m as a function of the ratio r for initial polarization states S_{10} , S_{20} , and S_{30} of (1) 0, 0, 1; (2) 0, 0.5, 1; (3) 0.4, 0.4, 1; (4) 0, 1, 0; (5) -0.5, 0, 0.3.

dependent and thereby nonlinear. Thus, the behavior of the output polarization depend on input intensity as well as fiber's axis.



Chapter 7

CONCLUSIONS

The purpose of this work was to investigate the nonlinear polarization effects in a birefringent single mode optical fiber. Stokes parameters were used to analyze these effects. Evolution equations for the polarization states in a birefringent optical fiber were derived and general solutions for Stokes parameters of the propagating light beam were obtained. The methods of the unified formalism for polarization optics was utilized to obtain several Mueller matrices which characterize the perturbations resulting from birefringence and dichroism over the optical path of the fiber. The basic assumption in this approach was that the interaction of the light with the fiber was considered linear. When the light beam was assumed to be intense so that nonlinear effects were considered as the light propagates, the use of Jacobi elliptic functions were employed to obtain the solutions in terms of Stokes parameters which described the nonlinear polarization dynamics at the output. This thesis successfully model the evolution of the Stokes parameters as functions of fiber length and orientation angle for different kinds of perturbations. Graphical illustrations showing the variation in output polarization due to both linear and nonlinear effects were also successfully obtained in this work.

Several interesting results were obtained and presented in this thesis. The character of the results were different depending on whether the fiber response to the propagating wave was considered linear or nonlinear and depending on whether the fiber was assumed

to have losses or not. A significant aspect of the results presented in this work is that when the fiber is considered linear, the output Stokes parameters are either periodic or a constant function of length or orientation angle. When the solutions are periodic, the three Stokes parameters are observed to have the same periods. However, when the input light is intense so that the fiber response to the propagating field is considered nonlinear, the output Stokes parameters are doubly periodic and the three Stokes parameters do not have the same periods. In addition, some cases of aperiodicity was observed. The results obtained may have potential applications in polarization-dependent devices.

The unified formalism which was used to develop and analyze the model to describe an evolution of the state of polarization in a birefringent optical fiber is a phenomenological linear theory since the Mueller matrices that were deduced from the formalism are linear operators whose elements can be measured. Strictly speaking, however, the Mueller matrix calculi in that formalism cannot handle a truly nonlinear propagation in an optical fiber. To do this, in our view, would require a higher order tensor. Thus, further work is needed to include the nonlinear polarization effects in the formalism. In any case, the Mueller matrix valid for nonlinear propagation can be obtained by measurement in a laboratory experiment. We believe, therefore, that a general higher order tensor for the nonlinear case when added to the linear-case Mueller matrix will yield the most general characterization for propagation of a light wave along a birefringent optical fiber.

Chapter 8

REFERENCES

1. C. S. Brown and A. E. Bak, "Unified formalism for polarization optics with application to polarimetry on a twisted optical fiber," *Opt. Eng.* **34** (6), 1625-1635, (1995).
2. B. Daino, G. Gregori, and S. Wabnitz, "New all-optical devices based on third-order nonlinearity of birefringent fibers," *Opt. Lett.* **11**, 42-44, (1986).
3. S. C. Rashleigh, "Origin and control of polarization effects in single-mode fibers," *J. Lightwave Technol.*, **LT-1**, 312-331, (1983).
4. S. M. Baker and J. N. Elgin, "Solitons in randomly varying birefringent fibre," *Quantum Semiclass. Opt.*, **10**, 251-261, (1998).
5. G. P. Agrawal, **Fiber-Optic Communication Systems**, Wiley, New York, (1992).
6. G. P. Agrawal, **Nonlinear Fiber Optics**, Second Edition, Academic Press, (1995).
7. H. G. Winful, "Self-induced polarization changes in birefringent optical fibers," *Appl. Phys. Lett.*, **47**, 213-215, (1985).
8. H. G. Winful, "Polarization instabilities in birefringent nonlinear media: application to fiber-optic devices," *Opt. Lett.*, **11**, 33-35, (1986).
9. F. Matera and S. Wabnitz, "Nonlinear polarization evolution and instability in a twisted birefringent fiber," *Opt. Lett.* **11**, 467-469, (1986).

10. S. Trillo, S. Wabnitz, R. H. Stolen, G. Assanto, C. T. Seaton and G. I. Stegeman, "Experimental observation of polarization instability in a birefringent optical fiber," *Appl. Phys. Lett.* **49** (19), 1224-1226, (1986).
11. S. Trillo, S. Wabnitz, "Nonlinear dynamics and instabilities of coupled waves and solitons in optical fibers," in **Anisotropic and Nonlinear Waveguides**, C. G. Someda and G. Stegeman, (Editors), Elsevier Science Publishers B.V., 185-236; (1992).
12. A. Vatarescu, "Intensity discrimination through nonlinear power coupling in birefringent fibers," *Appl. Phys. Lett.* **49**, (2), 61-63, (1986).
13. Y. P. Svirko and N. I. Zheludev, **Polarization of Light in Nonlinear Optics**, John Wiley and Sons, (1998).
14. G. C. Ishiekwene, "Polarization dispersion in single mode fibers," in Proceedings of Second Regional Workshop on Development of Radio Communication in Africa, 315-321, (1997).
15. E. Collett, **Polarized Light: Fundamentals and Applications**, Marcel Dekker, New York, (1993).
16. S. Huard, **Polarization of Light**, John Wiley and Sons, Chichester, (1997).
17. M. Born and E. Wolf, **Principles of Optics**, Pergamon Press, Oxford, (1970).
18. R. D. Guenther, **Modern Optics**, John Wiley and Sons, New York, (1990).
19. L. Mandel and E. Wolf, **Optical Coherence and Quantum Optics**, Cambridge University Press, Cambridge, (1995).
20. N. Bloembergen, **Nonlinear Optics**, Fourth Edition, Benjamin, Reading, New York, (1982).
21. R. W. Boyd, **Nonlinear Optics**, Academic Press, San Diego, (1992).
22. Y. R. Shen, **The Principles of Nonlinear Optics**, Wiley, New York, (1984).
23. A. Yariv, **Quantum Electronics**, Third Edition, Wiley, New York, (1989).
24. P. D. Maker and R. W. Terhune, "Study of optical effects due to an induced polarization third order in the electric field strength," *Phys. Rev.*, **137** (3A), A801-A818, (1965).

25. S. A. Akhmanov and V. I. Zharikov, "Nonlinear optics of gyrotropic media," *JETP Lett.* **6**, 137-140, (1967).
26. K. L. Sala, "Nonlinear refractive-index phenomena in isotropic media subjected to a dc electric field: Exact solutions," *Phys. Rev. A*, **29** (4), 1944-1956, (1984).
27. G. Gregori and S. Wabnitz, "New exact solutions and bifurcations in the spatial distribution of polarization in third-order nonlinear optical interactions," *Phys. Rev. Lett.* **56** (6), 600-603, (1986).
28. M. V. Tratnik and J. E. Sipe, "Nonlinear polarization dynamics I. The single-pulse equations," *Phys. Rev. A*, **35** (7), 2965-2975, (1987).
29. H. G. Winful and A. Hu, "Intensity discrimination with twisted birefringent optical fibers," *Opt. Lett.* **11** (10), 668-670, (1986).
30. B. Daino, G. Gregori, and S. Wabnitz, "Stability analysis of nonlinear coherent coupling," *J. Appl. Phys.* **58** (12), 4513-4514, (1985).
31. F. X. Kartner, L. Joneckis, and H. A. Haus, "Classical and quantum dynamics of a pulse in a dispersionless non-linear fibre," *Quantum Opt.* **4**, 379-396, (1992).
32. M. W. Shute, Sr., "Polarization maintaining optical fiber as a sensor of shell vibrations," Ph.D. Thesis, The George W. Woodruff School of Mechanical Engineering, Georgia Institute of Technology, August (1994).
33. A. E. Bak, C. S. Brown, G. C. Ishiekwene, and M. W. Shute, Sr., "A review of the unified polarization calculus based on the lorentz group," to be published
34. I. P. Kaminow, "Polarization in optical fibers," *IEEE J. Quantum Electron.*, **QE-17** (1), 15-22, (1981).
35. C. R. Menyuk, "Nonlinear pulse propagation in birefringent optical fibers," *IEEE J. Quantum Electron.*, **QE-23** (2), 174-176, (1987).
36. Y. Louis, A. P. Sheppard, and M. Haelterman, "Domain walls of linear polarization in isotropic kerr media," *Opt. Com.* **141** (3 - 4), 167-172, (1997).
37. I. I. Gancheryonok, I. V. Shapochkina, P. G. Zhavrid, V. A. Gaisyonok, and Y. Fujimura, "Polarization-sensitive spectroscopy of polarization-inhomogeneous molecular

media," J. Mol. Structure **410-411**, 517-520, (1997).

38. R. Ulrich and A. Simon, "Polarization optics of twisted single-mode fibers," App. Opt. **18** (13), 2241-2251, (1979).

39. D. Marcuse, "Coupled mode theory of round optical fibers," Bell Syst. Tech. J., **52**, 817-842, (1973).

40. P. D. Maker, R. W. Terhune and C. M. Savage, "Intensity-dependent changes in the refractive index of liquids," Phys. Rev. Lett., **12** (18), 507-509, (1964).

41. P. A. Franken, A. E. Hill, C. W. Peters, and G. Weinreich, Generation of optical harmonics, "Phys. Rev. Lett., **7** (4), 118-119, (1961).

42. E. Cojocar, "Direction cosines and vectorial relations for extraordinary-wave propagation in uniaxial media," App. Opt. **36** (1), (1997).

43. B. J. Stagg and T. T. Charalampopoulos, "Source-optics polarization effects on ellipsometry analysis," App. Opt. **33** (16), 3493-3501, (1994).

44. J. Blake, "Polarization behavior of axially strained two-mode fibers," Opt. Lett., **17** (8), 589-591, (1992).

45. J. F. Reintjes, "Nonlinear optical processes," in **Encyclopedia of Lasers and Optical Technology**, R. A. Meyers, (Editor), Academic Press Inc., 331-384, (1991).

46. C. S. Brown, A. E. Bak, and M. W. Shute, Sr., "Stochastic aspects of the unified formalism for polarization optics: applications to depolarization phenomena in optical fibers," (unpublished)

47. P. S. Hague, "Mueller matrix ellipsometry with imperfect compensators," J. Opt. Soc. Am. **68** (11), 1519-1528, (1978).

49. M. Kauranen, "Fundamentals of nonlinear optics, in Proceedings of Winter College on Optics, ICTP, Trieste, Italy, H4.SMR/1058-3 (1998).

50. D. I. Pushkarov and S. Tanev, "Solitary wave propagation in the normal dispersion region of optical waveguides with third and fifth-order nonlinearities," ICTP preprint IC/96/225, (1996).

51. J. P. Gordon, "Solitons in randomly birefringent fibers," Proceedings of Confer-

ence on Ultrafast Transmission Systems in Optical Fibres, ICTP, Trieste, Italy H4.SMR/842-5, (1995).

52. M. V. Tratnik and J. E. Sipe, "Bound solitary waves in a birefringent optical fiber," *Phys. Rev. A* **38** (4), 2011-2017, (1988).

53. C. R. Menyuk and P. K. A. Wai, "Polarization evolution and dispersion in fibers with spatially varying birefringence," *J. Opt. Soc. Am.* **B11** (7), 1288-1296, (1994).

54. R. Dandliker, "Rotational effects of polarization in optical fibers," in **Anisotropic and Nonlinear Waveguides**, C. G. Someda and G. Stegeman, (Editors), Elsevier Science Publishers B. V., 39-76, (1992).

55. F. Matera and C. G. Someda, "Random birefringence and polarization dispersion in long single-mode optical fibers," in **Anisotropic and Nonlinear Waveguides**, C. G. Someda and G. Stegeman, (Editors), Elsevier Science Publishers B. V., 1-37, (1992).

56. P. Diament, **Wave Transmission and Fiber Optics**, Macmillan, Inc., (1990).

57. L. B. Jeunhomme, "Single Mode Fiber Optics Principles and Applications," Marcel Dekker, Inc., (1990).

58. C. K. Kao, "Optical Fibre," Peter Peregrinus Ltd., (1988).

59. W. K. Tung, "Group Theory in Physics," Philadelphia, World Scientific, (1985).

60. J. F. Nye, "Physical Properties of Crystals: Their Representation by Tensors and Matrices," Second Edition, Clarendon Press, Oxford, (1985).

61. P. F. Byrd and M. D. Friedman, "Handbook of Elliptical Integrals for Engineers and Scientists," Second Edition, Springer-Verlag, New York, (1971).

62. B. Hutter, C. De Barros, B. Gisin, and N. Gisin, "Polarization-induced pulse spreading in birefringent optical fibers with zero differential group delay," *Opt. Lett.*, **24**, (6), 370-372, (1999).

63. S. R. Nagel, J. B. MacChesney, and K. L. Walker, in **Optical Fiber Communications**, Vol 1, Chap. 1, T. Li, (Editor), Academic Press, Orlando, (1985).

64. A. J. Morrow, A. Sarkar and P. C. Schultz, in **Optical Fiber Communications**,

Vol 1, Chap. 2, T. Li, (Editor); Academic Press, Orlando, (1985).

65. N. Niizeki, N. Inagaki, and T Edahire, in **Optical Fiber Communications**, Vol 1, Chap. 3, T. Li, (Editor), Academic Press, Orlando, (1985).

66. B. J. Ainslie and C. R. Day, *J. Lightwave Technology*, **LT-4**, 967, (1986).

67. R. Ulrich, *Opt. Lett.* **1**, 109 (1977).

68. N. Minorsky, **Nonlinear Oscillations**, Van Nostrand, Princeton, N.J., (1962).

69. J. Yumoto and K. Otsuka, *Phys Rev. Lett.* **54**, 1806, (1985).

70. F. Muhammad and C.S. Brown, "Lorentz transformations on Stokes vectors," in *Polarization Analysis and Measurement*, D. H. Goldstein and R. A. Chipman, (Editors), *Proc. SPIE* **1746**, 183-196, (1992).

71. F. Muhammad and C.S. Brown, "Lorentz group underpinnings for the Jones and Mueller Calculi," in *Polarization Analysis and Measurement II*, D. H. Goldstein and R. A. Chipman, (Editors), *Proc. SPIE* **2265**, 337-348, (1994).

72. R. F. Fox, "Gaussian stochastic processes in physics," *Phys. Rep.* **48**, 179-283, (1978).

73. D. Marcuse, "Theory of dielectric optical waveguides," Academic, New York, (1974).

74. H. Kogelnik, "Theory of dielectric waveguides," in *Integrated Optics* T. Tamir, (Editor), Springer, Berlin, (1979).

75. B. Crossignani, A. Cutolo, and P. Porto, "Guiding diffraction and confinement of optical radiation," Academic, New York, (1986).

76. E.T. Whittaker and G. N. Watson, **A Course of Modern Analysis**, Cambridge University Press, Cambridge, England, (1958).

77. A. Erdelyi, W. Magnus, F. Oberhettinger, and F. G. Tricomi, **Higher Transcendental Functions**, McGrawhill, New York, (1953).

78. N. Ginsin, "Statistics of polarization dependent losses" *Optics Communications*, **114**, 399-405, (1995).

79. P. L. D. Julian, J. Zhang, V. A. Handerek, A. J. Rogers, "Polarization switching

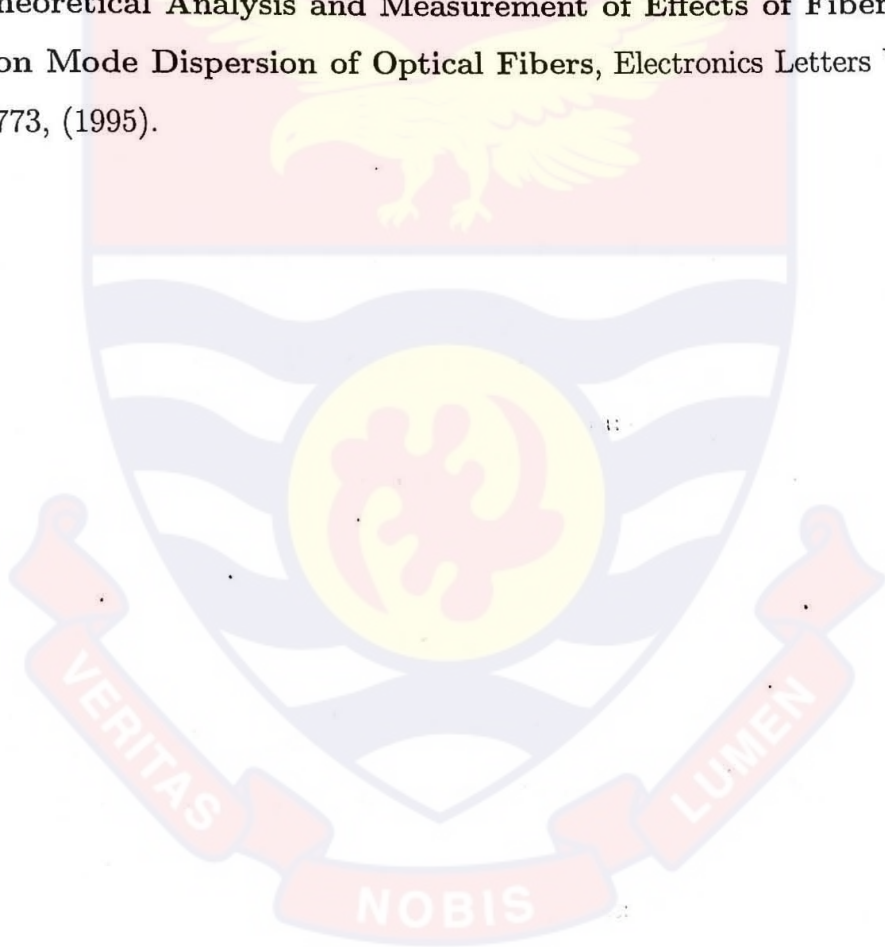
for distributed transverse stress sensing in optical fibers using the optical Kerr effect," J. of Lightwave Technology, Vol. 16, No. 12, 2378-84, (1998).

80. D. V. Vlassov and V. P. Zaitseva, JETP Lett., **13**, 112, (1971).

81. D. S. Klinger, J. W. Lewis and G. E. Randall, **Polarized Light in Optics and Spectroscopy**, Academic Press, Oxford, (1977).

82. J. G. Ellison, A. S. Siddiqui, **A Fully Polarimetric Optical Time-Domain Reflectometer**, IEEE Photonics Technology Letters, Vol 10, No. 2, 246-248, (1998).

83. R.E. Schuh, E. S. R. Sikora, N. G. Walker, A. S. Siddiqui, L. M. Gleeson, D. H. O. Bebbington, **Theoretical Analysis and Measurement of Effects of Fiber Twist on Polarization Mode Dispersion of Optical Fibers**, Electronics Letters Vol. 31, No. 20, 1772-1773, (1995).



Appendix A

Derivation of the Coupled-Mode Equation

Derivation of the coupled-mode equation begins with Maxwell's equations

$$\nabla \times \mathbf{H} = \mathbf{J} + \frac{\epsilon \partial \mathbf{E}}{c \partial t} \quad (\text{A.1})$$

$$\nabla \times \mathbf{E} = -\frac{\mu \partial \mathbf{H}}{c \partial t} \quad (\text{A.2})$$

$$\nabla \cdot \mu \mathbf{H} = 0 \quad (\text{A.3})$$

$$\nabla \cdot \epsilon \mathbf{E} = \rho \quad (\text{A.4})$$

In an optical fiber, there are no excess charges, thus, $\rho = 0$, and $\mathbf{J} = 0$.

Taking the curl of Eq.(A.2) and using Eq.(A.1) to eliminate the field vector \mathbf{H} one obtains the following wave equation

$$\nabla \times \nabla \times \mathbf{E} = -\frac{\mu \epsilon \partial^2 \mathbf{E}}{c^2 \partial t^2} \quad (\text{A.5})$$

Equation (A.5) can be expressed as

$$\nabla^2 \mathbf{E} + \nabla(\nabla \cdot \mathbf{E}) = \frac{\mu\epsilon}{c^2} \frac{\partial^2 \mathbf{E}}{\partial t^2} \quad (\text{A.6})$$

where the vector identity $\nabla \times \nabla \times \mathbf{E} = \nabla(\nabla \cdot \mathbf{E}) - \nabla^2 \mathbf{E}$ has been used.

Consider an initially ideal cylindrically symmetric single mode fiber with an unperturbed dielectric function $\epsilon_0(r, \theta)$, where r and θ are the polar parts of the cylindrical coordinates (r, θ, z) . Then, the permittivity of the ideal fiber becomes

$$\epsilon = \epsilon_0(r, \theta) \quad (\text{A.7})$$

Assuming that the corresponding transverse monochromatic fields traveling along the length of the fiber can be expressed as

$$\mathbf{E}^T = \sum_{n=1}^2 a_n \mathbf{E}_n^T(r, \theta) \exp[i(k_n z - \omega t)] \quad (\text{A.8})$$

and using the fact that the transverse and longitudinal parts of the del operator $\nabla = \nabla_T + \frac{\partial}{\partial z} \mathbf{e}_z$, and that of the Laplacian $\nabla^2 = \nabla_T^2 + \frac{\partial^2}{\partial z^2}$, Eq.(A.6) can be rewritten as

$$\left(\nabla_T^2 + \frac{\partial^2}{\partial z^2} \right) \mathbf{E}^T - \nabla(\nabla_T \cdot \mathbf{E}^T) = \frac{\mu\epsilon}{c^2} \frac{\partial^2 \mathbf{E}^T}{\partial t^2} \quad (\text{A.9})$$

Furthermore, using Eq.(A.7), Maxwell's equation (A.4) can now be written as

$$\nabla \cdot \epsilon \mathbf{E} = \epsilon_0 \nabla \cdot \mathbf{E} + \mathbf{E} \cdot \nabla \epsilon_0 = 0 \quad (\text{A.10})$$

and considering only transverse components, the above expressions in Eq.(A.10) yield

$$\nabla_T \cdot \mathbf{E}^T = -\mathbf{E}^T \cdot \nabla_T \ln \epsilon_0 \quad (\text{A.11})$$

Therefore, the general wave equation (A.9), can be rewritten as

$$\left(\nabla_T^2 + \frac{\partial^2}{\partial z^2}\right) \mathbf{E}^T + \nabla \left(\mathbf{E}^T \cdot \nabla_T \ln \epsilon_0\right) - \frac{\mu\epsilon}{c^2} \frac{\partial^2 \mathbf{E}^T}{\partial t^2} = 0 \quad (\text{A.12})$$

Substituting Eq.(A.8) into Eq.(A.12) leads to the following transverse ideal mode equation for an unperturbed fiber

$$\sum_{n=1}^2 a_n \exp [i (kz - \omega t)] \left\{ \nabla_T^2 \mathbf{E}_n^T + \left(\mu_0 \epsilon_0 \frac{\omega^2}{c^2} - k^2 \right) \mathbf{E}_n^T + \nabla_T \left(\mathbf{E}_n^T \cdot \nabla_T \ln \epsilon_0 \right) \right\} = 0 \quad (\text{A.13})$$

Note that in obtaining Eq.(A.13), the fiber is assumed to be isotropic so that, $k_1 = k_2 = k$ a constant.

Now, assuming that there are small perturbations in the fiber resulting from length dependent disturbances of the dielectric function, the total dielectric function can be expressed as

$$\epsilon(r, \theta, z) = \epsilon_0(r, \theta) + \Psi(r, \theta, z) \quad (\text{A.14})$$

where Ψ characterizes the perturbations. It should be noted that in the presence of perturbations, the constant field amplitudes in Eq.(A.8) become functions of z thereby containing the effects due to the perturbations. Therefore, it is assumed that the general electric field in the perturbed fiber can be represented as

$$\mathbf{E}^T = \sum_{n=1}^2 a_n(z) \mathbf{E}_n^T(r, \theta) \exp [i (k_n z - \omega t)] \quad (\text{A.15})$$

Using equations (A.4) and (A.14), the following relation is obtained

$$\nabla \cdot (\epsilon_0 \mathbf{E}) + \nabla \cdot (\Psi \mathbf{E}) = \mathbf{E}^T \cdot \nabla_T \ln \epsilon_0 + \nabla \cdot \mathbf{E} + \frac{1}{\epsilon_0} \nabla \cdot (\Psi \mathbf{E}) = 0 \quad (\text{A.16})$$

so that

$$\nabla \cdot \mathbf{E} = -\mathbf{E}^T \cdot \nabla_T \ln \epsilon_0 - \frac{1}{\epsilon_0} \nabla \cdot (\Psi \mathbf{E}) \quad (\text{A.17})$$

$$\mathbf{E}^Z = \sum_{n=1}^2 a_n(z) \mathbf{E}_n^Z(r, \theta) \exp[i(k_n z - \omega t)] \quad (\text{A.18})$$

so that the total fields become

$$\mathbf{E} = \mathbf{E}^T + \mathbf{E}^Z \quad (\text{A.19})$$

Using equations (A.17) and (A.19), the transverse part of the wave equation (A.6) can be written as

$$0 = \nabla^2 \mathbf{E}^T + \nabla_T \left[\mathbf{E}^T \cdot \nabla_T \ln \epsilon_0 + \frac{1}{\epsilon_0} \nabla \cdot (\Psi \mathbf{E}) \right] - \frac{\mu \epsilon}{c^2} \frac{\partial^2 \mathbf{E}^T}{\partial t^2} = S_A + S_B + S_C \quad (\text{A.20})$$

where S_A , S_B , and S_C are three vector sums when equations (A.15) and (A.18) are utilized. The first sum

$$S_A \equiv \sum_{n=1}^2 a_n(z) \left\{ \nabla_T^2 \mathbf{E}_n^T + \left(\mu_0 \epsilon_0 \frac{\omega^2}{c^2} - k_n^2 \right) \mathbf{E}_n^T + \nabla_T \left(\mathbf{E}_n^T \cdot \nabla_T \ln \epsilon_0 \right) \right\} \exp[i(k_n z - \omega t)] \quad (\text{A.21})$$

vanishes because it satisfies the ideal mode equation for a perturbed fiber. The second term

$$S_B \equiv \sum_{n=1}^2 \left\{ \mathbf{E}_n^T \frac{d^2 a_n}{dz^2} + a_n(z) \nabla_T \left(\frac{E_n^Z}{\epsilon_0} \frac{d\Psi}{dz} \right) + \nabla_T \left(\frac{\Psi E_n^Z}{\epsilon_0} \frac{da_n}{dz} \right) \right\} \exp[i(k_n z - \omega t)] \quad (\text{A.22})$$

which are negligible because it consists of second order small terms. Hence, it follows that

$$S_C \equiv \sum_{n=1}^2 \left[2ik_n \mathbf{E}_n^T \frac{da_n}{dz} + a_n(z) \mu_0 \Psi \frac{\omega^2}{c^2} (\Psi \mathbf{E}_n^T) + a_n(z) \nabla_T U_n \right] \exp[i(k_n z - \omega t)] \approx 0 \quad (\text{A.23})$$

where

$$U_n = \frac{1}{\epsilon_0} \left[\nabla_T \cdot (\Psi \mathbf{E}_n^T) + ik_n (\Psi E_n^z) \right] \quad (\text{A.24})$$

$$\int_0^{2\pi} d\theta \int_0^\infty r dr (\mathbf{E}_n^T \times \mathbf{H}_m^{T*}) \cdot \mathbf{e}_z = I_{mn}^0 \delta_{mn} \quad (\text{A.25})$$

on Eq.(A.23), the following expression is obtained

$$0 = \sum_{n=1}^2 \int_0^{2\pi} d\theta \int_0^\infty r dr \left[2ik_n a'_n(z) \mathbf{E}_n^T + a_n(z) \mu_0 \frac{\omega^2}{c^2} (\Psi \mathbf{E}_n^T) + a_n(z) \nabla_T U_n \right] \exp [i(k_n z - \omega t)] \times \quad (\text{A.26})$$

Equation (A.26) can be written in a more concise form as

$$\sum_{n=1}^2 \left\{ 2ik_n a'_n(z) I_{mn}^1 \delta_{mn} + a_n(z) \left[\mu_0 \frac{\omega^2}{c^2} I_{mn}^2 + I_{mn}^3 \right] \right\} \exp [i(k_n z - \omega t)] = 0 \quad (\text{A.27})$$

where

$$I_{mn}^1 = \int_0^{2\pi} d\theta \int_0^\infty r dr (\mathbf{E}_n^T \times \mathbf{H}_m^{T*}) \cdot \mathbf{e}_z \quad (\text{A.28})$$

$$I_{mn}^2 = \int_0^{2\pi} d\theta \int_0^\infty r dr (\Psi \mathbf{E}_n^T) \times \mathbf{H}_m^{T*} \cdot \mathbf{e}_z \quad (\text{A.29})$$

$$I_{mn}^3 = \int_0^{2\pi} d\theta \int_0^\infty r dr (\nabla_T U_n) \times \mathbf{H}_m^{T*} \cdot \mathbf{e}_z \quad (\text{A.30})$$

Therefore taking sums,

$$\sum_{n=m}^{1,2} 2ik_m a'_m(z) \exp [i(k_m z - \omega t)] I_{mm}^1 \delta_{mm} + \sum_{n=1}^2 a_n(z) \left[\mu_0 \epsilon \frac{\omega^2}{c^2} I_{mn}^2 + I_{mn}^3 \right] \exp [i(k_n z - \omega t)] = 0 \quad (\text{A.31})$$

Thus,

$$a'_m(z) = i \sum_{n=1}^2 P_{mn} a_n(z) \quad (\text{A.32})$$

where

$$P_{mn} = \left\{ \frac{\mu_0 \epsilon \frac{\omega^2}{c^2} I_{mn}^2 + I_{mn}^3}{2k_m I_{mm}^1} \right\} \exp [i(k_n - k_m) z] \quad (\text{A.33})$$

$$\frac{da(z)}{dz} = i \hat{P} \cdot a(z) \quad (\text{A.34})$$



Appendix B

Derivation of the Stokes Parameters Equation of Motion

To derive the Stokes parameters equation of motion, it is useful to begin with the coherency matrix defined by a matrix product in terms of the field amplitudes as

$$\mathcal{I}(z) = a(z) a^\dagger(z) \quad (\text{B.1})$$

where the symbol \dagger indicates the Hermitian conjugate which makes $a^\dagger(z)$ a row vector. Taking the derivative of Eq.(B.1) and using the coupled mode equation derived in Appendix A,

$$\frac{d}{dz} a(z) = i \hat{\mathbf{P}}(z) \cdot a(z) \quad (\text{B.2})$$

and its Hermitian conjugate

$$\frac{d}{dz} a^\dagger(z) = -i a^\dagger(z) \cdot \hat{\mathbf{P}}^\dagger(z) \quad (\text{B.3})$$

one obtains the following expression

$$\frac{d\mathcal{I}(z)}{dz} = i [\hat{\mathbf{P}}(z) \mathcal{I}(z) - \mathcal{I}(z) \hat{\mathbf{P}}^\dagger(z)] \quad (\text{B.4})$$

Recall that the coupling term can be expressed in complex form in terms of the birefringent and dichroic operators as follows:

$$\hat{\mathbf{P}}(z) = \hat{\mathbf{B}}(z) + i\hat{\mathbf{D}}(z) \quad (\text{B.5})$$

and its hermitian conjugate as

$$\hat{\mathbf{P}}^\dagger(z) = \hat{\mathbf{B}}^\dagger(z) + i\hat{\mathbf{D}}^\dagger(z) \quad (\text{B.6})$$

then, substituting Eq.(B.5) and its complex conjugate Eq.(B.6) into Eq.(B.4), will yield

$$\frac{d\mathcal{I}(z)}{dz} = i [\hat{\mathbf{B}}(z), \mathcal{I}(z)] - \{\hat{\mathbf{D}}(z), \mathcal{I}(z)\} \quad (\text{B.7})$$

where $[B, I] = [BI - IB]$ is called the commutator and $\{D, I\} = [DI - ID]$ is the anti commutator. Note that in order to obtain Eq.(B.7), the Hermiticity of $\hat{\mathbf{B}}(z)$ and $\hat{\mathbf{D}}(z)$ that is $\hat{\mathbf{B}}(z) = \hat{\mathbf{B}}^\dagger(z)$ and $\hat{\mathbf{D}}(z) = \hat{\mathbf{D}}^\dagger(z)$ were used.

The Stokes parameters can also be defined in terms of the field amplitudes as

$$\begin{aligned} S_0 &= a_1^* a_1 + a_2^* a_2 \\ S_1 &= a_1^* a_1 - a_2^* a_2 \\ S_2 &= a_1^* a_2 + a_2^* a_1 \\ S_3 &= i(a_1^* a_2 - a_2^* a_1) \end{aligned} \quad (\text{B.8})$$

so that with the use of equations (B.1) and (B.8), the relation between the Stokes parameters and the coherency matrix may be deduced and written as a 2×2 matrix

$$\mathcal{I}(z) = \frac{1}{2} \begin{bmatrix} S_0 + S_1 & S_2 - iS_3 \\ S_2 + iS_3 & S_0 - S_1 \end{bmatrix} \quad (\text{B.9})$$

From Eq.(B.9), it is observed that the coherency matrix equals its complex conjugate transpose and is thus hermitian. Hence, $\mathcal{I}(z)$ can be represented in terms of the Pauli spin matrices and the 2×2 identity matrix as

$$\mathcal{I}(z) = \frac{1}{2} \sum_{l=0}^3 S_l(z) \hat{\sigma}_l \quad (\text{B.10})$$

where

$$\sigma_0 = \begin{pmatrix} 1 & 0 \\ 0 & 1 \end{pmatrix} \quad \sigma_1 = \begin{pmatrix} 1 & 0 \\ 0 & -1 \end{pmatrix} \quad \sigma_2 = \begin{pmatrix} 0 & 1 \\ 1 & 0 \end{pmatrix} \quad \sigma_3 = \begin{pmatrix} 0 & -i \\ i & 0 \end{pmatrix} \quad (\text{B.11})$$

In the 2×2 operator representation of the general Jones matrix, the field amplitudes can be written as

$$a(z) = \hat{\mathbf{J}}(\hat{\mathbf{B}}(z), \hat{\mathbf{D}}(z)) \cdot a(z_0) \quad (\text{B.12})$$

where $\hat{\mathbf{J}}$ is the Jones matrix and z_0 is some reference value of z . Since $\hat{\mathbf{B}}(z)$ and $\hat{\mathbf{D}}(z)$ are physically measurable quantities, the operators representing them must be hermitian and thus can also be expressed in terms of the 2-dimensional identity and pauli spin matrices of Eq.(B.11). Thus,

$$\hat{\mathbf{B}}(z) = \frac{1}{2} \sum_{l=0}^3 \beta_l(z) \hat{\sigma}_l \quad (\text{B.13})$$

and

$$\hat{\mathbf{D}}(z) = \frac{1}{2} \sum_{l=0}^3 d_l(z) \hat{\sigma}_l \quad (\text{B.14})$$

Substituting equations (B.10), (B.13), and (B.14) into Eq.(B.7), one obtains the coherency matrix in a parametric form

$$\frac{d}{dz} \sum_{l=0}^3 S_l(z) \hat{\sigma}_l = \frac{1}{2} \sum_{k=0}^3 \left\{ i \sum_{i=0}^3 \beta_i S_k [\hat{\sigma}_i, \hat{\sigma}_k]_- - \sum_{j=0}^3 d_j S_k [\hat{\sigma}_j, \hat{\sigma}_k]_+ \right\} \quad (\text{B.15})$$

The Pauli matrices obey an algebra such that their multiplication property is defined by

$$\hat{\sigma}_i \hat{\sigma}_j = \delta_{ij} + i \epsilon_{ijs} \hat{\sigma}_s \quad (\text{B.16})$$

With the use of Eq.(B.16), Eq.(B.15) can now be expressed as

$$\sum_{l=0}^3 \frac{d}{dz} S_l(z) \hat{\sigma}_l = (\mathbf{S}(z) \times \boldsymbol{\beta}) \cdot \hat{\sigma}_s - d_0 S_0 - d_0 (\mathbf{S} \cdot \hat{\sigma}) - S_0 (\mathbf{d} \cdot \hat{\sigma}) - (\mathbf{d} \cdot \mathbf{S}) \quad (\text{B.17})$$

The left hand side of Eq.(B.17) can also be written as

$$\sum_{l=0}^3 \frac{d}{dz} S_l(z) \hat{\sigma}_l = \frac{d}{dz} S_0(z) \hat{\sigma}_0 + \sum_{l=1}^3 \frac{d}{dz} S_l(z) \hat{\sigma}_l \quad (\text{B.18})$$

Comparing equations (B.17) and (B.18), and taking the scalar and vector parts separately one obtains

$$\frac{d}{dz} S_0(z) = -d_0(z) S_0(z) - \mathbf{d}(z) \cdot \mathbf{S}(z) \quad (\text{B.19})$$

and

$$\frac{d}{dz} \mathbf{S}(z) = \mathbf{S}(z) \times \vec{\beta}(z) - d_0(z) \mathbf{S}(z) - S_0(z) \mathbf{d}(z) \quad (\text{B.20})$$

Appendix C

Derivation of the Mueller Matrix for an Optically Active Birefringent Fiber Without Dichroism

Derivation of the Mueller matrix for an optically active birefringent fiber begins with the differential equations describing the evolution of Stokes parameters

$$\frac{dS_0}{dz} = -\frac{\omega}{2c} \text{Im} \left[(4n + \Omega_0) S_0 + (\Omega \cdot \vec{S}) \right] \quad (\text{C.1})$$

and

$$\frac{dS_\mu}{dz} = -\frac{\omega}{2c} \text{Im} \left[(4n + \Omega_0) S_\mu + \Omega S_0 + i (\Omega \times \vec{S}) \right] \quad (\text{C.2})$$

where $\Omega = (\Omega_1, \Omega_2, \Omega_3)$ is a vector in Stokes space known as the self action vector and $\mu = 1, 2, 3$. The self action vector is in general complex and can be expressed as

$$\Omega = \vec{\beta} + i \vec{d} \quad (\text{C.3})$$

where $\vec{\beta}$ is the birefringence 3-vector and \vec{d} represents the dichroism 3-vector.

$$\frac{dS_0}{dz} = - \left[d_0 S_0 + \vec{d} \cdot \vec{S} \right] \quad (C.4)$$

and

$$\frac{d\vec{S}}{dz} = - \left[d_0 \vec{S} + \vec{d} S_0 + \vec{\beta} \times \vec{S} \right] \quad (C.5)$$

where $d_0 = \frac{\omega}{2c} \text{Im} (4n + \Omega_0)$ represents the isotropic loss of a the fiber. Consequently,

$$\vec{\beta} = \frac{\omega}{2c} \text{Re} \Omega \quad (C.6)$$

and

$$\vec{d} = \frac{\omega}{2c} \text{Im} \Omega \quad (C.7)$$

Now, if the fiber is initially assumed to be lossless, then there is no dichroism so that $\text{Im} \Omega = 0$ and Ω is real. Hence, Eq.(C.1) becomes

$$\frac{dS_0}{dz} = 0 \quad (C.8)$$

and Eq.(C.2) takes the form

$$\frac{d\vec{S}}{dz} = - \frac{\omega}{2c} \left(\Omega \times \vec{S} \right) \quad (C.9a)$$

which describes a precession of the Stokes vector around Ω which accounts for small anisotropy in the dielectric tensor of the fiber. The action vector can be expressed in terms of the Pauli matrices as

$$\Omega = \sigma_{ji}^{(\alpha)} u_{ij} \quad (C.10)$$

Here,

$$u_{ij} = \frac{1}{n} \left(\epsilon_{ij} + ik_m \Gamma_{ijm}^1 - n^2 \delta_{ij} \right) \quad (C.11)$$

is a rank-two tensor that represents the coupling in the field amplitudes due to perturbations. If it is further assumed that the fiber is isotropic, then $\epsilon_{ij} = n^2 \delta_{ij}$ and the coupling

$$u_{ij} = i \frac{\omega}{c} \Gamma^a e_{ijz} \tag{C.12}$$

where Γ^a is the magnitude of the optical nonlocality and e_{ijz} is the Levi Civita antisymmetric tensor. Note that Γ^a is a measure of the optical activity effects in a fiber.

It has been shown in the text that the action vector Ω for an isotropic optically active birefringent fiber has the following components

$$\Omega_1 = \frac{1}{n} \tag{C.13}$$

$$\Omega_2 = 0$$

$$\Omega_3 = -\frac{2\omega}{c} \Gamma^a$$

where $\Delta\epsilon = \epsilon_{11} - \epsilon_{33}$. It may be advantageous to express Eq.(C.9a) in tensor form as

$$\frac{dS_\alpha}{dz} = -\frac{\omega}{2c} e_{\alpha\beta\gamma} (\Omega_\beta S_\gamma) \tag{C.14}$$

where $\alpha, \beta,$ and γ have values 1, 2, and 3. With the use of Eq.(C.13) and Eq.(C.14), one can then obtain the following equations

$$\frac{dS_1}{dz} = 2GS_2 \tag{C.15}$$

$$\frac{dS_2}{dz} = 2GS_1 + 2\delta' S_3 \tag{C.16}$$

$$\frac{dS_3}{dz} = -2\delta' S_2 \tag{C.17}$$

and expressed in form of matrix equation will become

$$\frac{d}{dz} \begin{pmatrix} S_0 \\ S_1 \\ S_2 \\ S_3 \end{pmatrix} = \begin{pmatrix} 0 & 0 & 0 & 0 \\ 0 & 0 & -2G & 0 \\ 0 & 2G & 0 & 2\delta' \\ 0 & 0 & -2\delta' & 0 \end{pmatrix} \begin{pmatrix} S_0 \\ S_1 \\ S_2 \\ S_3 \end{pmatrix} \tag{C.18}$$

$G = \omega^2/2c^2\Gamma^a$ is the fiber's optical rotatory power, related to the circular birefringence and $\delta' = (\Delta\epsilon\omega/4cn)$ is a measure of the fiber's on-axis linear birefringence. Eq.(C.18) has solutions of the form

$$\vec{S}_\alpha = \exp(\vec{\beta} \cdot \hat{B}) z \cdot \vec{S}_{\alpha 0} = \exp \beta (e_\beta \cdot \hat{B}) z \cdot \vec{S}_{\alpha 0} \quad (C.19)$$

where $e_\beta = \cos 2\theta \vec{e}_1 + \sin 2\theta \vec{e}_3$ and $\beta = 2\sqrt{(\delta')^2 + G^2}$. Therefore,

$$e_\beta \cdot \hat{B} = \cos 2\theta \hat{B}_1 + \sin 2\theta \hat{B}_3 \quad (C.20)$$

from the Lorentz generators referred to in this work

$$\hat{B}_1 = \begin{bmatrix} 0 & 0 & 0 & 0 \\ 0 & 0 & 0 & 0 \\ 0 & 0 & 0 & 1 \\ 0 & 0 & -1 & 0 \end{bmatrix} \quad \text{and} \quad \hat{B}_3 = \begin{bmatrix} 0 & 0 & 0 & 0 \\ 0 & 0 & -1 & 0 \\ 0 & 1 & 0 & 0 \\ 0 & 0 & 0 & 0 \end{bmatrix} \quad (C.21)$$

so that

$$e_\beta \cdot \hat{B} = \begin{bmatrix} 0 & 0 & 0 & 0 \\ 0 & 0 & -\sin 2\theta & 0 \\ 0 & \sin 2\theta & 0 & \cos 2\theta \\ 0 & 0 & -\cos 2\theta & 0 \end{bmatrix} \quad (C.22)$$

or

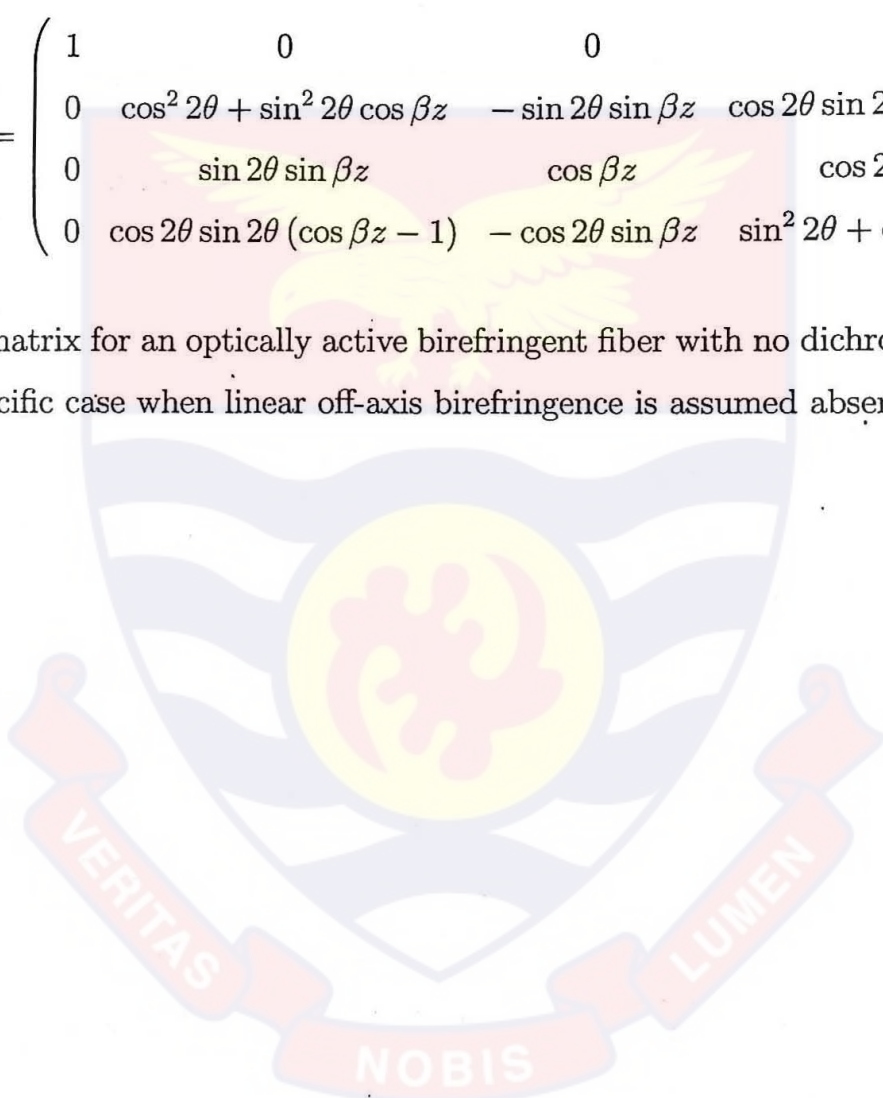
$$(e_\beta \cdot \hat{B})^2 = \begin{bmatrix} 0 & 0 & 0 & 0 \\ 0 & -\sin^2 2\theta & 0 & -\sin 2\theta \cos 2\theta \\ 0 & 0 & -1 & 0 \\ 0 & -\sin 2\theta \cos 2\theta & 0 & -\cos^2 2\theta \end{bmatrix} \quad (C.23)$$

$$\begin{aligned} \widehat{\mathbf{M}}(0, 0, \vec{\beta}, z) &= \exp(\vec{\beta} \cdot \hat{\mathbf{B}}) z \\ &= \left[\hat{\mathbf{I}} + (\vec{e}_\beta \cdot \hat{\mathbf{B}})^2 \right] - (\vec{e}_\beta \cdot \hat{\mathbf{B}})^2 \cos \beta z + (\vec{e}_\beta \cdot \hat{\mathbf{B}}) \sin \beta z \end{aligned} \tag{C.24}$$

where $\hat{\mathbf{I}}$ is the 4x4 identity matrix. Then,

$$\widehat{\mathbf{M}}(0, 0, \vec{\beta}, z) = \begin{pmatrix} 1 & 0 & 0 & 0 \\ 0 & \cos^2 2\theta + \sin^2 2\theta \cos \beta z & -\sin 2\theta \sin \beta z & \cos 2\theta \sin 2\theta (\cos \beta z - 1) \\ 0 & \sin 2\theta \sin \beta z & \cos \beta z & \cos 2\theta \sin \beta z \\ 0 & \cos 2\theta \sin 2\theta (\cos \beta z - 1) & -\cos 2\theta \sin \beta z & \sin^2 2\theta + \cos^2 2\theta \cos \beta z \end{pmatrix} \tag{C.25}$$

is the Mueller matrix for an optically active birefringent fiber with no dichroism assumed and for the specific case when linear off-axis birefringence is assumed absent.



Appendix D

Derivation of Exact Solutions for System of Coupled Nonlinear Equations

The coupled nonlinear evolution equations (Eq.5.25) can be rewritten as

$$\frac{dS_1}{dz} = -R_1 S_2 S_3 \quad (\text{D.1})$$

$$\frac{dS_2}{dz} = R_1 S_1 S_3 + R_0 S_3 \quad (\text{D.2})$$

$$\frac{dS_3}{dz} = -R_0 S_2 \quad (\text{D.3})$$

where $R_0 = \omega \Delta \epsilon / 2nc$, and $R_1 = 12\pi\omega \chi_{1122}^{(3)} / nc$. Multiplying Eq.(D.3) by S_3 one obtains

$$\frac{dS_3^2}{dz} = -2R_0 S_2 S_3 \quad (\text{D.4})$$

and dividing Eq.(D.1) by Eq.(D.4) yields

$$2R_0 \frac{dS_1}{dz} = R_1 \frac{dS_3^2}{dz} \quad (D.5)$$

or

$$\frac{d}{dz} (2R_0 S_1 - R_1 S_3^2) = 0 \quad (D.6)$$

so that

$$2R_0 S_1 - R_1 S_3^2 = C \quad (D.7)$$

where C is a constant. Integrating Eq.(D.6) gives

$$2R_0 (S_1 - S_{10}) = R_1 (S_3^2 - S_{30}^2) \quad (D.8)$$

Thus, one can deduce from either Eq.(D.6) or Eq.(D.7) that only one of the Stokes parameters is independent. To eliminate S_1 and S_2 , take the squared of Eq.(D.3) and the fact that

$$S_1^2 + S_2^2 + S_3^2 = 1 \quad (D.9)$$

to obtain

$$\left(\frac{dS_3}{dz}\right)^2 = R_0^2 [1 - (S_3^2 + S_1^2)] \quad (D.10)$$

and using Eq.(D.8), the above expressions in Eq.(D.10) can be simplified as

$$\left(\frac{dS_3}{dz}\right)^2 = -B_1 S_3^4 - B_2 S_3^2 + B_3 \quad (D.11)$$

where

$$\begin{aligned} B_1 &= \frac{1}{4} R_1^2 \\ B_2 &= R_0^2 + R_1 \left(R_0 S_{10} - \frac{1}{2} R_1 S_{30}^2 \right) \\ B_3 &= R_0^2 - \left(R_0 S_{10} - \frac{1}{2} R_1 S_{30}^2 \right) \end{aligned} \quad (D.12)$$

Now let $S_3^2 = \zeta$ then Eq.(D.11) can be written as

© University of Cape Coast <https://ir.ucc.edu.gh/xmlui>

$$\left(\frac{dS_3}{dz}\right)^2 = -B_1 \left(\zeta^2 + \frac{B_2}{B_1}\zeta - \frac{B_3}{B_1}\right) \quad (\text{D.13})$$

and with use of the quadratic formula, the right hand side of Eq.(D.13) has roots

$$\alpha_{1,2} = \frac{-B_2 \pm \sqrt{B_2^2 + 4B_1B_3}}{2B_1} \quad (\text{D.14})$$

so that Eq.(D.11) can now be expressed as

$$\left(\frac{dS_3}{dz}\right)^2 = -B_1 (S_3^2 - \alpha_1) (S_3^2 - \alpha_2) \quad (\text{D.15})$$

Now, using the tables of Elliptic Functions^[61] for integrands involving $\sqrt{a^2 + t^2}$ and $\sqrt{b^2 - t^2}$,

$$\int_y^b \frac{dt}{\sqrt{(a^2 + t^2)(b^2 - t^2)}} = g \int_0^{u_1} du = g \text{cn}^{-1}(\cos \phi, k) = g \mathcal{F}(\phi, k), \quad b > y \geq 0 \quad (\text{D.16})$$

where $k^2 = b^2/(a^2 + b^2)$, and $g = (a^2 + b^2)^{-\frac{1}{2}}$. Also, $\phi = \text{am } u_1 = \cos^{-1}(y/b)$ and $\text{cn } u_1 = \cos \phi$. Then, Eq.(D.15) can be rewritten in the form

$$\sqrt{B_1} \int_0^z dz = \pm \int_y^b \frac{dS_3}{\sqrt{(S_3^2 + a^2)(b^2 - S_3^2)}} \quad (\text{D.17})$$

where $a^2 = -\alpha_2$ and $b^2 = \alpha_1$. Thus,

$$\sqrt{B_1}z + C = g \text{cn}^{-1}(\cos \phi, k) \quad (\text{D.18})$$

or

$$\text{cn} \left(\frac{\sqrt{B_1}z}{g} + C ; k \right) = \cos \phi \quad (\text{D.19})$$

and

$$S_3 = \pm \sqrt{\alpha_1} \operatorname{cn} \left(\sqrt{B_1 (\alpha_1 - \alpha_2)} z + C ; k \right) \tag{D.21}$$

so that

where C is a constant. Now using Eq.(D.12),

$$\frac{B_2}{2B_1} = \frac{1}{r^2} \left[2(1 + rS_{10}) - r^2 S_{30}^2 \right] \tag{D.22}$$

and

$$\frac{B_3}{B_1} = \frac{4}{r^2} \left[1 - \left(S_{10} - \frac{r}{2} S_{30}^2 \right) \right] \tag{D.23}$$

where $r = R_1/R_0$. Thus, using equations (D.22) and (D.23), the roots in Eq.(D.14) can be expressed as

$$\alpha_{1,2} = \frac{1}{r^2} \left[r^2 S_{30}^2 - 2(1 + rS_{10}) \right] \pm \frac{2}{r^2} \left[(1 + rS_{10})^2 - r^2 S_{20}^2 \right]^{\frac{1}{2}} \tag{D.24}$$

In Eq.(D.24), α_1 is associated with the “+” sign and α_2 is associated with the “-” sign. Note that in obtaining Eq.(D.24), the invariance of the Stokes parameters, i.e. $S_1^2 + S_2^2 + S_3^2 = 1$ was used. Therefore,

$$\alpha_1 - \alpha_2 = \frac{4}{r^2} \left[(1 + rS_{10})^2 - r^2 S_{20}^2 \right]^{\frac{1}{2}} \tag{D.25}$$

Thus, Eq.(D.21) can now be written more compactly with the use of Eq.(D.25) as

$$S_3 = \pm \sqrt{\alpha_1} \operatorname{cn} (R_0 f z + C ; k) \tag{D.26}$$

where $f = \left[(1 + rS_{10})^2 - r^2 S_{20}^2 \right]^{\frac{1}{4}}$. Note also the fact that $B_1 = R_0^2 r^2 / 4$ has been used to obtain Eq.(D.26). But,

$$k = \frac{\sqrt{\alpha_1}}{\sqrt{\alpha_1 - \alpha_2}} \tag{D.27}$$

so that

$$\sqrt{\alpha_1} = \frac{2}{r}kf$$

Hence Eq.(D.29) can be expressed as

$$S_3 = \frac{2pkf}{r} \text{cn}(R_0fz + C; k) \quad (\text{D.29})$$

where $p = \pm 1 = \text{sgn}(S_{30})$ and with the sign defined as $\text{sgn}(x) = 1$ for $x \geq 0$ and $\text{sgn}(x) = -1$ for $x < 0$.

The solution for S_2 follows from the use of Eq.(D.3) and Eq.(D.29) yielding

$$-R_0S_2 = \frac{d}{dz} \left[\frac{2pkf}{r} \text{cn}(R_0fz + C; k) \right] \quad (\text{D.30})$$

Let $u = R_0fz + C; k$ then $\frac{d}{dz}(\text{cn } u) = -\text{sn } u \text{ dn } u \frac{du}{dz}$ and Eq.(D.30) becomes

$$S_2 = \frac{2pkf^2}{r} [\text{sn}(R_0fz + C; k)] \text{dn}(R_0fz + C; k) \quad (\text{D.31})$$

Similarly, with the use of Eq.(D.8), the solution for S_1 can be expressed as

$$S_1 = \frac{f^2}{r} \left\{ 1 - 2m [\text{sn}^2(R_0fz + C; k)] \right\} - 1 \quad (\text{D.32})$$